AD-A047 342   WASHINGTON UNIV SEATTLE DEPT OF OCEANOGRAPHY   F/G 8/11
A COMPILATION OF ARTICLES REPORTING RESEARCH SPONSORED BY THE O--ETC(U)
MAY 75   F A RICHARDS   N00014-A-0103-0014

UNCLASSIFIED   REF-M75-57   NL

1 OF 1
ADI
A047342

END
DATE
FILMED
1 -78
DDC

the department of

OCEANOGRAPHY

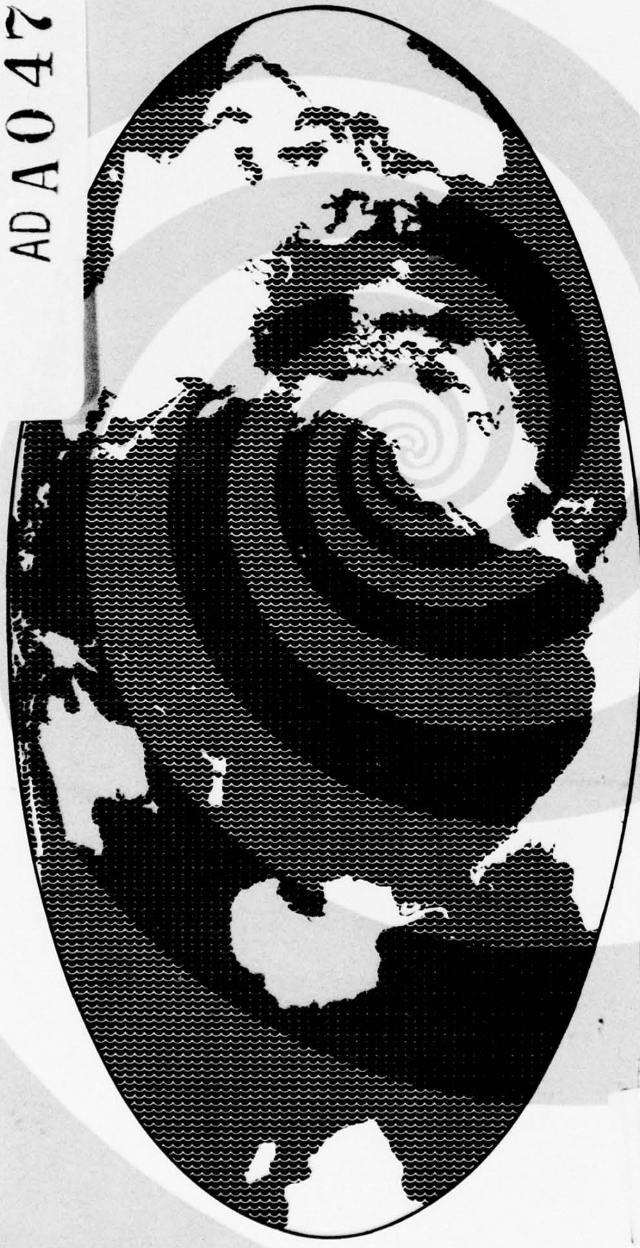

Technical Reports

Nos. 337, 338, 339, 340, 341

A COMPILATION OF ARTICLES REPORTING RESEARCH SPONSORED BY THE OFFICE OF NAVAL RESEARCH

Office of Naval Research
Contract Nonr-477(37)
and
N-00014-67-A-0103-0014
Project NR 083 012

Reference M75-57
June 1975

seattle, washington 98195

UNIVERSITY OF WASHINGTON
DEPARTMENT OF OCEANOGRAPHY
Seattle, Washington 98195

Technical Reports

Nos. 337, 338, 339, 340, 341

6 A COMPILATION OF ARTICLES REPORTING RESEARCH
SPONSORED BY
THE OFFICE OF NAVAL RESEARCH,

12 72p.

15
Office of Naval Research
Contract N-00014-A-0103-0014
Project Nr 083 012

14 Ref-M75-57

Reference M75-57
11 May 1975

J Richards
10 Francis A. Richards
Principal Investigator and
Assistant Chairman for Research

A 370280

ARTICLES REPORTING RESEARCH SPONSORED BY THE OFFICE OF NAVAL RESEARCH

contents:

Technical Report No. 337

THE PETROLOGIC NATURE OF THE LOWER OCEANIC CRUST AND UPPER MANTLE; by Nikolas I. Christensen. Geodynamics of Iceland and the North Atlantic Area: 165-176. 1974.

Technical Report No. 338

16. VELOCITIES OF COMPRESSIONAL AND SHEAR WAVES IN DSDP LEG 27 BASALTS; by N. I. Christensen, M. H. Salisbury, D. M. Fountain, and R. L. Carlson. Initial Reports of the Deep Sea Drilling Project 27:445-449. 1974.

Technical Report No. 339

STRUCTURE AND CONSTITUTION OF THE LOWER OCEANIC CRUST; by Nikolas I. Christensen and Matthew H. Salisbury. Reviews of Geophysics and Space Physics 13(1): 57-86. 1975.

Technical Report No. 340

27. ELASTIC WAVE VELOCITIES IN VOLCANIC AND PLUTONIC ROCKS RECOVERED ON DSDP LEG 31; by N. I. Christensen, R. L. Carlson, M. H. Salisbury, and D. M. Fountain. Initial Reports of the Deep Sea Drilling Project 31:607-609. 1975.

and

Technical Report No. 341

CONSTITUTION OF THE LOWER CONTINENTAL CRUST BASED ON EXPERIMENTAL STUDIES OF SEISMIC VELOCITIES IN GRANULITE, by Nikolas I. Christensen and David M. Fountain. Geological Society of america Bulletin 86:227-237. 1975.

B

THE PETROLOGIC NATURE OF THE LOWER OCEANIC CRUST AND UPPER MANTLE*

Nikolas I. Christensen

Department of Geological Sciences and Graduate Program in Geophysics, University of Washington, Seattle, Washington, U.S.A.

ABSTRACT. The compositions of the lower oceanic crust and upper mantle are investigated using data from high pressure experiments of compressional and shear wave velocities in rocks. Four compositional models for the lower oceanic crust are considered: 1) partially serpentinized peridotite, 2) gabbro, 3) metabasalt and metagabbro and 4) an ophiolite model consisting of metamorphosed sheeted dikes overlying late differentiates and cumulate gabbros. Comparisons of compressional wave velocities (V_p) from dredged oceanic rocks with layer 3 refraction velocities show that peridotites 30 to 40% serpentinized, unaltered gabbro, metagabbro and metabasalt all have velocities similar to observed lower crustal velocities. Thus compressional wave velocity measurements alone will not distinguish between the various crustal models. Although only a limited amount of refraction data on shear wave velocities (V_s) are available, it appears that lower crustal Poisson's ratios, calculated from V_p and V_s, are significantly lower than measured values in partially serpentinized peridotite and unaltered gabbro. In support of models 3 and 4 it is shown that Poisson's ratios of metabasalt and metagabbro, on the other hand, agree well with seismic data from the upper portion layer 3. The low Poisson's ratios reported for the lower crust of Iceland ($\sim$ 0.27) suggest that metabasalt and metagabbro are abundant constituents of layer 3. The 7.4 km/sec layer, often found between layer 3 and oceanic upper mantle in the Pacific Ocean, is interpreted as most likely being composed of peridotite, 10 to 20% serpentinized, or feldspathic

---

* This work has been supported in part by the Office of Naval Research and the National Science Foundation.

Kristjansson (ed.), Geodynamics of Iceland and the North Atlantic Area. 165-176.

peridotite. Compressional and shear wave velocities in eclogite and peridotite at appropriate pressures are similar to oceanic upper mantle velocities. An upper mantle of peridotite or dunite composition is favored, however, in regions where strong upper mantle anisotropy is observed.

1. INTRODUCTION

During the past few years several papers have been directly concerned with the petrologic nature of the oceanic crust and upper mantle. These papers have attracted much scientific attention because of the current interests in plate tectonics and the geological processes operating at ridge crests. Even though abundant geological and geophysical information is available on the crust and upper mantle, the relationship of this information to an understanding of composition is vague. Many rocks have been dredged from oceanic regions which offer clues to the petrologic nature of the lower levels of the crust and the upper mantle. However, it is impossible from geological criteria to accurately assess whether or not various rock types are abundant at different depth intervals. Similarly, ophiolite suites, which are believed by many to be on land exposures of oceanic crust, present complications because they are often dismembered and when complete differ significantly from one another in thickness, petrology and internal structure.

Much geophysical information on the crust and upper mantle, including heat flow, gravity and magnetic data, is also abstract and requires deciphering in order to interpret the physical significance of the measurements. Since the most direct information on the nature of the rocks beneath the oceans comes from seismology, it is appropriate to concentrate on seismic velocities of the lower oceanic crust and upper mantle. In the following discussion models of the mineralogical composition of the lower oceanic crust and upper mantle will be evaluated with the aid of experimental data on velocities in rocks.

2. SEISMIC STRUCTURE

Seismologists now recognize several layers within the oceanic crust. Average oceanic crustal structure [1] is often referred to in terms of a three layer crust in which the uppermost layer (layer 1) consists of a thin veneer of unconsolidated to semiconsolidated sediments, usually less than 1 km thick. Layer 2, often referred to as basement, is generally between 1.0 and 2.5 km in thickness and is believed to consist of basalt which is metamorphosed at its lower levels. Layer 3, immediately overlying the mantle, is quite variable in thickness (usually between 3 and 6 km) and at present is of unknown composition. Although many recent seismic studies have found a three layered crust, it now has become

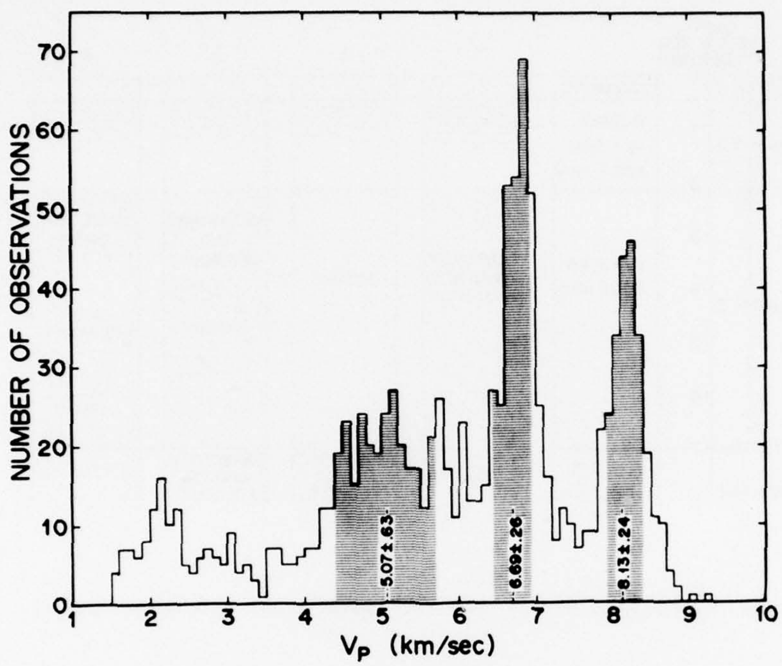

Fig. 1. Crustal and upper mantle compressional wave velocities.

increasingly apparent that in many regions crustal structure is much more complicated than this simple model. Examples include crust under ridge crests [2,3] and the high velocity basal crustal layer common in some oceanic regions [4].

In Fig. 1 crustal and upper mantle compressional wave velocities are shown in histogram form for 415 sites located in main oceanic basins. In addition, the average velocities of Raitt [1] are shown for layers 2 and 3 and the upper mantle. As can be seen from the diagram, the subdivisions of Raitt still hold, however many observed velocities fall outside the reported standard deviations. Thus even though it may be appropriate to envision the oceanic crust as containing three more or less well defined layers, such a simple model must be treated cautiously.

Much less information is available on shear velocities in the oceanic crust and the available data to 1970 have been summarized by Christensen [5]. In general for lower crustal velocities between 6.60 and 7.00 km/sec, shear wave velocities vary from 3.61 to 3.89 km/sec and calculated Poisson's ratios are between 0.25 and 0.29. It will be shown later that these values are extremely

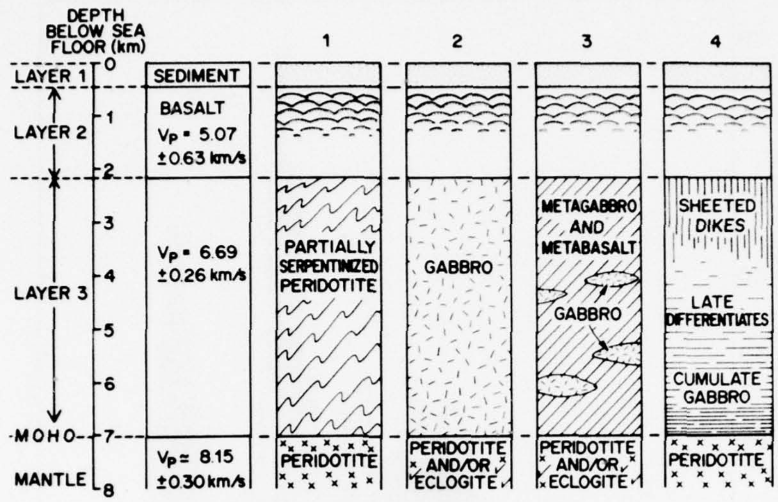

Fig. 2. Petrologic models for the lower crust and upper mantle.

important in interpreting composition from laboratory measurements of seismic velocities.

3. PETROLOGIC MODELS OF THE LOWER OCEANIC CRUST

Although the composition of the oceanic crust has been of considerable interest for the past decade, surprisingly few models have been seriously considered as viable representations of the petrologic nature of the crust. These are illustrated in Fig. 2 along with the average seismic structure of Raitt [1]. It should be emphasized that all four models are probably correct at least locally. Also it seems probable that all of these models are greatly oversimplified. However, the relative abundance of the rocks given in these simple sections is still a matter of speculation and a subject which can be clarified by comparisons of seismic refraction velocities with laboratory measurements.

Through the success of the Deep Sea Drilling Project, the upper portion of layer 2 has been found to consist of basalt at several localities. The laboratory measured velocities in these basalts agree well with refraction velocities of layer 2 [6]; because of this it is probable that basalt is the abundant rock type below the sea floor sediments. It also appears that the lower por-

tion of layer 2 has undergone metamorphic recrystallization [7], since the magnetic anomalies of the oceanic crust probably originate in only the upper half kilometer of layer 2.

The serpentinite lower crustal model (model 1, Fig. 3), originally proposed by Hess [8], assumes that the lower oceanic crust is generated under oceanic ridges by hydration of mantle peridotite. This model is attractive in several ways; serpentinite is simple to generate at ridge crests from an upper mantle composed of peridotite and as emphasized by Hess [8] serpentinite is easily disposed of at subduction zones by dehydration. Nevertheless this model has been strongly criticized by proponents of a mafic lower crust, three different models of which are shown in Fig. 3.

Model 2, which assumes that the lower crust consists of gabbro, has been proposed in several papers [1,9,10,11]. A slight variation of this model has hornblende gabbro as an abundant lower crustal rock, if sufficient water is present during the crystallization of basic magma within the lower crust [12].

As has been suggested as an alternative to the serpentinite and gabbro models, [12,13,14], metabasalts and metagabbros may be abundant constituents of the lower crust. For this model (model 3, Fig. 2) gabbros are assumed to occur within the lower crust as dikes and sills which have intruded the metamorphics. It is usually assumed that the metamorphism (greenschist to amphibolite facies) originates at ridge crests where high thermal gradients prevail, and the metabasalts and metagabbros are transported laterally by sea floor spreading.

Model 4 of Fig. 2 is based on rocks from ophiolites, believed by many to represent oceanic crust [15,16,17]. The hard rock portion of these sequences usually begin from the top with pillow basalts overlying sheeted dikes. The sheeted dikes, which are usually equated with the upper portion of layer 3, are vertical or near vertical and often metamorphosed to greenschist and amphibolite facies grade. Beneath the sheeted dikes are cumulate gabbros often containing abundant hornblende. Diorites, granophyres and trondhjemites, representing late stage products of differentiation, are common between the sheeted dikes and the gabbros. The lower portion of the ophiolite column (interpreted to represent mantle) consists of an uppermost ultramafic cumulate phase, containing abundant dunite and harzburgite, which overlies ultramafic tectonite composed of harzburgite.

4. LOWER CRUSTAL COMPOSITION

Since the dominant physical variable within the lower crust and upper mantle is pressure, experimental studies of seismic velocities in rocks at high pressure are the most significant for the analysis of seismic refraction velocities. Pressures within the lower oceanic crust and immediately beneath the Mohorovicic discontinuity are usually between 1 and 3 kbars. Compressional wave velo-

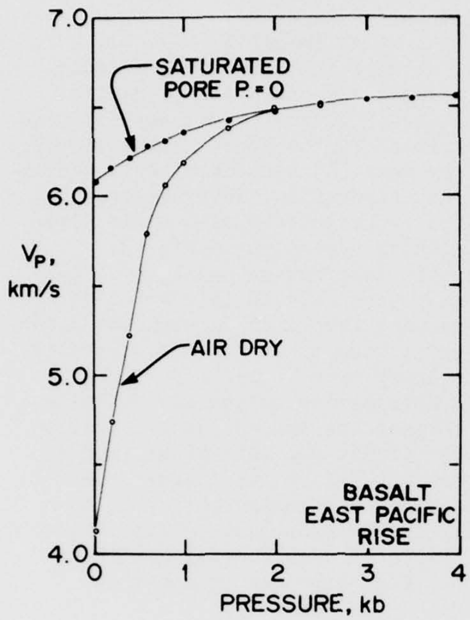

Fig. 3. Compressional wave velocities for saturated and air-dry basalt.

cities for a sample of oceanic basalt to 4 kbars, illustrated in Fig. 3, show two important features of rock velocities. First, velocities increase rapidly over the initial few kilobars increase in pressure, a finding ascribed to closure of grain boundary cracks [18]. At higher pressures grain boundary porosity is essentially eliminated, and the velocities are primarily related to the elastic properties of the minerals within the rocks. Second, it is significant that low pressure compressional wave velocities are higher if the rock pore spaces are water saturated. Since for most rocks the effect of pore water on velocities is usually minimal above 1 to 2 kbars, water saturation is an important variable only in velocity measurements of possible oceanic crustal rocks and has little importance in the interpretation of mantle velocities.

Since the classic works of Birch [18,19], in which compressional wave velocities were reported to 10 kbars for a wide variety of igneous and metamorphic rocks, several papers have presented data on velocities in rocks which are pertinent to a discussion of crustal and upper mantle composition. An extensive listing will not be at-

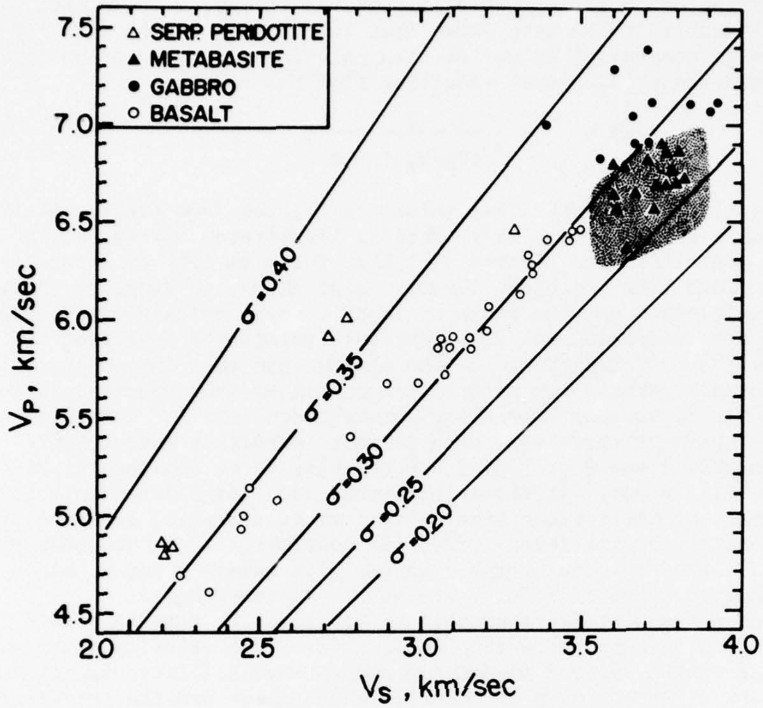

Fig. 4. The range of observed refraction velocities for layer 3 (stippled area) and rock velocities at 1 kbar.

tempted here; however, in addition to Birch's papers, much use will be made of the studies of Simmons [20], Christensen [5,12,21,22], Christensen and Shaw [23], and Christensen and Ramananantoandro [24]. Many of these papers also include data on shear wave velocities at elevated pressures, which provide important constraints on crustal and upper mantle composition when combined with compressional wave velocities.

Compressional wave velocities reported for layer 3 are similar to laboratory measurements of velocities in gabbro [12,18,21], amphibolite [12,18,21] and greenstone [22]. In addition, lower crustal velocities in the range of 6.7 to 6.9 km/sec agree with laboratory measurements in partially serpentinized peridotite containing

between 30 and 40% serpentine [5,12]. Thus if only oceanic compressional wave velocity refraction data are compared with rock velocities, all of the models illustrated in Fig. 3 are probable.

Recently it has been shown that the Poisson's ratios (σ) of partially serpentinized peridotites calculated from compressional (V_p) and shear (V_s) wave velocities from the relation

$$2\sigma = 1 - \frac{1}{(V_p/V_s)^2 - 1},$$

are usually much higher than values calculated from lower oceanic crustal refraction data [5]. This is illustrated in Fig. 4, in which velocities are plotted at 1 kbar for a variety of water saturated rocks from the ocean floors. Also shown are lines of constant Poisson's ratio and the range of lower crustal refraction data for which both compressional and shear wave velocities have been reported [5]. Of importance is the observation that Poisson's ratios for oceanic gabbros are generally much higher than observed values for layer 3, whereas laboratory measurements of σ for metabasalts and metagabbros agree well with seismic refraction measurements. Thus models 1 and 2 of Fig. 3 are unlikely to be abundant within the oceanic crust. It should be emphasized that refraction theory assumes that layer velocities are for waves traveling near the upper boundary of the layer. Thus the conclusion that the upper portion of layer 3 is metamorphic agrees with models 3 and 4, since the sheeted dikes of model 4 are usually metamorphosed.

At present it is impossible to distinguish between models 3 and 4 from seismic refraction data; however the velocity distributions within layer 3 of the two models should differ significantly. The late differentiates of model 4, which occur beneath the sheeted dikes, have very low velocities [18] and, if abundant, should form a low velocity region within layer 3. Also Poisson's ratio in the lower regions of layer 3 should be high if cumulate gabbros are abundant.

Crustal studies by seismic refraction techniques in Iceland provide abundant data on crustal values of Poisson's ratios for the crust of this region. Pálmason [3] reports average lower compressional and shear velocities of 6.35 km/sec and 3.53 km/sec, respectively, with Poisson's ratios near 0.27. The low velocities, which are also common in the upper mantle, are most likely related to the high temperature gradient in the region. Poisson's ratio, on the other hand, shows little change with temperature; thus from Fig. 4 it appears that metabasalt and metagabbro are abundant within the lower crust of Iceland.

A high velocity basal crustal layer with compressional wave velocities averaging 7.4 km/sec and a thickness of about 3 km has been found in several locations in the Pacific Ocean basin [4]. At present no shear velocity data have been published for this layer, so one can only speculate as to its nature using compressional wave velocity measurements. The velocities for this layer are in general

much higher than those observed for amphibolite and gabbro. Nevertheless, appropriate velocities have been reported for specific directions in anisotropic varieties of these rocks [21]. The most probable composition for this layer, not to be confused with "anomalous mantle" under ridge crests, is that of peridotite 10 to 20% serpentinized or feldspathic peridotite, both of which have appropriate velocities. Either of these compositions is consistent with model 3 of Fig. 3. Feldspathic peridotite does not occur in sufficient amounts within ophiolites to form a 3 km thick basal crustal layer. Thus a serpentinized peridotite origin for the 7.4 km/sec layer is the most favored for model 4.

5. UPPER MANTLE COMPOSITION

Compressional wave velocities in the oceanic upper mantle are generally between 7.8 and 8.6 km/sec, with a mean of approximately 8.2 km/sec (Fig. 1). The velocities severely limit permissible mineralogies, such that the most likely upper mantle rocks are peridotite and eclogite. The relative abundances of these two rock types, however, are still highly debated.

Recently Hart and Press [25] reported lithospheric S_n velocities ranging from 4.58 to 4.71 km/sec. Based on calculated velocities for various upper mantle petrologic models [26], they concluded that the upper mantle is composed of an eclogite-peridotite mix, because shear velocities of 4.71 km/sec are higher than that of peridotite. This, however, does not agree with laboratory measurements of shear wave velocities in fresh peridotites and dunites [24,27], which show that at pressures of 6 to 10 kbars unaltered peridotites have shear velocities between 4.6 and 4.8 km/sec. Similar shear velocities have been reported for eclogites [27]. Thus, in contrast with lower crustal studies, shear velocities are of

TABLE 1. Compressional wave velocities (km/sec) and anisotropies at 2 kbars

Rock	Highest Velocity	Lowest Velocity	Difference, % of mean	Reference
Dunite (North Carolina)	8.35	7.61	9.3	[18]
Dunite (Washington)	8.85	7.92	11.1	[18]
Dunite (New Zealand)	8.25	7.48	9.8	[18]
Dunite (Washington)	8.96	8.22	8.6	[28]
Dunite (Washington)	8.62	7.81	9.9	[24]
Dunite (Washington)	9.00	7.70	15.6	[24]
Eclogite (Colorado)	8.34	8.23	1.3	[29]
Eclogite (Colorado)	8.04	7.96	1.0	[29]
Eclogite (Japan)	8.54	8.40	1.8	[29]
Eclogite (Japan)	8.12	7.88	3.0	[29]

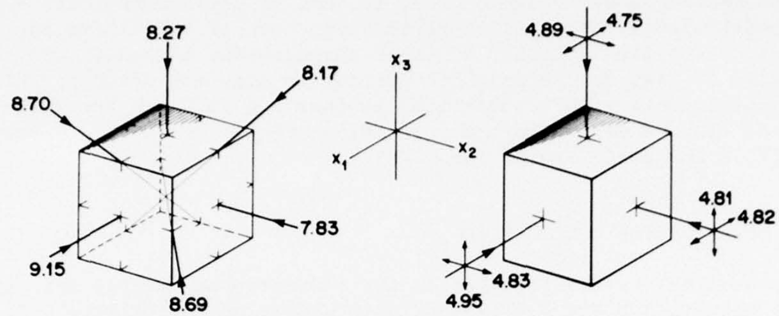

Fig. 5. Seismic velocities for an anisotropic dunite [24].

little value in deciphering upper mantle composition.

The elastic properties of rocks are usually considered to be isotropic, in which the elastic responses such as seismic wave velocities do not vary with direction. Under this simplifying assumption of isotropy, only two independent constants are required to completely describe elastic behavior. However, several recent investigations have shown that most ultramafic rocks are not adequately described by isotropic models, but require anisotropic elastic descriptions.

Compressional wave velocities and associated anisotropies at high pressure for several ultramafics and eclogites are given in Table 1. As was originally shown by Birch [18,19], the strong variation of compressional wave velocity with propagation direction in ultramafic rocks is related to preferred olivine orientation. Single crystal olivine is highly anisotropic with a maximum compressional wave velocity of 9.9 km/sec for propagation parallel to the a crystallographic axis and a minimum velocity of 7.7 km/sec for propagation parallel to the b axis. More recent studies of seismic anisotropy [24,28,29] have shown that the degree of preferred mineral orientation controls the magnitude of the anisotropy. Also, studies of shear wave propagation in olivine bearing ultramafic rocks have found that shear wave velocities within rocks with strong fabrics vary with displacement direction as well as propagation direction [24,30]. These relationships and the magnitude of anisotropy for a specimen of dunite with strong olivine orientation are illustrated in Fig. 5.

Detailed seismic refraction studies of the upper mantle in the northeast Pacific [31,32,33] have clearly shown that compressional wave velocities vary significantly with azimuth, the highest velocities being normal and the lowest parallel to ridge crests. The magnitude of the anisotropies are usually between 0.3 and 1.0 km/sec, in agreement with many laboratory measurements in olivine-rich ultramafics.

It is significant that eclogites, in general, do not show the strong anisotropy characteristic of many ultramafics [18,27,34]. Thus the observed anisotropies in the Pacific are most likely accounted for by dunite and peridotite with preferred olivine orientation. Upper mantle seismic velocities in other oceanic regions, however, which do show anisotropy may very well be accounted for by an eclogite model.

REFERENCES

1. R. Raitt, The Crustal Rocks, in: The Sea, ed. by M. N. Hill, New York, 1963.
2. X. LePichon, R. E. Houtz, C. L. Drake and J. E. Nafe, J. Geophys. Res., 70, 319, 1965.
3. G. Pálmason, Crustal Structure of Iceland from Explosion Seismology, Soc. Sci. Islandica, 40, Reykjavik, 1971.
4. G. H. Sutton, G. L. Maynard and D. M. Hussong, Widespread Occurrence of a High-Velocity Basal Layer in the Pacific Crust Found with Repetitive Sources and Sonobuoys, in: The Structure and Physical Properties of the Earth's Crust, ed. by J. G. Heacock, AGU, Washington D.C., 1971.
5. N. I. Christensen, J. Geol., 80, 709, 1972.
6. N. I. Christensen and M. H. Salisbury, Earth Planet. Sci. Lett., 19, 461, 1973.
7. TJ.H. van Andel, J. Mar. Res., 26, 144, 1968.
8. H. H. Hess, History of the Ocean Basins, in: Petrologic Studies. Buddington Vol., ed. by A. E. J. Engel, H. L. James and B. F. Leonard, Geol. Soc. Am., New York, 1962.
9. J. Ewing and M. Ewing, Bull. Geol. Soc. Am., 70, 291, 1959.
10. B. Gutenberg, Physics of the Earth's Interior, Academic Press, New York, 1959.
11. P. J. Fox, E. Schreiber and J. J. Peterson, J. Geophys. Res., 78, 5155, 1973.
12. N. I. Christensen, Marine Geol., 8, 139, 1970.
13. J. R. Cann, Geophys. J. R. Astron. Soc., 15, 331, 1968.
14. A. Miyashiro, F. Shido and M. Ewing, Deep-Sea Res., 17, 109, 1970.
15. I. G. Gass, Nature, 220, 39, 1968.
16. A. Gansser, Econ. Geol. Helv., 52, 659, 1959.
17. J. F. Dewey and J. M. Bird, J. Geophys. Res., 76, 3179, 1971.
18. F. Birch, J. Geophys. Res., 65, 1083, 1960.
19. F. Birch, J. Geophys. Res., 66, 2199, 1961.

20. G. Simmons, J. Geophys. Res., 69, 1123, 1964.
21. N. I. Christensen, J. Geophys. Res., 70, 6147, 1965.
22. N. I. Christensen, Bull. Geol. Soc. Am., 81, 905, 1970.
23. N. I. Christensen and G. H. Shaw, Geophys. J. R. Astron. Soc., 20, 271, 1970.
24. N. I. Christensen and R. Ramananantoandro, J. Geophys. Res., 76, 4003, 1971.
25. R. S. Hart and F. Press, J. Geophys. Res., 78, 407, 1973.
26. D. W. Forsyth and F. Press, J. Geophys. Res., 76, 7963, 1971.
27. N. I. Christensen, J. Geophys. Res., 79, 407, 1974.
28. N. I. Christensen, J. Geophys. Res., 71, 5921, 1966.
29. M. Kumazawa, H. Helmstaedt and K. Masaki, J. Geophys. Res., 76, 1231, 1971.
30. N. I. Christensen, J. Geophys. Res., 71, 3549, 1966.
31. R. W. Raitt, G. G. Shor and T. J. G. Francis, J. Geophys. Res., 74, 3095, 1969.
32. G. B. Morris, R. W. Raitt and G. G. Shor, J. Geophys. Res., 74, 4300, 1969.
33. C. E. Keen and D. L. Barrett, Can. J. Earth Sci., 8, 1056, 1971.
34. N. L. Carter, D. W. Baker and R. P. George Jr., Seismic Anisotropy, Flow, and Constitution of the Upper Mantle, in: Flow and Fracture of Rocks, ed. by H. C. Heard, I. Y. Borg, N. L. Carter and C. B. Raleigh, AGU, Washington D. C., 1972.

Reprinted from Veevers, J. J., Heirtzler, J. R., et al., September 1974
Initial Reports of the Deep Sea Drilling Project, Volume XXVII, Washington (U.S. Government Printing Office)

16. VELOCITIES OF COMPRESSIONAL AND SHEAR WAVES IN DSDP LEG 27 BASALTS

N. I. Christensen, M. H. Salisbury, D. M. Fountain, and R. L. Carlson,
Department of Geological Sciences, University of Washington, Seattle, Washington

INTRODUCTION

Two holes drilled during Leg 27 into basalt achieved significant penetrations of 38.5 meters at Site 259 and 47.5 meters at Site 261. Compressional and shear wave velocities have been measured to hydrostatic pressures of 6.0 kb for five basalt samples from Site 259 and seven basalt samples and one interlayered limestone from Site 261. The experimental technique used to obtain the velocities is similar to that described by Birch (1960), with the important exception that samples were water saturated prior to the measurements.

The purposes of this study were to: (a) investigate variations in velocities and related elastic properties of basement rocks from each site, (b) determine, if possible, if velocity gradients exist in the uppermost portion of Layer 2, (c) compare velocity-density relations of Leg 27 basalts with similar Atlantic and Pacific data, and (d) compare the laboratory-measured velocities with seismic-refraction velocities.

Samples 259-35-1, 128-131 cm and 259-36-2, 66-70 cm are altered, pale green, fractured basalts with intergranular to intersertal textures. The fractures are healed with dark green to reddish-brown vein fillings and white carbonate. Samples 259-37-2, 105-109 cm and 259-39-1, 135-138 cm (basalts) are both highly weathered, fine grained, and dark grayish-green in color. Sample 259-41-3, 53-56 cm is similar in texture to the overlying basalts, but is slightly coarser grained and highly vesicular.

Sample 261-33-1, 55-59 cm, the uppermost basalt of Site 261, contains highly altered plagioclase and pyroxene with a variolitic texture. Samples 261-33-1, 131-134 cm and 261-34-3, 69-73 cm were obtained beneath a half-meter-thick layer of recrystallized limestone (Sample 261-33-1, 67-71 cm), from a 10-meter-thick sill of relatively fresh coarse-grained basalt with a variolitic-textured groundmass containing clots of larger plagioclase and pyroxene crystals. Sample 261-35-3, 84-87 cm (basalt) is a medium-grained, highly altered rock with a variolitic texture. This sample may represent the lower portion of the sill, or, perhaps it is part of an underlying flow which has been altered by the intrusion. The lowest three samples studied (261-37-2, 92-95 cm; 261-38-2, 23-26 cm; and 261-38-5, 94-97 cm) are all extremely fine-grained basalts with felty-textured groundmasses. Alteration appears to decrease with depth in these three samples.

DATA

Bulk densities, obtained from the weights and dimensions of cylindrical samples, and compressional and shear-wave velocities are given in Table 1. Velocities were measured in only one core from each sample, since previous velocity studies (Christensen and Salisbury, 1972; 1973) have demonstrated low anisotrophy in other basalts from the DSDP samples, and petrographic examination of thin sections cut from the Leg 27 samples showed no evidence of strong preferred mineral orientation. For all samples included in the present study, wave propagation directions were parallel to the hole axes.

The samples were water saturated and 100-mesh screens were placed between the samples and copper jackets to obtain minimal pore pressures during the runs. Several studies (e.g., Dortman and Magid, 1968; Nur and Simmons, 1969; and Christensen, 1970; 1973) have shown significant increases in compressional wave velocities at pressures below approximately 2 kb after water saturation. This is illustrated in Figure 1 where compressional wave velocities were obtained from the same core of basalt under saturated conditions and again after the sample had been air dried at room temperature for several days.

Ratios of compressional to shear velocities (V_p/V_s), Poisson's ratios (σ), seismic parameters (ϕ), bulk moduli (K), compressibilities (β), shear moduli (μ), Young's moduli (E), and Lame's constants (λ) calculated from the densities and velocities are given in Table 2 at selected pressures.

VELOCITY-DENSITY RELATIONSHIPS

Christensen and Salisbury (1972; 1973) have shown that compressional- and shear-wave velocities of basalts in DSDP samples show excellent correlation with bulk density. The Leg 27 basalts show a range of densities from 2.081 g/cc to 2.997 g/cc, with corresponding compressional-wave velocities of 3.47 km/sec and 6.50 km/sec, respectively. The range of shear wave velocities is from 1.78 km/sec to 3.61 km/sec. The extremely wide range of densities for these rocks results primarily from the variation in stages of weathering apparent in the samples.

In Figures 2 and 3 compressional and shear wave velocities measured at 0.5 kb are plotted against density for 12 Leg 27 basalt samples together with 45 points from the Atlantic and Pacific oceans compiled by Christensen and Salisbury (1973). While the distribution of points for Leg 27 compressional-wave data is in excellent agreement with the Atlantic and Pacific point distributions, the Leg 27 shear-wave velocities appear to be slightly higher for given densities.

Also included in Figures 2 and 3 are least-squares regression lines computed by Christensen and Salisbury (1973) on the basis of 32 Pacific data points:

$$V_p = 3.22\rho - 3.55 \text{ km/sec}$$
$$V_s = 2.15\rho - 3.04 \text{ km/sec}$$

TABLE 1
Compressional (P) and Shear (S) Wave Velocities

Sample (Interval in cm)	Bulk Density	Mode	Velocity (km/sec) at Varying Pressures 0.2 kb	0.4 kb	0.6 kb	0.8 kb	1.0 kb	2.0 kb	4.0 kb	6.0 kb
259-35-1,	2.255	P	3.58	3.74	3.81	3.85	3.89	4.03	4.24	4.45
128-131	2.255	S	1.86	1.90	1.94	1.98	2.01	2.15	2.29	2.35
259-36-2,	2.081	P	3.38	3.44	3.49	3.53	3.56	3.70	3.93	4.14
66-70	2.081	S	1.68	1.76	1.80	1.84	1.88	1.97	2.06	2.10
259-37-2,	2.430	P	4.22	4.26	4.28	4.30	4.32	4.38	4.49	4.61
105-109	2.430	S	2.26	2.26	2.27	2.28	2.28	2.30	2.33	2.34
259-39-1,	2.551	P	4.60	4.64	4.67	4.70	4.72	4.81	4.96	5.11
135-138	2.551	S	2.48	2.50	2.51	2.52	2.53	2.56	2.61	2.66
259-41-3,	2.662	P	4.90	4.93	4.96	4.98	4.99	5.06	5.17	5.27
53-56	2.662	S	2.75	2.77	2.78	2.79	2.80	2.83	2.86	2.89
261-33-1,	2.587	P	4.92	4.96	4.98	5.01	5.03	5.10	5.21	5.32
55-59	2.587	S	2.61	2.62	2.63	2.63	2.64	2.66	2.69	2.72
261-33-1,	2.676	P	5.50	5.58	5.64	5.69	5.73	5.87	6.00	6.07
67-71	2.676	S	2.85	2.89	2.92	2.94	2.96	3.02	3.07	3.10
(Sedimentary)										
261-33-1,	2.790	P	5.52	5.54	5.56	5.57	5.58	5.63	5.71	5.80
131-134	2.790	S	2.83	2.85	2.86	2.87	2.88	2.90	2.91	2.93
261-34-3,	2.997	P	6.48	6.49	6.51	6.52	6.55	6.59	6.65	6.68
69-73	2.997	S	3.59	3.60	3.61	3.61	3.62	3.64	3.65	3.66
261-35-3,	2.599	P	4.43	4.46	4.48	4.50	4.52	4.59	4.73	4.87
84-87	2.599	S	2.26	2.29	2.31	2.33	2.34	2.38	2.43	2.46
261-37-2,	2.722	P	5.32	5.34	5.35	5.37	5.38	5.42	5.49	5.56
92-95	2.722	S	2.91	2.92	2.93	2.93	2.93	2.95	2.96	2.97
261-38-2,	2.745	P	5.48	5.49	5.51	5.52	5.53	5.56	5.62	5.68
23-26	2.745	S	2.80	2.81	2.82	2.83	2.84	2.85	2.86	2.87
261-38-5,	2.800	P	5.75	5.76	5.78	5.79	5.80	5.83	5.89	5.96
94-97	2.800	S	3.17	3.18	3.18	3.19	3.19	3.20	3.21	3.22

While it appears from the distribution of points in either figure that a nonlinear solution may provide a better fit, it is apparent that the linear solutions will predict velocities accurate to within approximately 0.2 km/sec for densities greater that 2.3 g/cc.

VELOCITY-DEPTH RELATIONSHIPS

The relatively deep drill penetrations into Layer 2 at Sites 259 and 261 provide a unique opportunity to examine variations in seismic velocity as a function of depth and thus to measure seismic-velocity gradients in the upper levels of Layer 2 directly.

In Figure 4 the compressional- (V_p) and shear-(V_s) wave velocities of representative samples from Sites 259 and 261 are presented as a function of recovery depth in Layer 2. Neglecting the effects of a sill in the upper 10 meters in Site 261, both sites display marked velocity gradients in both V_p and V_s (Table 3). From both hand-sample and thin-section analyses, this effect can be clearly attributed to differential submarine weathering. The uppermost extrusives at either site are profoundly weathered, in keeping with their ages (120 and 150 m.y., respectively). Their low velocities are consistent with both the velocity-density relations presented in this paper and our earlier findings of a marked decrease in density and seismic velocity of basalts from DSDP samples with age and weathering (Christensen and Salisbury, 1972; 1973). With increasing depth at both sites, weathering effects become less pronounced (feldspars and interstitial pyroxenes become less altered, for example) and seismic velocities increase. Projecting the observed velocity gradients downward, it is apparent that weathering extends to at least 70 and 55 meters at Sites 259 and 261, respectively. (Beyond these depths, if possible effects of changing lithology or metamorphic grade are ignored, seismic velocities would presumably be that of fresh basalt, Vp = 6.5 km/sec and Vs = 3.5 km/sec.)

COMPARISONS WITH REFRACTION DATA

The proximity of seismic refraction surveys (Francis and Raitt, 1967) to Sites 259 and 261 afford an excellent opportunity to compare laboratory-measured compressional wave velocities of Leg 27 basalts to velocities determined for Layer 2 from refraction work in the eastern Indian Ocean. The locations of profiles run by Francis and Raitt (1967) and the locations of Sites 259 and 261 are shown in Figure 5. A Layer-2 velocity of 4.98 km/sec was reported for Profile 49. The closest agreement with the refraction data is obtained for the basalt recovered from the 37-meter basalt penetration depth (Figure 4). Two profiles were determined by Francis and Raitt (1967) near Site 261, but a refracted Layer-2 arrival was not reported for the closest profile

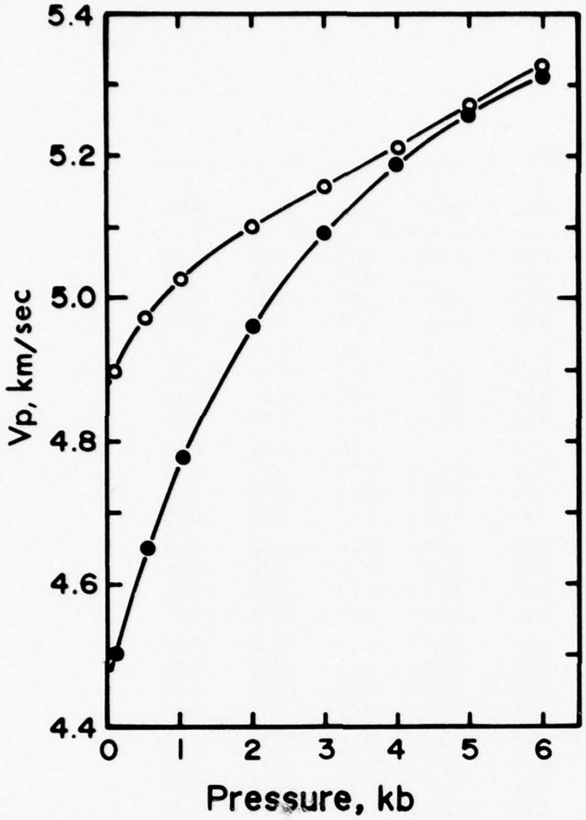

Figure 1. *Velocities for Sample 261-33-1, 55-59 cm (basalt), water saturated (open circles) and air dry (solid circles).*

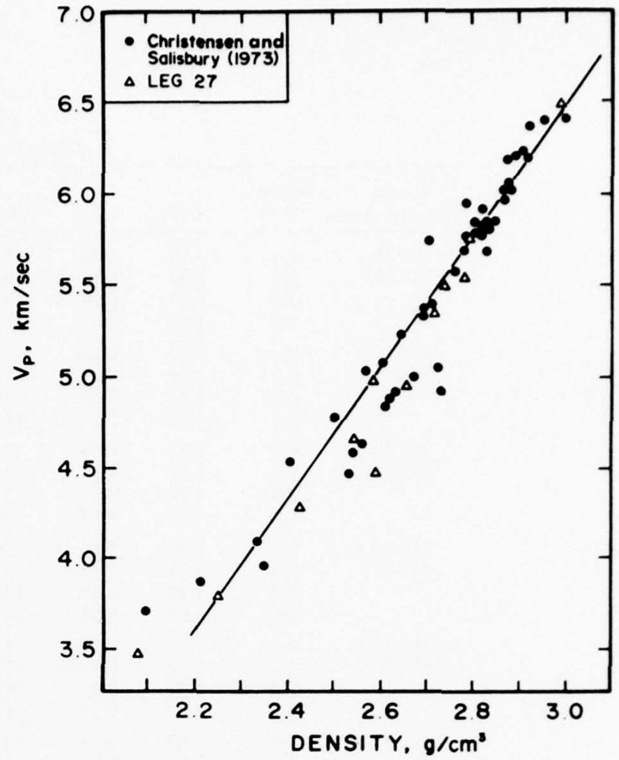

Figure 2. *Compressional wave velocities versus densities at 0.5 kb.*

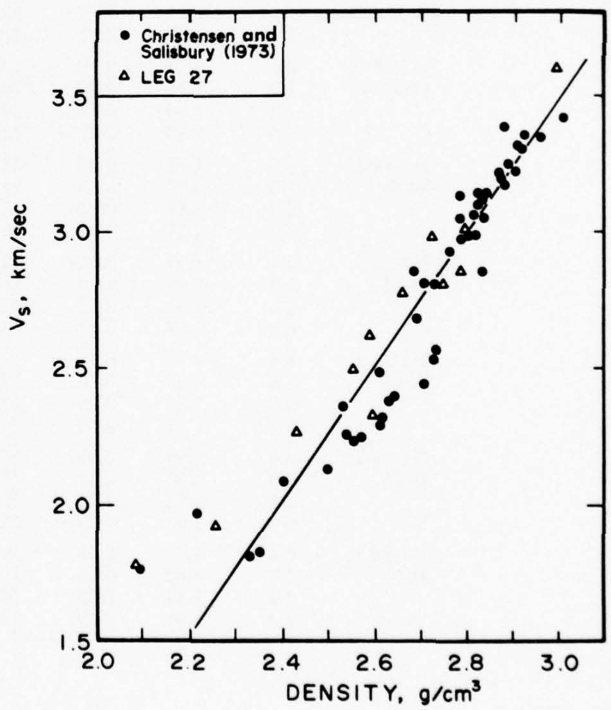

Figure 3. *Shear wave velocities versus densities at 0.5 kb.*

and the assumed velocity is not presented here. The compressional wave velocity reported for Refraction Station 58 is 5.18 km/sec, which compares most favorably with the basalt from a penetration depth of about 32 meters (Figure 4).

The refraction velocities noted above are higher than the velocities measured in the uppermost extrusive samples recovered from Layer 2 at each site (the effects of a thin sill at Site 261 may be neglected). The measured refraction velocities are lower, however, than those predicted from the velocity gradients of Figure 4 for greater depths. It is thus apparent that the refraction arrivals reported for these sites sampled intermediate levels producing an effective velocity similar to that measured directly in samples recovered 30 to 40 meters below the surface of Layer 2.

ACKNOWLEDGEMENTS

We wish to thank Robert McConaghy for his help in operating and maintaining the high-pressure system. This investigation was supported by National Science Foundation grant GA-36138 and the Office of Naval Research Contract N-00014-67-A-0103-0014.

TABLE 2
Elastic Constants, Leg 27

Sample (Interval in cm)	Pressure (kb)	Vp/Vs	σ	ϕ (km/sec)^2	K (Mb)	β (Mb^{-1})	μ (Mb)	E (Mb)	λ (Mb)
259-35-1,	0.4	1.97	0.33	9.15	0.21	4.84	0.08	0.22	0.15
128-131	1.0	1.93	0.32	9.73	0.22	4.54	0.09	0.24	0.16
	2.0	1.87	0.30	10.01	0.23	4.39	0.10	0.27	0.16
	6.0	1.90	0.31	12.32	0.28	3.52	0.12	0.33	0.20
259-36-2,	[illegible]	1.96	0.32	7.72	0.16	6.21	0.06	0.17	0.12
66-70	[illegible]	[illegible]	0.31	7.96	0.17	6.00	0.07	0.19	0.12
	[illegible]	[illegible]	0.30	8.39	0.18	5.66	0.08	0.21	0.12
	[illegible]	[illegible]	0.33	11.09	0.24	4.22	0.09	0.25	0.18
259-37-2,	[illegible]	[illegible]	0.30	11.27	0.27	3.64	0.12	0.32	0.19
105-109	1.0	[illegible]	0.31	11.69	0.29	3.51	0.13	0.33	0.20
	2.0	1.90	0.31	12.03	0.29	3.40	0.13	0.34	0.21
	6.0	1.97	0.33	13.80	0.34	2.93	0.13	0.35	0.25
259-39-1,	0.4	1.86	0.30	13.19	0.34	2.97	0.16	0.41	0.23
135-138	1.0	1.86	0.30	13.71	0.35	2.85	0.16	0.42	0.24
	2.0	1.88	0.30	14.32	0.37	2.72	0.17	0.44	0.26
	6.0	1.92	0.32	16.59	0.43	2.33	0.18	0.48	0.31
259-41-3,	0.4	1.78	0.27	14.11	0.38	2.66	0.20	0.52	0.24
53-56	1.0	1.78	0.27	14.44	0.39	2.59	0.21	0.53	0.25
	2.0	1.79	0.27	14.83	0.40	2.52	0.21	0.54	0.25
	6.0	1.82	0.29	16.49	0.44	2.25	0.22	0.57	0.30
261-33-1,	0.4	1.89	0.31	15.42	0.40	2.50	0.18	0.46	0.28
55-59	1.0	1.91	0.31	15.96	0.41	2.42	0.18	0.47	0.29
	2.0	1.92	0.31	16.52	0.43	2.33	0.18	0.48	0.31
	6.0	1.96	0.32	18.33	0.48	2.08	0.19	0.51	0.35
261-33-1,	0.4	1.93	0.32	19.93	0.53	1.87	0.22	0.59	0.38
67-71	1.0	1.94	0.32	21.16	0.57	1.76	0.23	0.62	0.41
(Sedimentary)	2.0	1.94	0.32	22.27	0.60	1.67	0.24	0.65	0.44
	6.0	1.96	0.32	23.94	0.65	1.55	0.26	0.68	0.48
261-33-1,	0.4	1.94	0.32	19.87	0.55	1.80	0.23	0.60	0.40
131-134	1.0	1.94	0.32	20.14	0.56	1.78	0.23	0.61	0.41
	2.0	1.94	0.32	20.47	0.57	1.74	0.23	0.62	0.42
	6.0	1.98	0.33	22.00	0.62	1.61	0.24	0.64	0.46
261-34-3,	0.4	1.81	0.28	24.91	0.75	1.34	0.39	0.99	0.49
69-73	1.0	1.81	0.28	25.34	0.76	1.32	0.39	1.01	0.50
	2.0	1.81	0.28	25.73	0.77	1.29	0.40	1.02	0.51
	6.0	1.82	0.28	26.52	0.80	1.25	0.40	1.04	0.53
261-35-3,	0.4	1.95	0.32	12.88	0.34	2.98	0.14	0.36	0.24
84-87	1.0	1.93	0.32	13.07	0.34	2.93	0.14	0.37	0.25
	2.0	1.93	0.32	13.42	0.35	2.85	0.15	0.39	0.25
	6.0	1.98	0.33	15.53	0.41	2.44	0.16	0.42	0.30
261-37-2,	0.4	1.83	0.29	17.17	0.47	2.14	0.23	0.60	0.31
92-95	1.0	1.83	0.29	17.44	0.48	2.11	0.23	0.60	0.32
	2.0	1.84	0.29	17.71	0.48	2.07	0.24	0.61	0.33
	6.0	1.87	0.30	19.04	0.52	1.91	0.24	0.63	0.36
261-38-2,	0.4	1.95	0.32	19.64	0.54	1.85	0.22	0.57	0.39
23-26	1.0	1.95	0.32	19.82	0.55	1.83	0.22	0.58	0.40
	2.0	1.95	0.32	20.08	0.55	1.81	0.22	0.59	0.40
	6.0	1.98	0.33	21.18	0.59	1.70	0.23	0.60	0.44
261-38-5,	0.4	1.81	0.28	19.73	0.55	1.81	0.28	0.72	0.36
94-97	1.0	1.82	0.28	19.99	0.56	1.78	0.29	0.73	0.37
	2.0	1.82	0.28	20.24	0.57	1.76	0.29	0.74	0.38
	6.0	1.85	0.29	21.53	0.61	1.64	0.29	0.75	0.41

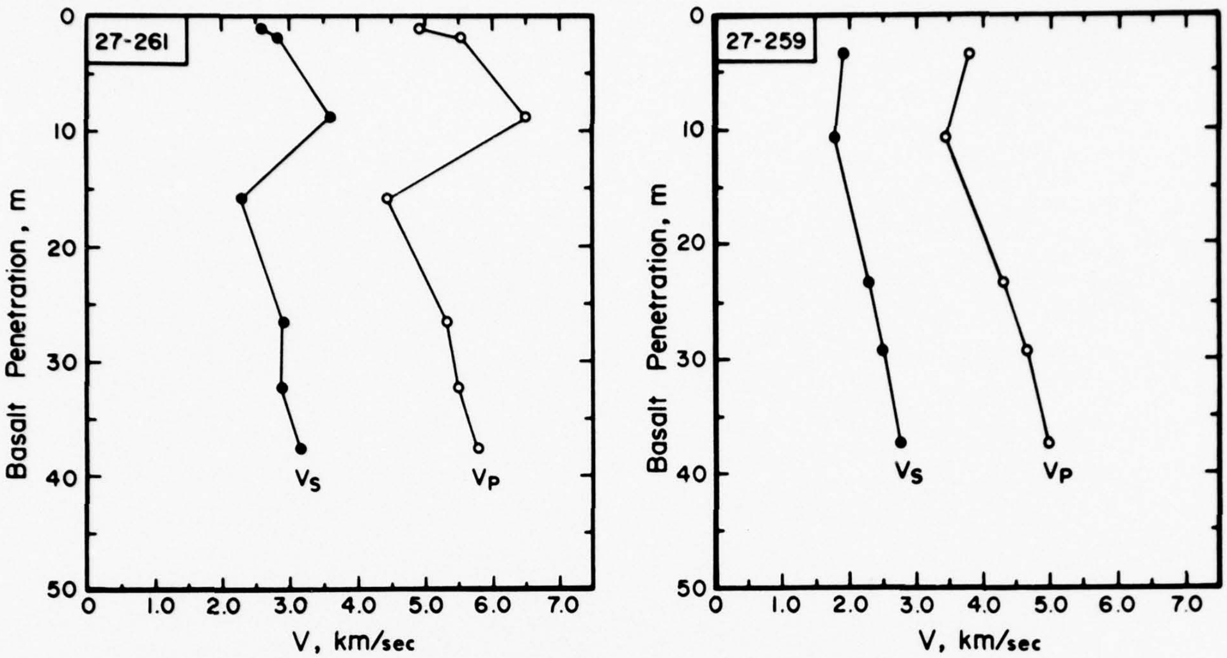

Figure 4. *Compressional and shear wave velocities at 0.5 kb versus recovery depth in Layer 2.*

TABLE 3
Compressional and Shear Wave Velocity Gradients

	$\partial V_p/\partial_z$ $\frac{(km/sec)}{m}$	$\partial V_s/\partial_z$ $\frac{(km/sec)}{m}$
Site 259	0.041	0.028
Site 261[a]	0.038	0.022

[a]Compiled from deepest three samples below sill.

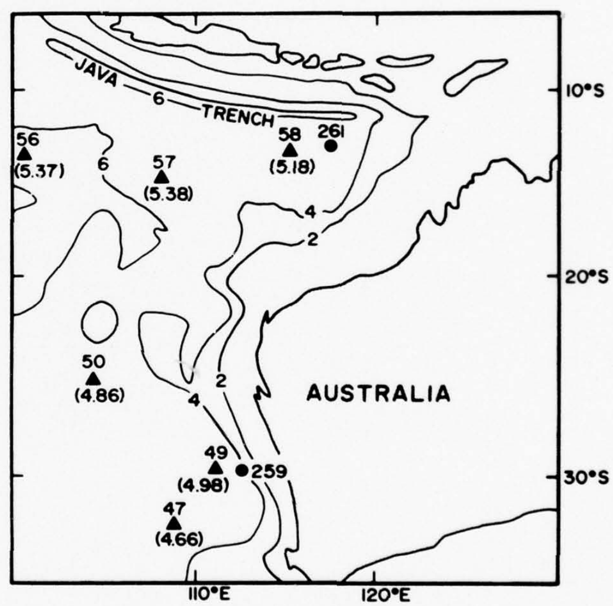

Figure 5. *Layer 2 seismic refraction velocities (km/sec) in the vicinity of DSDP Leg 27 Sites 259 and 261.*

REFERENCES

Birch, F., 1960. The velocity of compressional waves in rocks to 10 kilobars, I: J. Geophys. Res., v. 65, p. 1083.

Christensen, N. I., 1970. Compressional wave velocities in basalts from the Juan de Fuca Ridge: J. Geophys. Res., v. 75, p. 2773.

———, 1973. Compressional and shear wave velocities and elastic moduli of basalts, DSDP, Leg 19. *In* Creager, J. S., Scholl, D. W., et al., Initial Reports of the Deep Sea Drilling Project, Volume 19: Washington (U.S. Government Printing Office), p. 657.

Christensen, N. I. and Salisbury, M. H., 1972. Sea floor spreading, progressive alteration of Layer 2 basalts, and associated changes in seismic velocities: Earth Planet. Sci. Lett., v. 15, p. 367.

———, 1973. Velocities, elastic moduli and weathering-age relations for Pacific Layer 2 basalts: Earth Planet. Sci. Lett., v. 19, p. 461.

Dortman, N. B. and Magid, H. Sh., 1968. Velocity of elastic waves in crystalline rocks and its dependence on moisture content: Dokl. Akad. Nauk SSSR, Earth Sci. Sec., English Transl., v. 179, p. 1.

Francis, T. J. G. and Raitt, R. W., 1967. Seismic refraction measurements in the southern Indian Ocean: J. Geophys. Res., v. 72, p. 3015.

Nur, A. and Simmons, G., 1969. The effect of saturation on velocity in low porosity rocks. Earth Planet. Sci. Lett., v. 7, p. 183.

Structure and Constitution of the Lower Oceanic Crust

NIKOLAS I. CHRISTENSEN

MATTHEW H. SALISBURY

Reprinted from
REVIEWS OF GEOPHYSICS AND SPACE PHYSICS
Volume 13 Number 1 February 1975

Structure and Constitution of the Lower Oceanic Crust

NIKOLAS I. CHRISTENSEN

Department of Geological Sciences and Graduate Program in Geophysics
University of Washington, Seattle, Washington 98195

MATTHEW H. SALISBURY

Department of Geological Sciences, University of Washington, Seattle, Washington 98195

Any petrologic model of the lower oceanic crust must be consistent with three sets of data: (1) the seismic structure of the oceanic crust, (2) the petrology of oceanic dredge samples, and (3) laboratory measurements of seismic velocity through such samples. A review of these data indicates that within the framework of earlier three-layer models of oceanic seismic structure the crust is internally complex and varies markedly with age, azimuth, and tectonic province. Mantle compressional wave velocities V_p are anomalously low under the ridge (7.2–7.7 km/s) but increase to 8.0–8.3 km/s beyond 15 m.y.; layer 3 thickens by 2 km within 40 m.y. of formation and decreases in V_p from 6.8 to 6.5 km/s within 80 m.y.; both the mantle and layer 3 are statistically anisotropic. Dredge lithologies consist predominantly of serpentinized ultramafics and mafic igneous rocks ranging from basalt to gabbro, the gabbro often showing evidence of fractionation. Metamorphism of mafic rocks from zeolite to amphibolite facies grade is common. Velocities in oceanic serpentinites and basalts are generally lower than layer 3 refraction velocities. Unaltered gabbros have compressional wave velocities of approximately 7.0 km/s, which is high for layer 3, together with shear wave velocities V_s of 3.8 km/s and values of Poisson's ratio σ of 0.30. Metabasites containing hornblende and plagioclase have values of V_p = 6.8 km/s, V_s = 3.8 km/s, and σ = 0.28, in good agreement with those of layer 3. On the basis of petrology and velocity it is suggested that layer 3 is composed of hornblende metagabbro underlain by normal gabbro. In a model consistent with geophysical observations of heat flow, seismicity, gravity, and seismic structure at the ridge it is proposed that layer 2 and the upper levels of layer 3 form near the median valley but that deeper levels of layer 3 thicken for 40 m.y. by intermittent offridge intrusion fed from the underlying anomalous mantle. Ophiolites in such a model represent segments of thin immature ridge crest obducted onto continental margins during subduction of a spreading ridge.

CONTENTS

INTRODUCTION

The concepts of sea floor spreading and plate tectonics have provided a framework within which significant advances have been made in understanding the tectonic evolution of the ocean basins and continents. Serious deficiencies remain, however, in our understanding of the geological processes that create new oceanic crust at the ridge crests. One reason is that although the oceanic crust and upper mantle have been defined structurally through seismic studies, little is known about their mineralogic constitution. Only when sufficiently detailed information on the distribution of rock types with depth, as well as on possible lateral variations of mineralogy within the crust and upper mantle, is obtained will an understanding of the geologic processes that form the oceanic crust be possible.

Through the success of the Deep-Sea Drilling Project (DSDP), samples representative of the entire sediment column have been recovered from more than 200 ocean basin sites. Although basalts have been recovered from the underlying basement at many of these sites, only the uppermost few percent of the oceanic crust below the sediment column have been directly sampled by drilling. The rest of the column is known only from dredge samples and from geophysics. Models of oceanic crustal structure are thus based on and expressed largely in terms of seismology, important constraints being provided by dredge sample petrology, gravity, heat flow, and magnetic data. Not surprisingly, interpretations of these data have resulted in several speculative petrologic models of the oceanic crust that differ significantly from one another.

This paper distinguishes which of these petrologic models are plausible and which are improbable through a comparison of the seismic velocity structure of the oceanic crust with velocities measured in the laboratory from samples recovered from the ocean basins. To this end, three sets of primary data are examined: (1) oceanic refraction data in the form of a new compilation of data published or summarized since 1964, (2) petrologic descriptions of oceanic dredge samples, and (3) laboratory velocity measurements of oceanic rocks, many presented here for the first time. No model presented in the literature to date appears to be entirely consistent with the constraints imposed by these data. A petrologic model of the oceanic crust satisfying these constraints is suggested. In addition, a mechanism is proposed by which such crust might be generated at the ridge crest.

SEISMIC STRUCTURE

Field Techniques

The last two decades have witnessed a remarkable increase in our knowledge of the structure of the oceanic crust, an increase due largely to seismic refraction studies at sea. The bulk of the data available from these studies has been acquired by

using the unreversed, split, and reversed techniques developed by *Ewing et al.* [1937, 1939] and more recently described by *Hill* [1952], *Shor* [1963], and *Officer et al.* [1959].

One of the more persistent problems in marine refraction studies over this period has been the proper selection of shot spacing; for operational reasons it has often been difficult to provide spacing close enough to detect layers that appear only as first arrivals over a limited shooting interval. A very promising technique introduced by *Sutton et al.* [1969], *Maynard et al.* [1969], and *Ewing and Houtz* [1969] appears to resolve this problem by producing a marked decrease in shot spacing through the use of repetitive air gun sound sources, sonobuoys, and precision echo-recording equipment. The structural resolution introduced by this technique (several previously unsuspected layers are now often detected) promises a revolution in marine refraction studies.

In increasing recognition of the complexity of the oceanic crust and upper mantle, important new shooting techniques have been developed for the study of specific problems of seismic structure. For example, following the suggestion of *Hess* [1964*a*] that seismic anisotropy may exist in the upper mantle, *Raitt et al.* [1971], *Keen and Barrett* [1971], and *Whitmarsh* [1971] have conducted orthogonal and ring surveys at sea. In perhaps the most recent instrumental development *Hussong et al.* [1969], *Francis and Porter* [1973], *Carmichael et al.* [1973], and *Lister and Lewis* [1974] have begun testing both recoverable and nonrecoverable ocean bottom seismometers used in conjunction with both conventional and air gun sources. The unique capability of these instruments to monitor both compressional and shear waves directly may be crucial to the interpretation of oceanic seismic structure in terms of petrology.

Interpretation of oceanic refraction data is relatively straightforward, and the results are generally uncomplicated. It must be emphasized, however, that such complications as velocity gradients and inversions, generally not incorporated in determinations of seismic structure, have been detected by means of amplitude and wave form analysis [*Helmberger*, 1968; *Helmberger and Morris*, 1969, 1970]. Where such complications are present but unresolved, determinations of seismic structure, particularly layer thicknesses, may be significantly in error. Evaluation of the importance of these effects and of the validity of refraction determinations of seismic structure must await the results of additional sonobuoy and ocean bottom seismometer studies, the general application of sophisticated data analysis techniques, and, ultimately, deep basement drilling.

Oceanic Refraction Data

Compilations. More than 2000 ocean basin refraction lines have been published since the late 1930's. Since the reservations outlined above do not imply that velocities obtained from these studies are incorrect but that, at worst, they are merely incomplete, there is considerable value in compiling these data for review and interpretation. For excellent compilations of this sort the reader is referred to the works of *McConnell et al.* [1966] and *Shor et al.* [1971*a*].

Since much of the refraction data gathered by means of new techniques, as well as a large body of newly available information from back arc basins, has not been included in these compilations, it has been necessary, for the purposes of this study, to assemble a new compilation of recent refraction results. To this end, refraction velocities, layer thicknesses, and standard deviations of the data, together with water depths, profile geodetic end points and azimuths, instrumental techniques, and shooting procedures, have been compiled for 529 ocean basin sites published since 1964. In addition, an attempt has been made to assign a sea floor age to each site on the basis of magnetic anomalies and deep-sea drilling results, to classify each site in terms of tectonic province (e.g., median valley, ridge flank, back arc basin), and finally, for studies of seismic anisotropy and structure, to determine the azimuth of each profile with respect to nearby fracture zones and magnetic anomaly orientations or, for back arc basins, with respect to the axial trends of nearby island arcs and behind-arc ridges. Although extensive use will be made of this compilation below, compressional wave velocity data will be presented here in summary form only, since they can, for the most part, be found elsewhere in the literature [*Le Pichon et al.*, 1965; *Francis and Shor*, 1966; *Keen and Loncarevic*, 1966; *Ludwig et al.*, 1966, 1968, 1971, 1973; *Francis and Raitt*, 1967; *Fenwick et al.*, 1968; *Furumoto et al.*, 1968, 1971; *Murauchi et al.*, 1968, 1973; *Shor et al.*, 1968, 1971*a*, *b*; *Bunce et al.*, 1969; *Den et al.*, 1969, 1971; *Ewing and Houtz*, 1969; *Helmberger and Morris*, 1969; *Matthews et al.*, 1969; *Bosshard and MacFarlane*, 1970; *Ewing et al.*, 1970, 1971; *Houtz et al.*, 1970; *Sutton et al.*, 1971; *Talwani et al.*, 1971; *Yoshii et al.*, 1973].

Remarkably few determinations of shear wave velocity from the oceanic crust have been reported owing to the inefficiency of P to S and S to P wave conversions. Measurements that have appeared in the literature from profiles in which both V_p and V_s were reversed are listed in Table 1, together with associated values of compressional wave velocity, unit thickness, and tectonic province. In addition, Poisson's ratio σ is computed from each set of velocities and presented in Table 1. This parameter is diagnostic of mineralogy [*Christensen*, 1972*a*] and is thus critical in the interpretation of refraction velocities in terms of petrology.

Velocities and layer thicknesses. Early studies by *Hill* [1957] and subsequent analysis of numerous refraction profiles by *Raitt* [1963] suggest that the average seismic structure of the oceanic crust is surprisingly uncomplicated. Raitt's synthesis of this structure (Table 2) loosely divides the oceanic crust into three successively deeper layers on the basis of seismic velocities and layer thicknesses. Layer 1 is a thin veneer, generally less than 1 km thick, of sediments ranging in velocity from 1.5 to approximately 3.5 km/s; layer 2 is a layer of intermediate and relatively well defined thickness (generally 1.0–2.5 km) but widely ranging velocity (3.5 to approximately 6.4 km/s, the most common values lying between 4.4 and 5.6 km/s); immediately overlying the mantle, layer 3 is a layer of considerable and highly variable thickness (commonly 3.4–6.3 km) but well-defined velocity (6.4–7.7 km/s, most values lying between 6.4 and 7.0 km/s).

As can be seen in Figure 1, in which the observed velocities from all 415 main basin sites from the present compilation are presented in histogram form, the velocity layering proposed by Raitt is broadly confirmed. The general validity of this subdivision is even more apparent in Figure 2*a*, in which each velocity from the main basin sites that might be characterized as tectonically 'normal' (data from such anomalous sites as fracture zones, offridge rises, plateaus, and linear island chains are purposely excluded) is plotted against its associated layer thickness. In addition, in Figure 2*b* each mantle velocity is plotted as a function of the thickness of the overlying crust. Although subdivision of the crust into more than three layers

TABLE 1. Oceanic Shear Velocity Measurements

V_p, km/s	V_s, km/s	Poisson's Ratio σ	Unit Thickness, km	Tectonic Province	Site	Reference
2.1	0.4	0.48	0.3	Abyssal plain	6-OBS 28, 30	*Sutton et al.* [1971]
2.7	0.6	0.47	0.97	Abyssal plain	6-OBS 28, 30	*Sutton et al.* [1971]
4.7	2.5	0.30	1.05	Abyssal plain	6-OBS 28, 30	*Sutton et al.* [1971]
6.02	3.50	0.25	1.25	Behind-arc basin	N24-N25	*Shor et al.* [1971*b*]
6.35	3.55	0.27	1.18	Abyssal plain	SH 31	*Helmberger and Morris* [1969]
6.54	3.88	0.21	8.83	Offridge rise	103b	*Bunce and Fahlquist* [1962]
6.60	3.68	0.28	5.72	Behind-arc basin	27	*Murauchi et al.* [1968]
6.62	3.81	0.25	5.0	Abyssal plain	5	*Ludwig et al.* [1966]
6.65	3.84	0.25	8.22	Abyssal plain	104a	*Bunce and Fahlquist* [1962]
6.65	3.88	0.24	8.37	Abyssal plain	104b	*Bunce and Fahlquist* [1962]
6.69	3.61	0.29	4.0	Abyssal plain	LSD-6, 7	*Francis and Shor* [1966]
6.72	3.79	0.27	7.94	Offridge rise	103a	*Bunce and Fahlquist* [1962]
6.74	3.55	0.31	5.50	Offridge rise	22	*Den et al.* [1971]
6.79	3.57	0.31		Ridge flank	V-10-6	*Le Pichon et al.* [1965]
6.81	3.68	0.29	4.42	Abyssal plain	21	*Den et al.* [1971]
6.82	3.81	0.27	3.96	Behind-arc basin	21	*Den et al.* [1971]
6.83	3.78	0.28	4.91	Behind-arc basin	24	*Murauchi et al.* [1968]
6.85	3.75	0.29	3.3	Abyssal plain	6-OBS 28, 30	*Sutton et al.* [1971]
6.91	3.74	0.29	8.15	Offridge rise	3	*Den et al.* [1969]
6.94	3.85	0.28	2.75	Abyssal plain	SH 31	*Helmberger and Morris* [1969]
7.09	3.61	0.32		Ridge flank	V-10-7	*Le Pichon et al.* [1965]
7.55	4.2	0.28	2.4	Abyssal plain	6-OBS 28, 30	*Sutton et al.* [1971]
7.77	4.25	0.29		Abyssal plain	LSD-6, 7	*Francis and Shor* [1966]
8.16	4.62	0.27		Back arc basin	26-56	*Officer et al.* [1959]
8.25	4.71	0.26		Abyssal plain	6-OBS 28, 30	*Sutton et al.* [1971]
8.3	4.65	0.27		Abyssal plain	6-OBS 27	*Sutton et al.* [1971]

causes dispersal in the more recent data, each of Raitt's crustal layers, as well as the mantle, can be seen to occupy a diffuse but clearly distinguishable velocity-thickness field.

As important as such crustal averages are, it is equally important to note that information can be lost in the averaging process. By way of example, if the matter of oceanic sediment thickness had been pursued no further than a compilation of its mean, its striking dependence upon sea floor age [*Ewing and Ewing*, 1967] would have remained undetected. It is thus appropriate to point out the wide ranges in velocity and thickness included even within the standard deviations describing the mean oceanic crustal layers and to inquire as to the causes of these departures from the mean.

Variations with age. Several authors have suggested that the seismic structure of the oceanic crust varies systematically with age. The most pronounced of these variations, and the least contested, is a marked increase in the thickness of layer 3 and the total thickness of the crust with age [*Le Pichon et al.*, 1965; *Le Pichon*, 1969; *Goslin et al.*, 1972]; it has further been suggested that layer 2 thins somewhat with age [*Le Pichon*, 1969] and decreases in velocity [*Christensen and Salisbury*, 1972, 1973; *Hart*, 1973].

To examine these questions and to determine the cause of the wide ranges of thickness and velocity observed for the

TABLE 2. Average Oceanic Crustal Structure [after *Raitt*, 1963]

	Velocity V_p, km/s	Thickness, km
Layer		
2	5.07 ± 0.63	1.71 ± 0.75
3	6.69 ± 0.26	4.86 ± 1.42
Mantle	8.13 ± 0.24	

oceanic crustal layers, main basin refraction velocities and layer thicknesses from normal oceanic sites that can be dated are examined as a function of age (Figures 3 and 4). Since it is difficult to assign the numerous observed refraction velocities falling outside the layer-defining standard deviations to a particular layer and since it is equally difficult, for those cases in which subdivisions of a given layer are observed, to decide which velocity is characteristic of a layer, the noncommital approach of plotting velocities in histograms appropriate to their ages has been taken in Figure 3. Changes in velocity with age will thus be seen in this figure as differences in form between

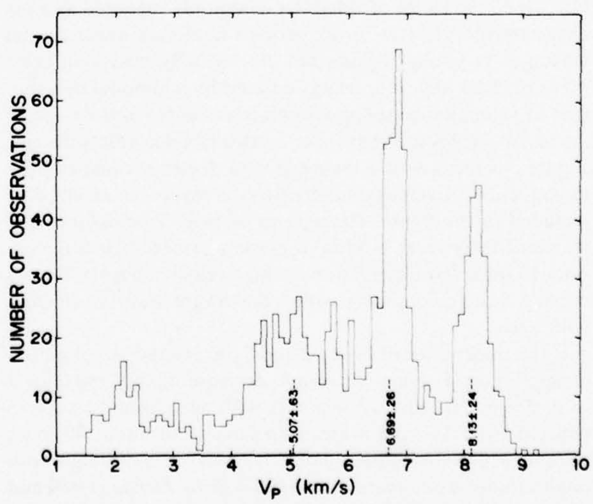

Fig. 1. Histogram of compressional wave refraction velocities from 415 main ocean basin sites. Superimposed are mean compressional wave velocities and standard deviations of velocity for layers 2, 3, and the mantle as computed by *Raitt* [1963].

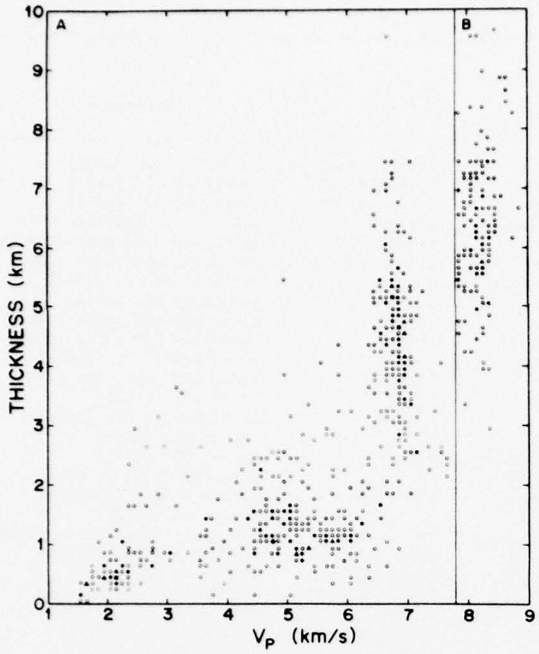

Fig. 2. (*a*) Compressional wave refraction velocities versus associated layer thicknesses from normal main ocean basin sites. (*b*) Mantle compressional wave velocity versus cumulative thickness of overlying crustal layers. Open circles indicate 1 observation; solid circles, 2 observations; solid triangles, 3 observations; solid squares, 4 observations; solid diamonds, 5 observations.

histograms. Two such changes are readily apparent. (1) 'Anomalous mantle' refraction velocities ranging between 7.1 and 7.8 km/s are frequently observed in young crust but are almost absent in crust more than 40 m.y. old. When velocities of this range are present, normal mantle velocities are usually absent, and layer 3 velocities are missing or slow. It should be pointed out that the presence of this phenomenon is spotty even in young crust; an equal number of sites are found with a normal seismic structure. (2) Velocities in the range 6.7–6.9 km/s (i.e., the range of velocities commonly regarded as most characteristic of layer 3) are seen to dominate lower crustal velocities in young regions but are virtually absent in crust more than 80 m.y. old, being replaced by a bimodal distribution of velocities centering around peaks at 6.5 and 7.0 km/s. As to the suggestion that layer 2 velocities decrease with age, Figure 3 is inconclusive owing to data dispersal caused by the introduction of velocity subdivisions in layer 2 in recent data included in the figure. Histograms of layer 2 velocities from standard three-layer models of oceanic crustal structure continue to show few observations of high velocity in layer 2 in old crust, a finding consistent with a downward shift in velocities with age.

If the thicknesses of layers 2 and 3 are plotted as a function of age (Figure 4), layer 2 is seen to decrease slightly and layer 3 to increase markedly in thickness with age (from 1.8 to 1.35 km and from 3.0 to 4.8 km, respectively) to about 40 m.y., beyond which time little change is observed. Although both observations are consistent with those of *Le Pichon* [1969] and although the observation that layer 3 thickens with age is almost certainly valid, the statement that layer 2 thins with age is misleading without further clarification. The majority of the young sites examined in this figure do not display an abnormally thick layer 2. A small number of young sites, however, have layer 2 thicknesses that are two to three times normal, and, as a consequence, the average thickness is slightly greater than that of old crust. An alternative and attractive interpretation of the data is not that layer 2 is abnormally thick but that layer 3 velocities are strongly depressed at these sites, these depressions causing layer 3 to be geophysically indistinguishable from layer 2 and thus added to its base. It is notable in this connection that young sites displaying such apparent thickening also display, almost invariably, anomalous mantle velocities. It is thus felt that abnormal layer 2 thicknesses, a thin or absent layer 3, and the presence of anomalous mantle velocities are interrelated phenomena at many young sites. The plate tectonic setting of these sites, their spotty geographic distribution, and their unusual structure suggest that they may be sites of active intrusion.

Menard [1967] and *Shor et al.* [1971*a*] have suggested alternatively that variations in layer 2 thickness are associated with variations in spreading rate, layer 2 being thickest at sites of slow spreading. Although this suggestion is attractive, it is difficult to evaluate. The argument hinges on data from a small number of ridge crest sites displaying slow spreading. Since the presence of an anomalous mantle is also associated with slow spreading, neither variable can be isolated as the cause of the high values of layer 2 thickness. It should be noted, however, that if the thickness of layer 2 is controlled by spreading rate only, Figure 4 implies that spreading is slower now than at any time during the previous 150 m.y., a conclusion considered unrealistic.

If many sites on the ridge crest are anomalous, it is more appropriate to compute the structure of the 'normal oceanic crust' from those sites in Figure 4 that are more than 40 m.y. old, as is done in Table 3. The mean layer velocities and standard deviations in this table are not significantly different from those in Table 2. It is worth noting, however, that the thickness of layer 2 and the standard deviations of the thicknesses of layers 2 and 3 are less than those of previous compilations.

Anisotropy. It is well established that seismic anisotropy exists in the uppermost mantle in many, though not all, areas of the main ocean basins, velocities generally being high perpendicular to ridge crests and slow parallel to ridge crests [*Hess*,

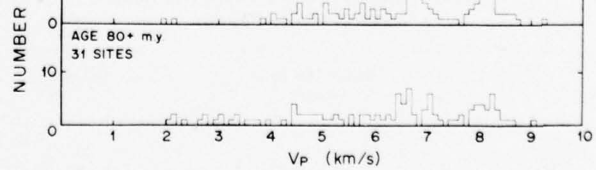

Fig. 3. Compressional wave refraction velocities from normal main ocean basin sites as a function of sea floor age.

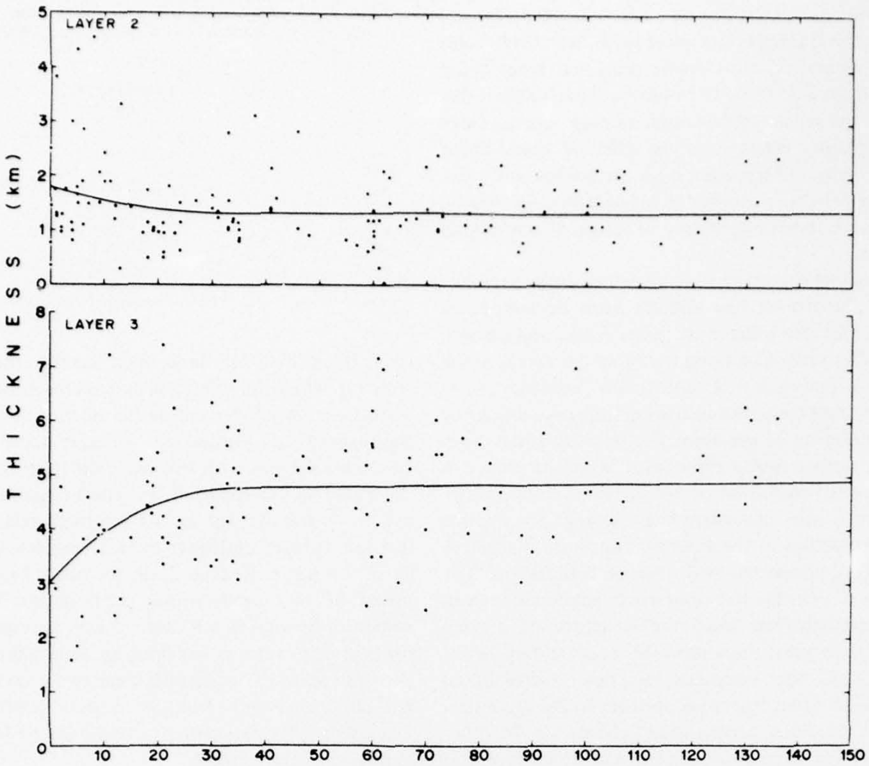

Fig. 4. Thicknesses of layers 2 and 3 at normal main ocean basin sites as a function of sea floor age. Curves are computed by running average techniques.

1964a; *Raitt et al.*, 1971; *Keen and Barrett*, 1971; *Whitmarsh*, 1971]. Little attention has been given, however, to whether anisotropy exists at higher levels in the oceanic crust, as was suggested by *Christensen* [1972b]. To resolve this question, velocities from the refraction profiles that were conducted over normal oceanic crust in the main ocean basins and that can be oriented with respect to either fracture zones or magnetic anomaly patterns (which are roughly perpendicular and parallel, respectively, to the ridge crests) are presented in histogram form in Figure 5. Profiles conducted subparallel to the ridge crests (i.e., profiles for which the difference in azimuth between the shot line and the ridge axis is <30°) are presented in the uppermost histogram, whereas those of intermediate (30°-60°) and subperpendicular (60°-90°) orientations are included in the middle and lower histograms, respectively.

The well-known anisotropy of the mantle can be clearly discerned as a marked increase in mantle velocities from a mean of 8.0 km/s subparallel to the ridge crest to a mean of 8.3 km/s subperpendicular to the ridge crest. More unexpectedly, layer 3 velocities decrease somewhat with increasing relative azimuth, a trend opposite in sense to that of the underlying mantle but consistent with recent observations by *Christensen* [1972b].

TABLE 3. Normal Oceanic Crustal Structure (This Study)

	Velocity V_p, km/s	Thickness, km
Layer		
2	5.04 ± 0.69	1.39 ± 0.50
3	6.73 ± 0.19	4.97 ± 1.25
Mantle	8.15 ± 0.31	

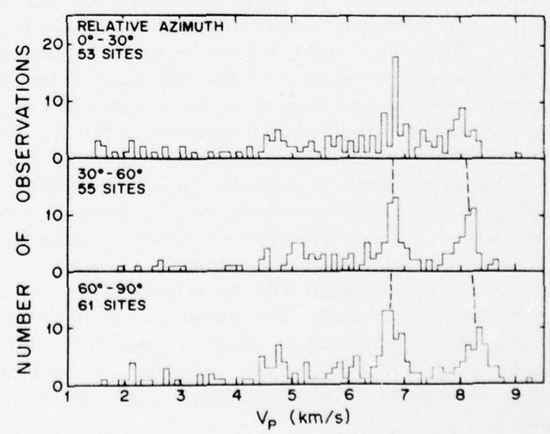

Fig. 5. Compressional wave refraction velocities from normal main ocean basin sites as a function of the azimuth of each refraction profile with respect to the local ridge axis; profiles shot subparallel to the ridge have relative azimuths of 0°-30°; those shot subperpendicular have relative azimuths of 60°-90°.

Regional variations. Despite an acknowledged genetic simplicity within the framework of plate tectonics, it is becoming increasingly clear that the oceanic crust, far from being simple, is tectonically complex. It would be remarkable if distinct features of the oceanic crust such as ridge crests, ridge flanks, abyssal plains, fracture zones, offridge rises, linear island chains, troughs and trenches, back arc basins, and rises, all clearly distinguishable in terms of topography, seismicity, and heat flow, were indistinguishable in terms of underlying seismic structure.

That major distinctions in seismic structure from province to province can be drawn has already been demonstrated (Figures 3 and 4) for the ridge crest, ridge flank, and abyssal plain provinces. Distinctions among the other provinces noted above cannot be demonstrated statistically because of insufficient data. Nonetheless, the following impressions can be noted from examination of the data. The fracture zones commonly display a conventional three-layer structure that can often be distinguished from that of normal crust in two ways. First, it is frequently thin, consistent with isostatic arguments; second, layer 2 velocities in the fracture zones are invariably low (4.2–5.4 km/s), consistent with intense brecciation. The crustal structures of offridge rises and linear island chains can commonly be distinguished from the structure of normal oceanic crust by their great thickness [*Den et al.*, 1969]. In the case of offridge rises, this increased thickness is distributed among all layers of what otherwise appears to be a conventional three-layer structure. Linear island chains, on the other hand, commonly have an unusual structure in which layer 2 is two to three times normal thickness and exhibits a wide range of velocities (3.5–6.1 km/s) distributed among several subdivisions, whereas layer 3 has somewhat low velocities and a normal thickness [*Furumoto et al.*, 1968, 1971]. Except for unusually thick sediment accumulations, the crustal structure of troughs, trenches, and back arc basins appears to be indistinguishable from that of normal oceanic crust [*Murauchi et al.*, 1968; *Ludwig et al.*, 1971]. Behind-arc rises, like main basin offridge rises, are distinguished chiefly by an unusually thick crust, the excess thickness again being distributed among layers of normal velocity [*Shor et al.*, 1971*b*].

Local structure. Recent studies using air gun–sonobuoy techniques suggest that the seismic structure of the oceanic crust may be far more complex than had previously been suspected [*Sutton et al.*, 1969; *Maynard et al.*, 1969; *Hussong*, 1972]. Although the results of routine refraction studies are generally consistent with those of sonobuoy studies [*Hussong*, 1972], the mean oceanic crustal layers of Raitt are only averages of layers that, in detail, are each seen to be composed of several subdivisions. In particular, layer 2 is frequently observed to have a thin low-velocity cap (2.5–3.8 km/s), and layer 3 is often observed to have a thick previously undetected basal layer with velocities ranging from 7.1–7.7 km/s. This layer is not to be confused with the anomalous mantle observed under ridge crests. The persistence of these subdivisions has prompted some authors [*Talwani et al.*, 1971; *Peterson et al.*, 1974] to suggest a redefinition of the mean oceanic crust based on sonobuoy data, such as the one in Table 4.

In view of the fact that only a small number of sites have been studied to date by sonobuoy techniques and that many of these show three or, in some instances, no subdivisions, such definitions seem premature. It is proposed that equally valid subdivisions of oceanic crustal structure can be drawn vertically. If the data for those main basin normal crust sonobuoy sites for which mantle returns have been observed (sufficient acoustic energy for examination of the entire column thus being insured) are plotted in a velocity-depth curve (Figure 6), two crustal types with distinctly different lower crustal (layer 3) structures are apparent. In type 1 (Figure 6) layer 3 is composed, on the average, of a 1-km-thick relatively low velocity (6.4 km/s) layer underlain by a 5-km-thick layer with a velocity of 7.1 km/s. In type 2, on the other hand, layer 3 is composed of two subdivisions, each about 3 km thick, with velocities averaging 6.8 and 7.5 km/s, respectively. Since no other criteria such as sea floor age, spreading rate, or tectonic province seem to distinguish these two crustal types (and there will almost certainly be more as more sonobuoy data become available), this variation is attributed to local structural or petrologic heterogeneity.

TABLE 4. Oceanic Crustal Structure From Sonobuoy Studies [after *Peterson et al.*, 1974]

	Velocity V_p, km/s	Thickness, km
Layer		
1	1.7-2.0	0.5
2A	2.5-3.8	0.5-1.5
2B	4.0-6.0	0.5-1.5
3A	6.5-6.8	2.0-3.0
3B	7.0-7.7	2.0-5.0
Mantle (4)	8.1	

In view of (1) the demonstrated lateral heterogeneity of the oceanic crust on both local and regional levels, (2) the impending overhaul of refraction studies and conclusions from sonobuoy data (for example, if a layer with a seismic velocity of 7.1–7.7 km/s is generally present at the base of layer 3, a slight revision of layer 3 and crustal thicknesses will be necessary), and (3) the likelihood that even this overhaul will be inaccurate owing to the presence of undetected velocity inversions and gradients, a revision of the estimates of mean oceanic crustal structure beyond that of Table 3 seems inappropriate at this time.

ROCKS FROM THE LOWER OCEANIC CRUST

The seismic structure of the oceanic crust must ultimately be interpreted in terms of petrology. It is thus important to consider what lithologies are actually recovered from the sea floor itself.

Through the efforts of deep-sea dredging and, more recently, the DSDP, igneous rocks comprising the uppermost hard-rock part of the oceanic crust have been obtained at many sites in the ocean basins. Although significant differences in chemistry exist among these rocks in restricted localities, numerous studies have shown that rocks from the uppermost basement are usually basaltic, and most have chemical characteristics that make it appropriate to call them tholeiites [*Engel and Engel*, 1964; *Engel et al.*, 1965; *Aumento*, 1967; *Miyashiro et al.*, 1969*b*; *Shido et al.*, 1971]. For more detailed information on the petrology and chemistry of submarine basalts, the reader is referred, in addition, to the excellent studies of *Aumento* [1968], *Hekinian and Aumento* [1973], and *Kay et al.* [1970].

Although several investigations [*Christensen*, 1970*a*, 1972*c*; *Christensen and Shaw*, 1970] have shown that compressional wave velocities measured in these basalts agree well with the

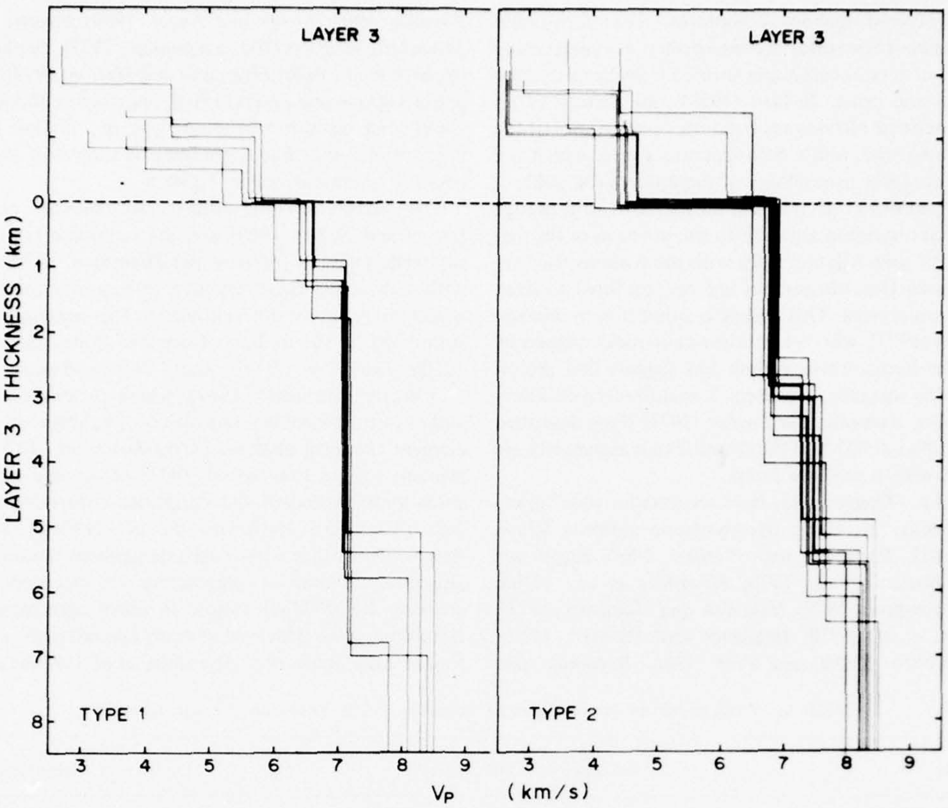

Fig. 6. Oceanic crustal types based on internal structure of layer 3 observed in sonobuoy studies conducted over normal main ocean basin sites. The range of commonly observed layer 3 refraction velocities is superimposed for comparison. Layers above the dotted line represent subdivisions of layer 2.

seismic velocities of layer 2, measured basalt velocities are generally much lower than the seismic velocities of the lower oceanic crust. For this reason we shall concentrate in the following discussion on reported occurrences and petrographic descriptions of metamorphic and coarse-grained igneous rocks dredged, for the most part, from the walls of median valleys, fracture zones, and trenches, which have been postulated to be important constituents of the lower oceanic crust. Because many of the papers that have reported the occurrences of these rocks were preliminary in nature, detailed data on the mineralogy and chemistry of possible lower crustal rocks, data that are critical in the interpretation of petrology in terms of mineralogy, are relatively limited.

Ultramafic rocks. Ultramafic rocks ranging from almost completely fresh to totally serpentinized are common constituents of fracture zones, central rift valleys, and walls of major trenches. Mineralogy indicates that the original ultramafics were dunite [*Bonatti*, 1968], lherzolite [*Engel and Fisher*, 1969; *Bonatti*, 1968; *Bonatti et al.*, 1970], harzburgite [*Cann and Funnell*, 1967; *Muir and Tilley*, 1966; *Fisher and Engel*, 1969; *Hekinian and Aumento*, 1973; *Bonatti et al.*, 1970], and picrite [*Melson and Thompson*, 1971; *Bonatti et al.*, 1970; *Ploshko and Bogdanov*, 1968]. Chemical analyses reported by *Hess* [1964*b*], *Chernysheva and Bezrukov* [1966], *Hekinian* [1968], *Bonatti* [1968], *Fisher and Engel* [1969], *Miyashiro et al.* [1969*a*], *Melson and Thompson* [1970], *Christensen* [1972*a*], and *Hekinian and Aumento* [1973] show trends related to the degree of serpentinization, sea floor weathering, and heterogeneity in the parent rocks from which the serpentinites and partially serpentinized ultramafics were formed. *Miyashiro et al.* [1969*a*] have attached particular significance to the CaO contents of oceanic serpentinites and have shown that with decreasing CaO and Al_2O_3, the K_2O and TiO_2 contents and the Fe/Mg ratio also tend to decrease. They attribute these findings to upper mantle heterogeneity and chemical migration during serpentinization.

Early studies of oceanic serpentinites [*Nicholls et al.*, 1964; *Quon and Ehlers*, 1963; *Bowin et al.*, 1966; *Hekinian*, 1968] reported antigorite as the most abundant serpentine mineral. The optical identification of antigorite has proven to be unreliable (e.g., antigorite was often equated with bastite), and more recent X ray diffraction studies have shown that lizardite is the most common serpentine mineral in oceanic ultramafics [*Miyashiro et al.*, 1969*a*; *Hekinian and Aumento*, 1973; *Aumento and Loubat*, 1971]. On the basis of oxygen and hydrogen isotopic analyses of 20 serpentinites from the mid-Atlantic ridge, the Blanco fracture zone, and the Puerto Rico trench, *Wenner and Taylor* [1973] conclude that seawater is the dominant type of water involved in the formation of oceanic serpentine from ultramafic rocks, although it is possible that up to 25% of the water involved in submarine serpentinization is magmatic in origin.

On the basis of reported occurrences, petrography, and chemistry, it is apparent that oceanic ultramafic rocks have formed under a wide variety of conditions. *Fisher and Engel* [1969] and *Melson and Thompson* [1970] have described collections of rocks from the Tonga trench and the Romanche fracture zone, respectively, that have textures and mineralogies

suggestive of layered igneous complexes. The ultramafics found within these rock suites are interpreted as representing the lower parts of crystal cumulates formed from basic magma trapped within the crust. *Bonatti* [1968] and *Bonatti et al.* [1970] have described ultramafics from the lower slopes of the Saint Paul, Romanche, and Chain fracture zones, which are overlain by a complex assemblage of metamorphics, gabbro, and basalt. *Miyashiro et al.* [1970*b*], on the basis of a dredge haul on a crestal mountain adjacent to the junction of the median valley of the mid-Atlantic ridge with the Atlantis fracture zone, have shown that ultramafics are not confined to deep levels of the oceanic crust. This finding is supported by *Thompson and Melson* [1972], who report ultramafic rocks capped by volcanics in the Vema fracture zone and suggest that the ultramafics, in this instance, represent a mantle-derived intrusion. In addition, *Aumento and Loubat* [1971] have described diapiric ultramafics at 45°N in the Atlantic that apparently are not associated with transform faults.

Gabbroic rocks. Dredge hauls have recovered a wide variety of gabbroic rocks, including two-pyroxene gabbros [*Quon and Ehlers*, 1963; *Bogdanov and Ploshko*, 1967; *Engel and Fisher*, 1969; *Bonatti et al.*, 1970; *Miyashiro et al.*, 1970*a*; *Melson and Thompson*, 1970; *Hekinian and Aumento*, 1973], norite [*Bonatti et al.*, 1970; *Bogdanov and Ploshko*, 1967], hornblende gabbro [*Cann and Vine*, 1966; *Bogdanov and Ploshko*, 1967; *Fisher and Engel*, 1969; *Bonatti et al.*, 1970; *Miyashiro et al.*, 1970*a*; *Thompson*, 1973], nepheline gabbro [*Bonatti et al.*, 1970; *Thompson and Melson*, 1972], anorthositic gabbro [*Quon and Ehlers*, 1963], anorthosite [*Engel and Fisher*, 1969], and troctolite [*Miyashiro et al.*, 1970*a*]. Petrographic descriptions and modal analyses of several of these gabbroic rocks are summarized in Table 5.

The association of gabbro, anorthosite, and lherzolite [*Engel and Fisher*, 1969] and the cumulate textures of some pryoxene gabbros [*Melson and Thompson*, 1970] indicate that within the crust there are layered basic complexes that have undergone gravity differentiation. This assumption is further supported by the finding of oceanic aplites [*Miyashiro et al.*, 1970*a*; *Thompson*, 1973], quartz diorite [*Bonatti et al.*, 1970], and diorite [*Aumento*, 1969], which probably represent late stages of fractional crystallization of gabbroic magma. Major eleme: : chemical analyses [*Miyashiro et al.*, 1970*a*] and trace element studies [*Thompson*, 1973] of oceanic gabbroic rocks show wide compositional variations controlled by fractional crystallization. *Miyashiro et al.* [1970*a*] have clearly demonstrated that within oceanic gabbros the decreases in the anorthite content of plagioclase are accompanied by increasing FeO*/MgO ratios, in close agreement with fractionation trends observed in many layered mafic complexes. In Figure 7 the analyses of *Miyashiro et al.* [1970*a*] are shown on

TABLE 5. Some Reported Occurrences of Gabbroic Rocks From the Oceanic Crust

Location	Petrographic Description	Reference
Mid-Atlantic ridge		
30°N	Granulated gabbros containing 40-50% plagioclase (An_{60}), 35-40% diopside, 5-8% hypersthene, 2% magnetite, and small amounts of amphibole and chlorite; altered gabbro with 40-45% labradorite, 30% diopside, and 10% hypersthene with zoisite and chlorite; anorthositic gabbro with 84% plagioclase (An_{60}), 5% diopside and bronzite, 6% amphibole, and 5% chlorite and biotite, with minor magnetite.	*Quon and Ehlers* [1963]
24°N	Tholeiitic gabbros showing strong differentiation; plagioclase composition varies from An_{47} to An_{79}; some gabbros are metamorphosed; primary hornblende is often present.	*Miyashiro et al.* [1970*a*]
1°S	Hornblende gabbro containing brown hornblende and aggregates of green amphibole, normal gabbro, olivine gabbro, and norite; mylonitized sections are common; titanomagnetite, prehnite, chlorite, iddingsite, and biotite are often present.	*Bogdanov and Ploshko* [1967]
3°S-8°N	Gabbro containing diopside, plagioclase, orthopyroxene and secondary amphibole; norite containing hypersthene, plagioclase and secondary chlorite, anthophyllite, hornblende, epidote, grunerite, and zoisite; olivine gabbro with enstatite, plagioclase, olivine, hornblende and secondary anthophyllite, talc, and chlorite; cataclastic gabbros containing clinopyroxene, plagioclase and secondary actinolite, hornblende, and chlorite; nepheline gabbro with titanaugite, plagioclase, nepheline, natrolite, aegirine, barkevikite, magnetite, and secondary chlorite.	*Bonatti et al.* [1970]
Equator	Gabbros, some of which show cumulate textures, containing plagioclase (An_{70}), augite, hypersthene, olivine(?) and secondary serpentine, chlorite, actinolite, talc, and opaques (mode of 46% pyroxene, 46% plagioclase, and 8% secondary minerals).	*Melson and Thompson* [1970]
53°N	Gabbro containing plagioclase (An_{65}), augite, orthopyroxene, olivine and secondary chlorite, serpentine, amphibole, iddingsite, and magnetite.	*Hekinian and Aumento* [1973]
Carlsberg ridge		
6°N	Granulated metamorphosed gabbro with hornblende, plagioclase (An_{50}), clinozoisite, chlorite, and sphene.	*Cann and Vine* [1966]
Tonga trench		
21°S, 173°W	Altered gabbro with plagioclase, augite and hornblende; cut by veinlets of alkali feldspar.	*Fisher and Engel* [1969]
Mid-Indian ridge		
14°S and 17°S	Coarse-grained massive gabbros at 17°S containing 63% plagioclase (bytownite), 25% augite, 5% olivine, 2% opaques, and 4% chlorite and hornblende; at 14°S one gabbro contains 67% plagioclase, 16% augite, 17% hypersthene, and minor chlorite, opaques, and antigorite; some gabbros are granulated, and others are altered to hornblende, chlorite, talc, and tremolite.	*Engel and Fisher* [1969]

a MgO-FeO*-(Na_2O + K_2O) diagram (where FeO* is total iron as FeO) along with plagioclase compositions and the fractionation trend of the Skaergaard intrusion [*Wager and Deer*, 1939].

Although hornblende gabbro, judging from its abundance in dredge hauls, is apparently an abundant constituent of the lower crust, the relationship of hornblende-bearing gabbros to cumulate gabbros is poorly understood. In many of these rocks the hornblende is clearly primary [*Miyashiro et al.*, 1970*a*; *Thompson*, 1973], whereas in others the amphiboles are secondary, having formed by uralitization and higher-grade metamorphism [*Quon and Ehlers*, 1963; *Cann and Vine*, 1966; *Engel and Fisher*, 1969; *Hekinian and Aumento*, 1973]. The latter gabbros contain primary igneous assemblages and secondary minerals formed by metamorphism and hydrothermal activity. The histories of such specimens are clearly complex; many of the reported mineral assemblages are not in equilibrium. It appears that gabbroic and metamorphic assemblages are formed in the context of high thermal gradients beneath the ridges. The lack of equilibrium often observed in these assemblages can be explained by rapid upward movement and exposure on the sea floor through faulting and diapiric intrusion or, alternatively, by rapid cooling associated with downward penetration of seawater.

Metabasites. Many rocks obtained from dredging along fracture zones and ridge median valleys that have been reported as gabbros and basalts are metamorphosed to some degree. Often, recrystallization is slight [*Miyashiro et al.*, 1970*a*], and unlike many continental metamorphics, relict igneous textures and minerals are common [*Cann and Funnell*, 1967; *Bonatti et al.*, 1970; *Miyashiro et al.*, 1971]. As is shown in Table 6, on the basis of mineralogy, metabasalts and metagabbros dredged from the ocean basins belong to the zeolite, greenschist, and amphibolite facies. The temperature of metamorphism for the higher-grade rocks must have exceeded 350°C, a value well above estimates of normal oceanic crustal temperature (calculated temperatures at the base of the crust are approximately 200°C in regions of normal heat flow). The crests of mid-ocean ridges, however, are characterized by

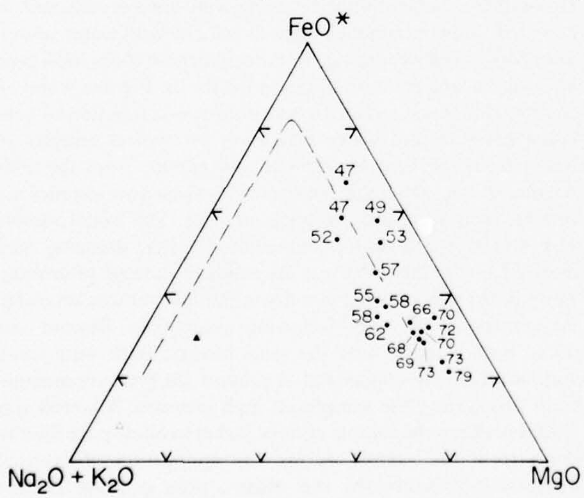

Fig. 7. A MgO-FeO*-(Na_2O + K_2O) diagram for gabbros and late differentiates dredged from the mid-Atlantic ridge at 24°N [*Miyashiro et al.*, 1970*a*; *Thompson*, 1973]. Numbers represent An content of modal plagioclase. The differentiation trend of the Skaergaard intrusion is included for comparison. Solid circles represent gabbro; solid triangles, diorite; open triangles, aplite.

high heat flow and high thermal gradients sufficient to produce metamorphic mineral assemblages at relatively shallow depths.

Schistose and nonschistose metabasites have been reported from ridge crests and fracture zones. Although only a limited number of samples have been studied, it appears that at least in the lower-grade oceanic metamorphics the proportion of nonschistose rocks is high. Accordingly, *Miyashiro et al.* [1971] have proposed the use of the terms burial metamorphism, mid-oceanic ridge metamorphism, or ocean floor metamorphism to emphasize the poor development of schistosity.

Prehnite-pumpellyite facies assemblages are apparently rare in oceanic rocks. *Hekinian and Aumento* [1973] have described low-grade metamorphic rocks from the Gibbs fracture zone and Minia seamount that they tentatively assigned to the prehnite-pumpellyite facies. Pumpellyite has been identified in oceanic rocks by *Melson and van Andel* [1966]. *Miyashiro et al.* [1971] have reported prehnite, apparently retrograde, within a schistose amphibolite from the mid-Atlantic ridge.

Zeolite facies rocks, the mineralogies of which are summarized in Table 6, have been reported from the mid-Atlantic ridge by *Miyashiro et al.* [1971]. Although chemical changes accompanying zeolite facies metamorphism are difficult to evaluate because of the intense weathering of the rocks so far reported, metabasalts of this facies generally show Na_2O and H_2O contents higher than those of abyssal tholeiites.

Greenschist facies metabasalts and metagabbros show a wide range of mineralogy and composition. In a detailed study of the petrology and chemistry of spilites from the Carlsberg ridge, *Cann* [1969] concluded that ocean floor spilites originate from greenschist facies metamorphism of once-cooled basalt. During this process, calcic plagioclase is replaced by albite, olivine and basaltic glass are replaced by chlorite, and augite may persist metastably or form actinolite. Changes in chemistry accompanying this metamorphism involve the loss of CaO, a gain in H_2O+, and an increase in Fe_2O_3, trends similar to those produced by ocean floor weathering [*Hart*, 1970; *Hekinian*, 1971]. Intense chemical migration and albitization resulting from hydrothermal activity are common in metabasites of the greenschist facies [*Miyashiro et al.*, 1971]. It should be noted, however, that igneous plagioclase (labradorite, bytownite) is often resistant to recrystallization; hence the mineral assemblage actinolite-chlorite-calcic plagioclase is also common.

Although amphibolites appear to be common in dredge hauls from the walls of fracture zones, only a limited number have been described. Oceanic rocks belonging to the amphibolite facies are usually metagabbros, often with their original textures and chemical compositions preserved [*Cann and Funnell*, 1967; *Miyashiro et al.*, 1971]. Some oceanic amphibolites, however, have strong schistosity and well-developed banding [*Bogdanov and Ploshko*, 1967; *Bonatti et al.*, 1970; *Miyashiro et al.*, 1971]. In many samples the interpretation of the petrography is difficult because of intense mylonitization and later retrograde metamorphism [*Cann and Vine*, 1966; *Cann and Funnell*, 1967].

COMPRESSIONAL AND SHEAR WAVE VELOCITIES IN OCEANIC ROCKS

Although compressional and shear wave velocities have been reported from a wide variety of continental rocks similar to dredge samples from ridge crests and fracture zones [*Birch*,

TABLE 6. Some Reported Occurrences of Metabasalts and Metagabbros From the Oceanic Crust

Location	Facies	Mineralogy	Reference
Mid-Atlantic ridge			
30°N	Greenschist	Quartz, epidote, magnetite	*Quon and Ehlers* [1963]
1°S	Amphibolite	Hornblende, plagioclase, actinolite, leucoxene	*Bogdanov and Ploshko* [1967]
22°N	Greenschist	Albite, chlorite, epidote, actinolite, nontronite, sphene	*Melson and van Andel* [1966]
3°S-8°N	Greenschist	Albite, epidote, chlorite, actinolite, quartz	*Bonatti et al.* [1970]
	Amphibolite	Hornblende, plagioclase	
24°N and 30°N	Zeolite	Natrolite, thomsonite, analcime, chabazite, laumontite, stilbite, mixed layer chlorite-smectite + vermiculite (relict pyroxene and plagioclase)	*Miyashiro et al.* [1971]
	Greenschist	Chlorite, quartz, epidote, actinolite, plagioclase (albite and relict labradorite or bytownite)	
	Amphibolite	Hornblende, plagioclase, chlorite	
11°N	Greenschist	Chlorite, albite, actinolite, sphene	*Melson and Thompson* [1971]
4°S	Greenschist	Chlorite, albite, actinolite	*Thompson and Melson* [1972]
53°N	Prehnite-pumpellyite(?)	Chlorite, epidote, prehnite, calcite, zeolite, partially albitized calcic plagioclase, clinopyroxene, magnetite	*Hekinian and Aumento* [1973]
Carlsberg ridge			
5°N	Greenschist	Albite, chlorite, augite, sphene, actinolite, epidote	*Cann* [1969]
	Amphibolite transitional to greenschist	Hornblende, plagioclase, clinozoisite, chlorite, sphene	*Cann and Vine* [1966]
Palmer ridge			
43°N	Amphibolite	Hornblende, plagioclase	*Cann and Funnell* [1967]
Bald Mountain			
45°N, 29°W	Greenschist	Albite, epidote, tremolite, chlorite, quartz, sphene, actinolite, hornblende	*Aumento and Loncarevic* [1969]

1960, 1961; *Simmons*, 1964; *Christensen*, 1965, 1966*a*, *b*, 1968], little information was directly available from oceanic igneous and metamorphic rocks prior to 1970. Although this situation has been largely remedied, the accuracy of laboratory velocity measurements through oceanic rocks is limited by factors peculiar to their provenance. At extremely high confining pressures the velocities measured in the laboratory represent an average of the intrinsic velocities of a rock's constituent minerals. Within the range of hydrostatic confining pressures of the oceanic crust, however (0.4–2.0 kbar), most rocks exhibit significant and variable grain boundary porosity. Since velocity is strongly lowered by such porosity and is, in addition, extremely sensitive to the presence of pore fluids in grain boundary cracks, it is necessary before examining rock velocity data to examine in detail the underlying assumptions and limitations of such measurements.

Water saturation. Early studies of elastic wave propagation in sedimentary rocks [*Hughes and Kelly*, 1952; *Wyllie et al.*, 1958] and recent investigations of igneous and metamorphic rocks [*Dortman and Magid*, 1969; *Nur and Simmons*, 1969; *Christensen*, 1970*c*] have emphasized the importance of water saturation for velocities at relatively low pressures. Figure 8 shows the compressional wave velocity of a water-saturated oceanic basalt as a function of time as the sample is allowed to dry at room temperature and pressure. The decrease in compressional wave velocity is the result of slow evaporation of water from grain boundary cracks within the sample. In comparable studies the effect of water saturation on shear wave velocities has been found to be negligible [*Dortman and Magid*, 1969; *Nur and Simmons*, 1969].

At low confining pressures the increase in velocity produced by water saturation depends primarily on the rock porosity. Unweathered serpentinites have relatively low porosity and, as expected, show minimal changes in velocity with water saturation. Most oceanic igneous and metamorphic rocks, however, have significant grain boundary porosity. In Figures 9 and 10 compressional wave velocities are shown as a function of confining pressure and water saturation for typical samples of basalt from the East Pacific rise and gabbro from the mid-Atlantic ridge. Although the curves for these two samples are similar, their saturation histories are not. The basalt sample was stored in seawater immediately after dredging and received in the laboratory in its original state of saturation. The gabbro was received in a dry condition but was saturated by immersion in water following evacuation. Beyond this point, both samples have the same history. Both were cored and jacketed with copper foil to prevent the pressure medium from penetrating the samples at high pressure. A screen was placed between the sample and the jacket to allow pore fluid to drain from the sample during the application of external hydrostatic pressure (by this means, pore pressure is kept minimal). Finally, velocities were measured for a range of pressures by means of the well-known pulse transmission technique [*Birch*, 1960]. After allowing the samples to dry in the atmosphere for one week, both samples were rerun. It is clear from these two cases that not only is velocity strongly in-

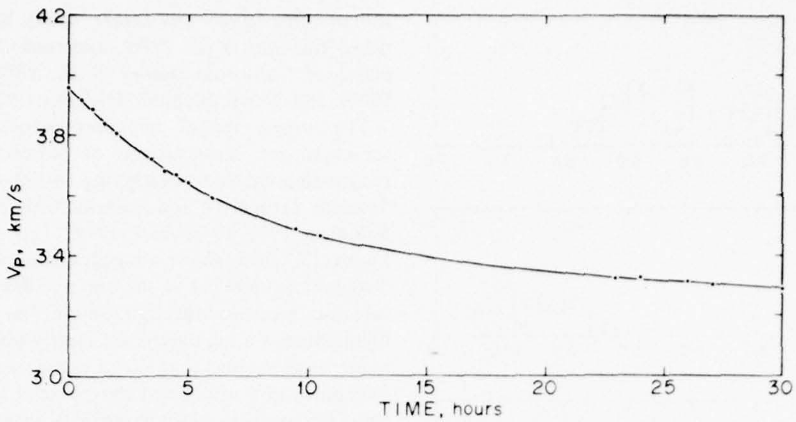

Fig. 8. Measured compressional wave velocity versus time for a sample of water-saturated basalt allowed to air dry at atmospheric pressure.

fluenced by water saturation at low pressures but also that initial conditions of water saturation can be reproduced by using laboratory techniques.

Since the range of in situ pressures within the oceanic crust is usually between 0.4 and 2.0 kbar, it is apparent from Figures 9 and 10 that the degree of water saturation of oceanic rocks constitutes an important factor that must be duplicated in the laboratory if laboratory velocity measurements are to be compared with oceanic crustal velocities. Although it has been suggested [*Fox et al.*, 1973] that the in situ interstitial water content of oceanic rocks is similar to that of air-dried laboratory samples, several independent lines of evidence suggest that it is not. Most oceanic rocks show abundant evidence of interaction with seawater, both through submarine weathering [*Hart*, 1970; *Hekinian*, 1971; *Christensen and Salisbury*, 1972] and various degrees of metamorphism in which water was an active constituent [*Miyashiro et al.*, 1971; *Cann and Funnell*, 1967; *Wenner and Taylor*, 1973]. In addition to spaces between grain boundaries, numerous fractures undoubtedly present within the oceanic crust allow water circulation. Further evidence that fractures and grain boundary cracks within the oceanic crust contain abundant water comes from studies of oceanic heat flow; measurements of heat flow on ridge crests and flanks require hydrothermal circulation as a dominant heat transfer process, since heat flow values along active oceanic ridges cannot be explained solely by conduction [*Elder*, 1965; *Deffeyes*, 1970; *Lister*, 1972]. This observation is consistent with the presence of hot springs and geysers in quasi-oceanic regions such as Iceland. Finally, the observed high electrical conductivity of the oceanic crust is most likely controlled by pore fluids [*Cox*, 1971], since most dry mafic rocks have extremely low conductivities at oceanic crustal temperatures and pressures.

Although oceanic rocks are probably saturated or nearly saturated in situ, the pore pressure of such interstitial water is not known. As was discussed by *Brace* [1971], pore pressure within crustal rocks probably varies between lithostatic, in which it balances the weight of the overlying rock and seawater, and hydrostatic, in which all pore space is continuously connected with seawater. In the course of measuring

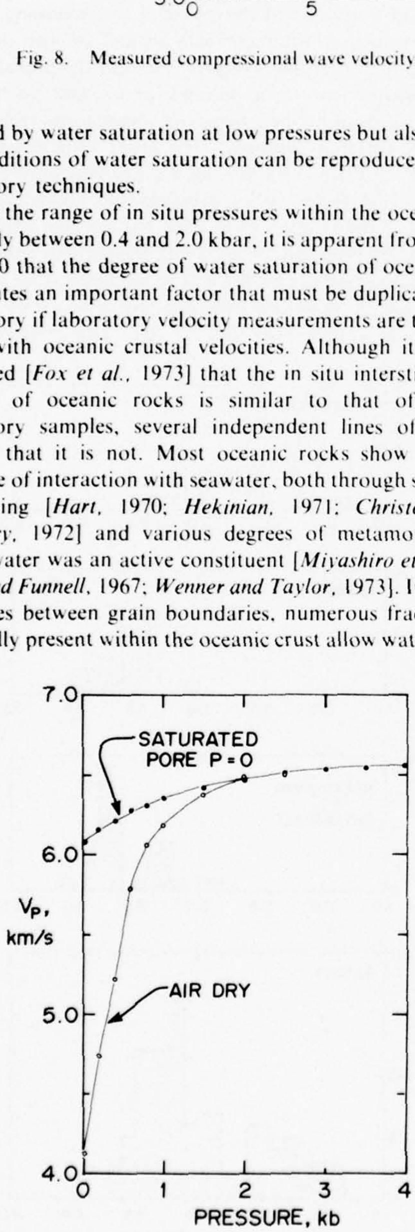

Fig. 9. Measured compressional wave velocities for air-dried and water-saturated basalt from the East Pacific rise as a function of confining pressure.

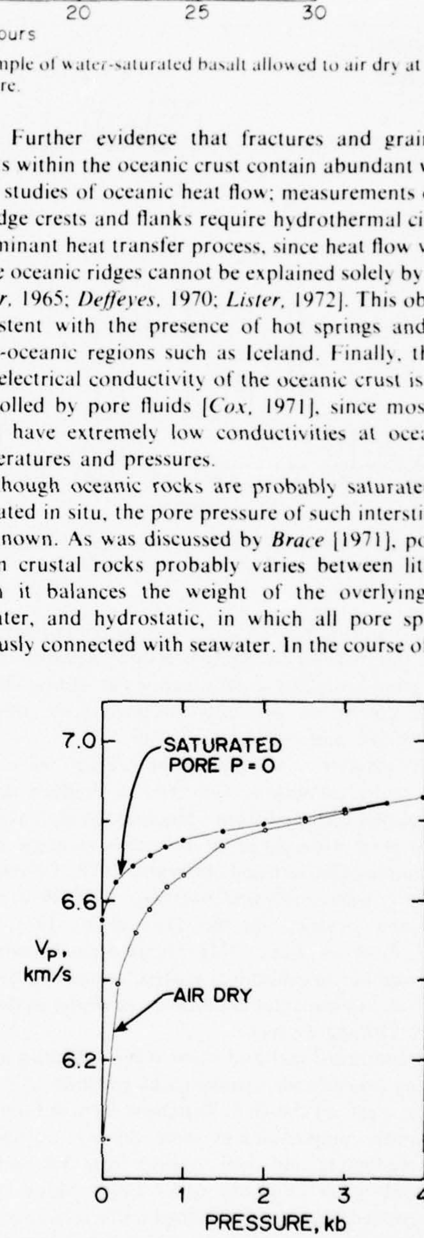

Fig. 10. Measured compressional wave velocities for air-dried and water-saturated gabbro from the mid-Atlantic ridge as a function of confining pressure.

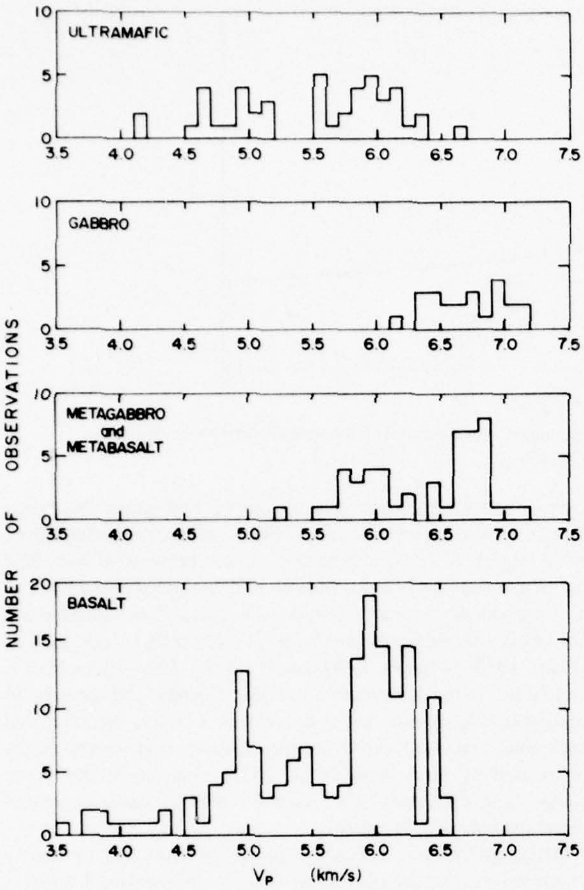

Fig. 11. Laboratory measurements of compressional wave velocity at 1 kbar for water-saturated oceanic rocks.

the velocities reported below, water was generally allowed to drain out of the rocks as confining pressure increased. To the extent that grain boundary cracks trap water during closure, experimental conditions probably produce pore pressures between lithostatic and hydrostatic values.

Ranges of velocity. A number of studies have been presented recently on seismic velocities in dredged oceanic rocks and samples collected from ophiolites. Many have been conducted over a wide range of pressures through water-saturated samples [*Barrett and Aumento*, 1970; *Christensen*, 1970*c*, 1972*a*, *c*; *Christensen and Salisbury*, 1972, 1973; *Hyndman*, 1973] and air-dried samples [*Fox et al.*, 1971, 1973; *Poster*, 1973; *Peterson et al.*, 1974]. The interested reader can find a large number of additional studies, conducted under a wide variety of experimental conditions, in *Initial Reports of the Deep-Sea Drilling Project*.

Measured compressional and shear wave velocities at a 1-kbar confining pressure for various rocks pertinent to a study of the oceanic crust are shown in histogram form in Figures 11 and 12; to make comparisons of some validity, we have included in these figures, and shall consider from this point on, velocities from water-saturated rocks only. Many of the velocities presented have been published in the references cited above. Previously unpublished data include velocities measured in our laboratory for a variety of rocks collected from the mid-Atlantic ridge [*Bonatti et al.*, 1970], the mid-Indian ridge [*Engel and Fisher*, 1969], basalts from the Lau ridge [*Hawkins et al.*, 1970], and rocks from ophiolite complexes in California [*Bailey et al.*, 1970], Oregon [*Thayer*, 1963], and Newfoundland [*Williams*, 1971].

The widest ranges of compressional and shear wave velocities are characteristic of basalts, primarily because progressive sea floor weathering causes submarine basalts to decrease in density and velocity with age [*Christensen and Salisbury*, 1972, 1973; *Hart*, 1973]. This point is illustrated in Figure 13, which shows a basalt compressional wave velocity distribution identical to the one in Figure 11 except that the velocities measured through samples less than 20 m.y. old are highlighted. Young basalts are clearly fast at the hand sample scale; basalts older than 20 m.y. old are slow. Whether this phenomenon is translated into a trend of decreasing layer 2 refraction velocities with age will depend on the depth of weathering, metamorphic overprinting, and the prevalence of such mesoscopic features as pillows, joints, and fractures.

The velocities of metagabbros and metabasalts (Figures 11 and 12) are distinctly bimodal. The lower velocities (5.2–6.3 km/s for V_p and 2.8–3.5 km/s for V_s) are typical of chlorite-rich greenschist facies rocks, whereas the higher velocities (6.4–7.2 km/s for V_p and 3.6–4.1 for V_s) are characteristic of rocks of the amphibolite facies. In all the metamorphic rocks studied the presence of chlorite was found to produce a significant lowering of velocities, whereas the presence of epidote and actinolite causes velocities to rise. The compressional

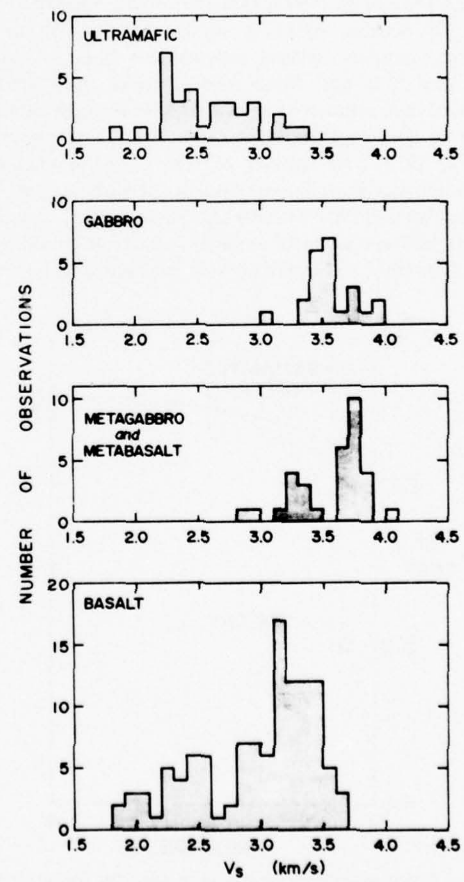

Fig. 12. Laboratory measurements of shear wave velocity at 1 kbar for oceanic rocks.

wave velocities shown in Figure 11 for greenschist facies rocks are significantly lower than the seismic velocities of the lower oceanic crust. Velocities measured to date from greenschist facies dredge samples, however, do not include many of the typical mineral assemblages characteristic of rocks described, for example, from the median valley of the mid-Atlantic ridge [*Melson and van Andel*, 1966]. Studies of velocities in continental greenschist facies rocks of equivalent mineralogy [*Christensen*, 1970*b*] show that it is possible to have greenschist facies rocks with compressional wave velocities similar to lower oceanic crustal velocities at appropriate pressures (see Table 7).

Many metamorphic rocks from dredge hauls and ophiolite complexes have significantly lower anisotropy than continental metabasalts and metagabbros. This difference is interpreted as being due to the metamorphism of oceanic rocks under conditions of low compressive stress dissimilar to those prevailing in continental orogenic regions. Nevertheless, we have found high anisotropy in some amphibolites dredged from the Vema fracture zone. An example is illustrated in Figure 14. Anisotropy in this specimen is clearly related to a strong orientation of hornblende, the maximum velocity being in the propagation direction parallel to a strong concentration of hornblende *c* axes. This anisotropy may have important implications in interpreting composition in lower oceanic crustal regions that possess seismic anisotropy [*Christensen*, 1972*b*].

The ranges of velocity shown in Figures 11 and 12 for gabbro are much less than those found for basalts, metamorphics, and ultramafics. The small number of high velocities ($V_p \simeq 7.0$ km/s, $V_s \simeq 3.8$ km/s) is characteristic of relatively fresh samples; samples that have been altered by deuteric processes or later hydrothermal activity display lower velocities.

Wide ranges of velocity in the ultramafic rocks examined are due largely to different degrees of serpentinization. Pure serpentinites have relatively low velocities; velocities increase linearly and sharply, however, with increasing density and decreasing percentage of serpentine [*Birch*, 1961; *Christensen*, 1966*b*]. As was discussed by *Christensen* [1972*a*], relatively high values of Poisson's ratio are diagnostic properties of serpentinites.

Influence of mineralogy. The influence of mineralogy on velocities and Poisson's ratio for many common oceanic rocks can be conveniently expressed by two sets of triangular composition diagrams in which the apexes are augite, hornblende, and plagioclase (An_{50}) and olivine, enstatite, and serpentine, respectively (Figure 15). Velocities measured for reasonably pure and isotropic monomineralic aggregates at 1 kbar have been selected for the end members, and contours of equal velocity and Poisson's ratio have been calculated from the velocities for intermediate points. Figure 15*a* contains mineral assemblages typical of unaltered gabbro and amphibolite. On the basis of this diagram a gabbro containing 50% plagioclase and 50% augite would have values of V_p = 7.0 km/s, V_s = 3.8 km/s, and σ = 0.30 at confining pressures of 1 kbar, similar to measured properties of several gabbros from oceanic and continental regions. Unaltered basalts of similar mineralogy have lower velocities (Figures 11 and 12) because of their finer grain size and hence greater grain boundary porosity. Amphibolites, which typically contain approximately 30% plagioclase and 70% hornblende, have values of V_p = 6.8 km/s, V_s = 3.8 km/s, and σ = 0.28. These predicted velocities again agree well with measured velocities. The plagioclase compositions of amphibolites are usually somewhat more sodic than the composition selected for Figure 15*a*, and thus the velocities would be lowered by about 0.1 km/s and there would be little effect on Poisson's ratio. The influence of mineralogy on velocities and elastic constants for rocks containing olivine, enstatite,

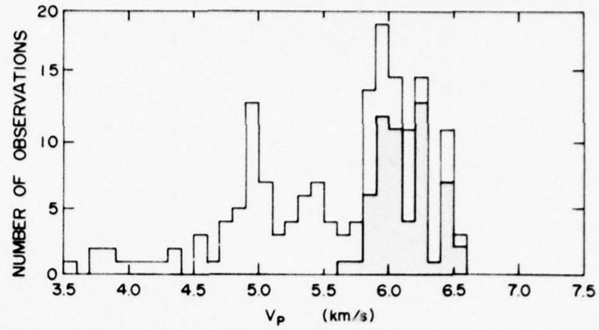

Fig. 13. Measured compressional wave velocities for oceanic basalts (from Figure 11) as a function of age. Shaded velocities are for samples from sites <20 m.y. old; the remaining sites range from 20 to 150 m.y. in age.

TABLE 7. Compressional Wave Velocity in Greenstones [*Christensen*, 1970*b*]

Sample	Density, g/cm^3	Velocity V_p, km/s 0.4 kbar	1.0 kbar	2.0 kbar	4.0 kbar	6.0 kbar
Metabasalt						
1 (Yreka, Calif.)*	2.88	6.74	6.78	6.82	6.86	6.89
	2.90	6.80	6.85	6.89	6.93	6.97
	2.94	6.83	6.90	6.99	7.08	7.12
Mean	2.91	6.79	6.84	6.90	6.96	6.99
2 (Luray, Va.)†	2.92	6.54	6.61	6.69	6.75	6.78
	2.94	6.54	6.60	6.66	6.72	6.77
	2.93	6.47	6.54	6.60	6.66	6.71
Mean	2.93	6.52	6.58	6.65	6.71	6.75
Epidosite (Luray, Va.)§	3.17	6.19	6.72	7.04	7.18	7.24
	3.17	6.40	6.78	7.03	7.15	7.22
	3.16	6.40	6.80	7.01	7.15	7.23
Mean	3.17	6.33	6.77	7.03	7.16	7.23

*Plagioclase, actinolite, clinozoisite, chlorite, and quartz.
†Albite, epidote, chlorite, actinolite, and magnetite.
§Epidote, quartz, albite, and actinolite.

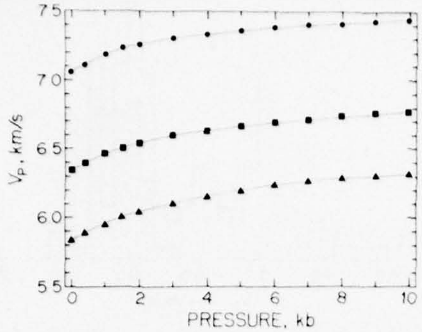

Fig. 14. Compressional wave velocities for three mutually perpendicular propagation directions in amphibolite from the Vema fracture zone.

and serpentine has been discussed in detail by *Christensen* [1966*b*]. Of significance here are the large changes in velocities and Poisson's ratio accompanying changes in serpentine content.

Velocity-density relations. Bulk densities, determined from the mass and dimensions of cylindrical samples, are almost universally reported in rock velocity studies. Relations between velocity and density are important because they allow estimates of crustal density to be made from seismic refraction velocities and, conversely, because rock densities can be used to predict elastic properties. The most frequently used velocity-density relation is that given by *Birch* [1961], in which for a given mean atomic weight the compressional wave velocity is assumed to be linearly related to density. Most samples from oceanic regions are mafic or ultramafic rocks that vary only slightly in mean atomic weight. Thus, to a first

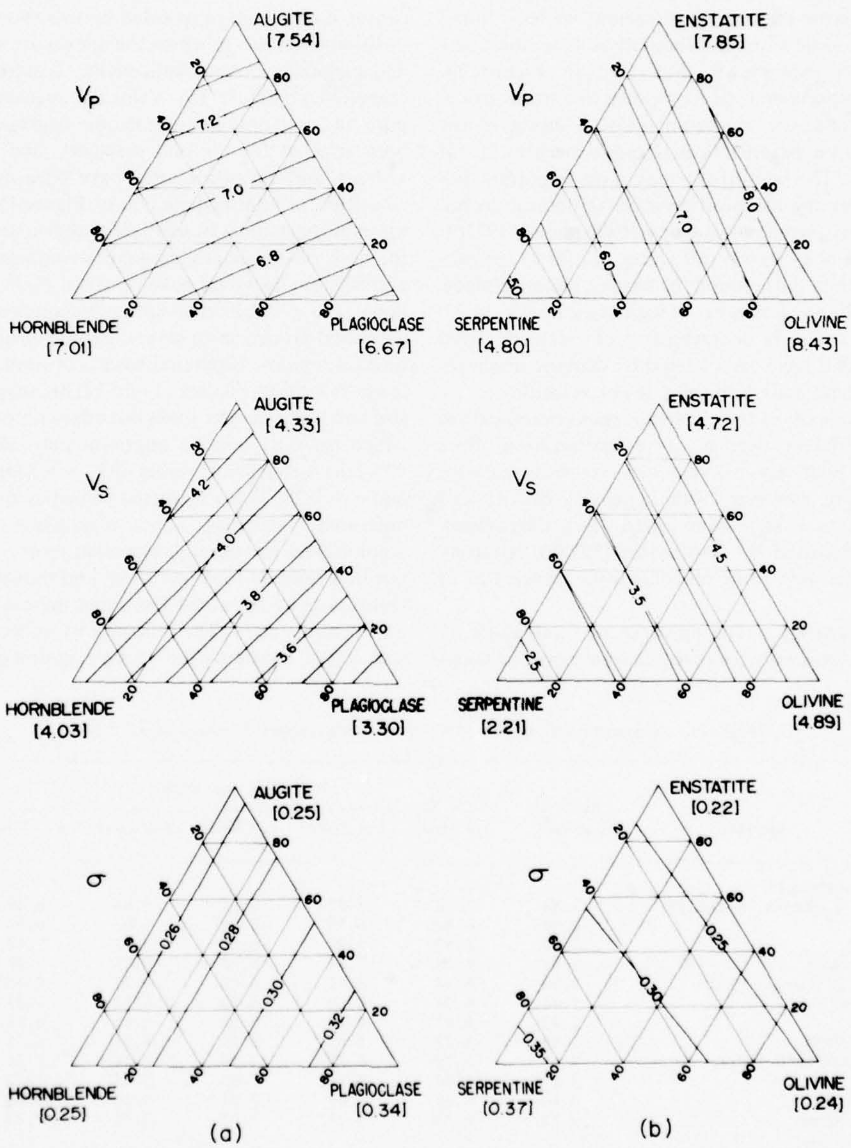

Fig. 15. Contours of constant compressional and shear wave velocity and Poisson's ratio σ at 1 kbar as a function of mineralogy in the ternary systems augite-hornblende-plagioclase and olivine-enstatite-serpentine, believed to represent lithologies common in the lower oceanic crust.

approximation, velocities of oceanic rocks should be linearly related to density. Similarly, estimates of density can be made from oceanic crustal velocities without knowledge of mean atomic weight. For this reason simple velocity-density relations are much more convenient than ones that require knowledge of rock chemistry.

In Table 8 the parameters of least squares solutions of the forms $V = a + b\rho$ and $\rho = c + dV$ are given for various groups of water-saturated oceanic rocks at pressures of 0.5 and 1.0 kbar. Owing to the lack of perfect linear correlation between velocity and density, the regression lines of V on ρ differ slightly from the regression lines of ρ on V, the latter usually having steeper slopes.

The best correlation between velocity and density is found for basalts obtained from the DSDP, as is illustrated in Figure 16. The relatively high velocities for the low-density basalts suggest that nonlinear solutions may be more appropriate than linear solutions. Thus, in Table 9, data are given in the form $V = a + b\rho^c$ for the various groups of rocks included in Table 8. The nonlinear solutions calculated for the DSDP basalts are also shown in Figure 16.

The correlation coefficients for the solutions in Table 8 that

TABLE 8. Regression Line Parameters

Solution	Pressure, kbar	n	a, km s^{-1}	b, km s^{-1}/g cm^{-3}	$S_{(V,\rho)}$, km s^{-1}	r	r^2, %
			$V_p = a + b\rho$				
DSDP basalts	0.5	77	-4.26	3.56	0.20	0.96	93
	1.0	77	-4.10	3.52	0.20	0.97	93
All basalts except vesicular rocks	0.5	131	-4.44	3.64	0.21	0.95	91
	1.0	131	-4.44	3.67	0.21	0.95	91
All metamorphics except serpentinites	0.5	50	-3.61	3.48	0.32	0.76	58
	1.0	50	-2.79	3.22	0.31	0.74	55
All rocks except serpentinites and vesicular basalts	0.5	215	-5.06	3.91	0.32	0.90	81
	1.0	215	-4.92	3.89	0.31	0.90	81
All rocks	0.5	286	-1.34	2.60	0.42	0.83	68
	1.0	386	-1.18	2.57	0.41	0.83	68
			$V_s = a + b\rho$				
DSDP basalts	0.5	75	-3.07	2.17	0.17	0.94	89
	1.0	75	-2.79	2.08	0.15	0.94	89
All basalts except vesicular rocks	0.5	115	-3.11	2.20	0.17	0.93	86
	1.0	115	-3.07	2.21	0.17	0.93	87
All metamorphics except serpentinites	0.5	32	-3.59	2.47	0.19	0.80	64
	1.0	32	-2.89	2.25	0.18	0.78	61
All rocks except serpentinites and vesicular basalts	0.5	175	-3.66	2.43	0.23	0.89	79
	1.0	175	-3.50	2.39	0.22	0.89	80
All rocks	0.5	213	-3.36	2.32	0.25	0.88	77
	1.0	213	-3.22	2.29	0.24	0.88	77

Solution	Pressure, kbar	n	a, g cm^{-3}	b, g cm^{-3}/km s^{-1}	$S_{(\rho,V)}$, g cm^{-3}	r	r^2, %
			$\rho = a + bV_p$				
DSDP basalts	0.5	77	1.30	0.261	0.06	0.96	93
	1.0	77	1.27	0.265	0.05	0.97	93
All basalts except vesicular rocks	0.5	131	1.36	0.249	0.06	0.95	91
	1.0	131	1.35	0.247	0.06	0.95	91
All metamorphics except serpentinites	0.5	50	1.80	0.166	0.07	0.76	58
	1.0	50	1.76	0.170	0.07	0.74	55
All rocks except serpentinites and vesicular basalts	0.5	215	1.58	0.207	0.07	0.90	81
	1.0	215	1.58	0.210	0.07	0.90	81
All rocks	0.5	286	1.22	0.262	0.13	0.83	68
	1.0	286	1.17	0.266	0.13	0.83	68
			$\rho = a + bV_s$				
DSDP basalts	0.5	75	1.56	0.407	0.07	0.94	89
	1.0	75	1.49	0.428	0.07	0.94	89
All basalts except vesicular rocks	0.5	115	1.60	0.392	0.07	0.93	86
	1.0	115	1.57	0.393	0.07	0.93	87
All metamorphics except serpentinites	0.5	32	1.96	0.258	0.06	0.80	64
	1.0	32	1.92	0.269	0.06	0.78	61
All rocks except serpentinites and vesicular basalts	0.5	175	1.78	0.324	0.08	0.89	79
	1.0	175	1.73	0.334	0.08	0.89	80
All rocks	0.5	213	1.75	0.331	0.09	0.88	77
	1.0	213	1.72	0.337	0.09	0.88	77

n is number of data points; $S_{(V,\rho)}$, standard error of estimate of V on ρ; $S_{(\rho,V)}$, standard error of estimate of ρ on V; r, correlation coefficient; r^2, coefficient of determination.

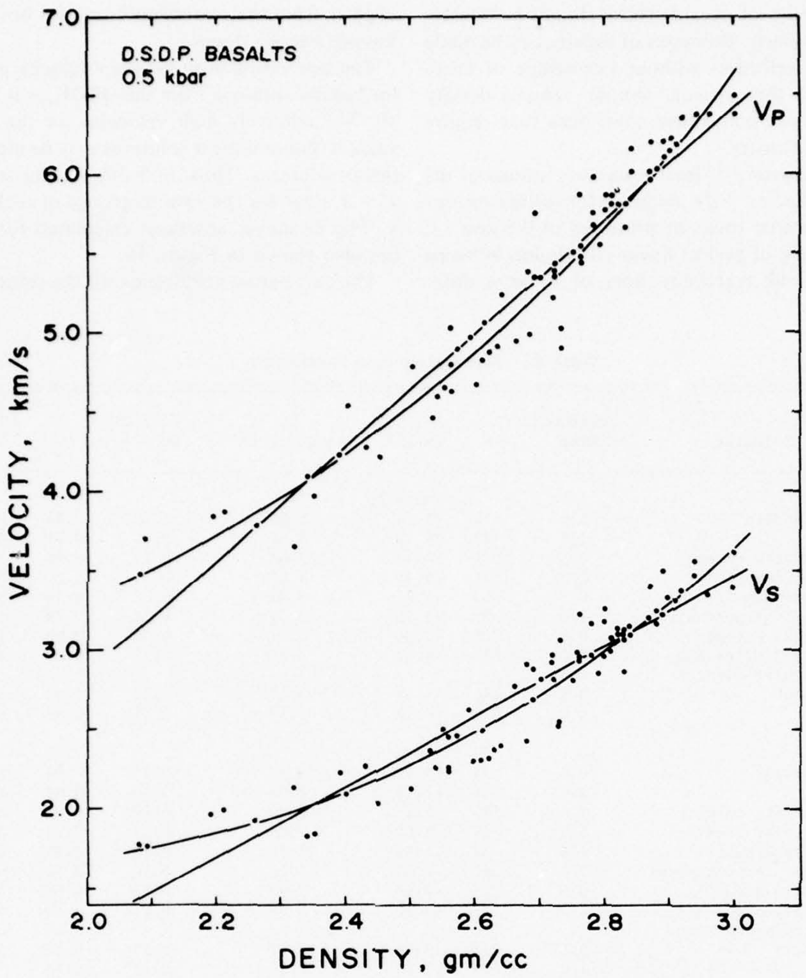

Fig. 16. Velocity-density relations for layer 2 basalts. Solutions are both linear and nonlinear.

include only metamorphic rocks are relatively low. This is interpreted as being primarily due to the presence of significant anisotropy in some of the metamorphic rocks examined.

For many of the solutions the slopes of the regression lines of V_p on ρ are between 3.5 and 3.9 km s^{-1}/g cm^{-3}. These are slightly higher than the solutions of *Birch* [1961] at 10 kbar for rocks of approximately constant mean atomic weight. Since the slopes of the regression lines of V_p on ρ commonly decrease with increasing pressure [*Christensen and Shaw*, 1970], higher slopes in Table 8 taken at 0.5 and 1.0 kbar are easily understood. An exception is noted in solution 5, in which the slope of the regression line for all rocks is only 2.6 km s^{-1}/g cm^{-3}. In Figure 17 the velocities for all rocks at 1 kbar are plotted as a function of density, together with the linear and nonlinear solutions of Tables 8 and 9 for all rocks except vesicular basalts and serpentinites. The 21 open circles with compressional wave velocities of approximately 5 km/s are measurements from relatively low bulk density high-velocity vesicular basalts from the Lau ridge. Shear velocities measured for two of these samples are shown as open circles with velocities of approximately 2.8 km/s. This figure suggests that basalt velocities are not significantly lowered by porosity arising from vesicularity (the energy follows a path of minimum travel time) and that, further, the anomalous slope of solution 5 (Table 8) is due to the relatively high velocities of vesicular basalts in relation to their bulk densities.

Velocities are also shown in Figure 17 for serpentinites and partially serpentinized ultramafics. Of importance is the fact that for a given density the compressional wave velocities for these rocks tend to be higher than velocities in gabbros, metagabbros, metabasalts, and nonvesicular basalts. Thus, as was observed earlier, the ratios of V_p to V_s and Poisson's ratio are relatively high for serpentine-bearing rocks.

The two samples in Figure 17 with the highest densities are ilmenite-rich norites dredged from the mid-Atlantic ridge. Although the presence of ilmenite in these rocks significantly increases density, compressional and shear velocities in these samples are similar to those of normal gabbros and norites. Since ilmenite-bearing norites have high mean atomic weights, these velocities are consistent with *Birch*'s [1961] observation that for rocks of the same density, velocities decrease with increasing mean atomic weight.

PETROLOGIC MODELS

A number of petrologic models have been proposed to explain the observed seismic structure of the oceanic crust. Most models assume that layer 2 consists of basalt that grades downward to low-grade metabasalt. The distributions and

TABLE 9. Nonlinear Solution Parameters

Solution	Pressure, kbar	No. of Data Points	a, km s^{-1}	b	c	Error Mean Square
		$V_p = a + b\rho^c$				
DSDP basalts	0.5	77	2.33	0.081	3.63	0.03
	1.0	77	2.37	0.085	3.57	0.03
All basalts except vesicular rocks	0.5	131	1.59	0.023	2.80	0.04
	1.0	131	1.50	0.027	2.70	0.04
All metamorphics except serpentinites	0.5	50	2.68	0.206	2.74	0.41
	1.0	50	2.93	0.165	2.73	0.43
All rocks except serpentinites and vesicular basalts	0.5	215	-0.58	1.050	1.77	0.10
	1.0	215	-0.95	1.268	1.65	0.10
All rocks	0.5	286	4.02	0.006	5.57	0.15
	1.0	286	4.10	0.007	5.49	0.14
		$V_s = a + b\rho^c$				
DSDP basalts	0.5	75	1.33	0.011	4.85	0.02
	1.0	75	1.43	0.011	4.84	0.02
All basalts except vesicular rocks	0.5	115	0.98	0.049	3.63	0.03
	1.0	115	1.11	0.040	3.79	0.03
All metamorphics except serpentinites	0.5	32	1.00	0.120	2.88	0.04
	1.0	32	1.22	0.120	2.81	0.04
All rocks except serpentinites and vesicular basalts	0.5	175	-0.09	0.311	2.27	0.05
	1.0	175	-0.02	0.319	2.24	0.05
All rocks	0.5	213	1.13	0.037	3.87	0.057
	1.0	213	1.25	0.031	3.98	0.054

relative abundances of the rock types believed to comprise the lower crust, however, are still highly debated. Having examined the seismic structure of the oceanic crust, as well as the petrology of samples recovered from the sea floor and the velocities through such samples, we are finally in a position to evaluate petrologic models of the lower crust.

Serpentinite Model

Noting the abundance of serpentinite at mid-ocean ridges and along the walls of trenches, *Hess* [1962], in a proposal that is still controversial, suggested that layer 3 is composed of serpentinized peridotite. According to Hess's model, partially serpentinized peridotite is generated by hydration of mantle peridotite along ridge crests at sites above the 500°C isotherm. Partially serpentinized peridotite, comprising layer 3, is carried laterally by sea floor spreading; the present Mohorovičić (M) discontinuity in this model represents a hydration boundary fossilized away from the ridge crests at lower temperatures of 150°–200°C. This model, later adopted by *Dietz* [1963], received considerable support when *Phillips et al.* [1969] observed that between 43°N and 43°30′N on the crest of the mid-Atlantic ridge there is an area of about 1500 km² in which dredging recovered serpentinized peridotite and no basalt. *Vine and Hess* [1971] suggested that within this region (which is in the vicinity of a major fracture zone and in which linear magnetic anomaly patterns are interrupted) layer 3 is directly exposed.

The first serious challenges to the concept of a partially serpentinized lower crust were presented by *Cann* [1968] and *Oxburgh and Turcotte* [1968]. *Cann* [1968] noted that (1) the supposed inverse thickness relationship between layers 2 and 3 over the mid-Atlantic ridge, observed by *Le Pichon et al.* [1965], suggests that the two layers are of similar composition, (2) the narrow range of velocities observed for layer 3 [*Raitt*, 1963] indicates a remarkably uniform degree of partial serpentinization, and (3) the absence of layer 3 over the mid-Atlantic ridge and its presence over the East Pacific rise imply that if layer 3 is composed of serpentinized peridotite, the 500°C isotherm should be within the crust under the mid-Atlantic ridge and at deeper levels under the East Pacific rise. This third point is contradicted, however, by the fact that heat flow values appear to be higher over the East Pacific rise. *Oxburgh and Turcotte* [1968], focusing on the nature of the crust-mantle transition, argued, in addition, that if the lower crust is partially serpentinized, one would expect a gradational boundary between the crust and underlying mantle. At that time, velocities in the range 7.1–7.7 km/s were not commonly

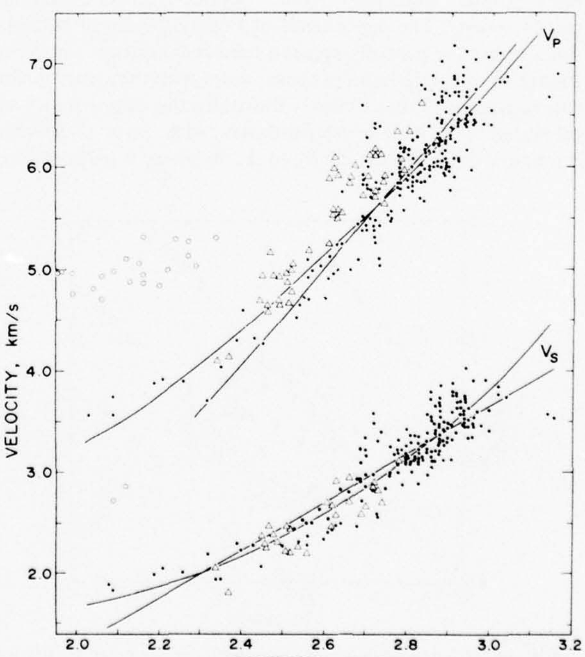

Fig. 17. Velocity-density relations for oceanic rocks at 1 kbar. Solutions are both linear and nonlinear. Open circles represent vesicular basalt; open triangles, serpentinized ultramafics.

observed in the lower oceanic crust, and it was assumed that the M discontinuity represented a sharp boundary between materials with velocities of 6.7 and 8.1 km/s. In view of these objections, Cann proposed that layer 3 is formed by metamorphism of basaltic crust to amphibolite, whereas Oxburgh and Turcotte supported the view that layer 3 is composed of gabbro or metabasite.

Le Pichon [1969] reviewed early ideas on lower crustal composition and concluded that there were no definitive arguments either for or against a serpentinite composition for layer 3. More recently, *Bottinga and Allegre* [1973], adopting a serpentinite crustal model, argued that Cann's objections to a serpentinized lower crust were erroneously based on the supposition of uniform velocities and thicknesses of layer 3 and a tenuous correlation between heat flow and layer 3 thickness. They emphasize that a considerable spread of seismic velocities is observed in the lower crust, and thus wide ranges are allowed in the degree of serpentinization. Also, because of the scatter in oceanic heat flow values, any relationship between heat flow and the thickness of layer 3 is questionable. An examination of Figures 1 and 2 shows that lower crustal velocities peak at 6.8 km/s, and it is thus suggested that peridotite of approximately 35% serpentine content may be abundant within the lower oceanic crust. However, the range of lower crustal compressional wave velocities is 6.4–7.7 km/s, which can be interpreted as evidence for variability in lower crustal serpentine content between approximately 50 and 10%. Thus uniform lower crustal velocities should not be regarded as sufficient reason for an easy rejection of a serpentinized lower crust.

The most damaging evidence against the serpentinized peridotite model for layer 3 is reported by *Christensen* [1972*a*], who shows that the ratios of V_p to V_s, and hence Poisson's ratios for partially serpentinized peridotites, are much higher than those observed from oceanic crustal seismic measurements. The dependence of Poisson's ratio on serpentine content for partially serpentinized peridotites is shown in Figure 15; a comparison of these values with the seismic data summarized in Table 1 clearly illustrates the inconsistency of measured velocities in serpentinites with layer 3 seismic refraction data. Ratios of V_p to V_s in many basaltic rocks,

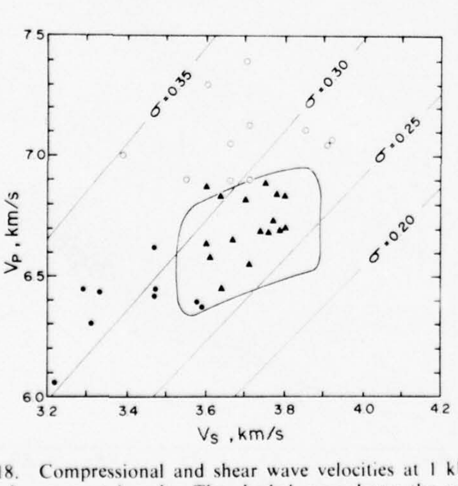

Fig. 18. Compressional and shear wave velocities at 1 kbar for possible lower crustal rocks. The shaded area shows the range of refraction velocities tabulated in Table 1. Solid triangles represent metabasite; open circles, gabbro, norite, and anorthositic gabbro; solid circles, altered gabbro and metabasite.

however, agree well with seismic observations [*Christensen*, 1972*a*]; thus it is clear that the serpentine content of the lower oceanic crust must be limited to a small fraction, probably less than 10%.

Metabasite and Gabbro Models

In addition to *Cann* [1968] and *Oxburgh and Turcotte* [1968], a number of authors have suggested that the lower crust is composed principally of gabbro or metabasite. On the basis of petrologic arguments and laboratory measurements of seismic velocities in rocks, *Christensen* [1970*a*] presented a model for the oceanic crust in which layer 3 consists of the mineral assemblage plagioclase and hornblende, occurring as hornblende gabbro and amphibolite. *Miyashiro et al.* [1970*b*] proposed that layer 3 contains metabasalt, metagabbro, and serpentinites formed by hydration of peridotites, the latter having intruded into fracture zones.

Several early papers [*Ewing and Ewing*, 1959; *Gutenberg*, 1959; *Raitt*, 1963] concerned with the seismic structure of the oceanic crust favored a simple gabbro composition for the lower crust. More recently, *Fox et al.* [1973], on the basis of a comparison of layer 3 refraction velocities with laboratory measurements of compressional wave velocities through rock samples dredged from the North Atlantic, reached this same conclusion, noting that of the oceanic rock types considered, only gabbros have velocities generally compatible with those of layer 3 (6.7–6.9 km/s) at appropriate pressures. Since we find in this study, and in earlier studies [*Birch*, 1960, 1961; *Christensen*, 1965, 1970*b*], that velocities in metabasites are, in many instances, also compatible with those of layer 3, we suggest that the composition of the lower crust is, in all probability, considerably more complex.

The principal difficulty with using only compressional wave velocities in interpreting crustal composition is that since many mineral assemblages can produce similar velocities, solutions based on this approach are nonunique. This problem is illustrated in Figure 15 for the three-component systems hornblende-plagioclase-augite and olivine-enstatite-serpentine; lower crustal compressional wave velocities ranging from 6.4 to 7.7 km/s include every possible mineral assemblage in the hornblende-plagioclase-augite system. Thus if one considers only this mineral assemblage, lower crustal compressional wave velocities can be equated with hornblendite, pyroxenite, anorthosite, amphibolite, and gabbro. Restricting consideration to velocities within the range 6.7–7.0 km/s still permits a wide variety of possible mineral assemblages to occur within the lower oceanic crust.

If both compressional and shear wave velocities are considered, however, the compositional resolution of velocity studies can be significantly improved. Unfortunately, little attention has been given by seismologists to obtaining shear velocities for crustal layers. Owing to problems in identifying and interpreting converted secondary shear arrivals characteristic of marine refraction studies, observational shear wave velocity data are extremely limited (Table 1) and subject to relatively large uncertainties. Nonetheless, the importance of these measurements in understanding crustal composition [*Christensen*, 1972*a*] makes it desirable to use what data are available.

Laboratory measurements of compressional and shear wave velocities are now available for most rock types postulated to be major constituents of the lower oceanic crust (Figures 11 and 12). In Figure 18 it can be seen that fresh gabbros, norites,

and anorthositic gabbros generally have higher Poisson's ratios and compressional wave velocities than metabasalts and metagabbros. Figure 15*a*, as was discussed earlier, also shows the variations of velocities and Poisson's ratio with mineral composition for anorthosites, gabbros, and amphibolites. Although little is known about the effect of mineralogy on the elastic properties of greenschist facies rocks, it is clear from Figures 15*a* and 18 that the metamorphism of gabbro to amphibolite facies mineral assemblages lowers Poisson's ratio to values generally between 0.26 and 0.28.

Figure 18 also shows the range of lower crustal compressional and shear wave velocities tabulated in Table 1. Although certainly more observational and experimental data are desirable, the agreement of lower crustal velocities with laboratory measurements in metabasites is striking. It should be emphasized that observed velocities are not consistent with the elastic properties of fresh gabbro. It must be noted, however, that the shear wave velocities so far determined for layer 3 are for crustal regions with compressional wave velocities of 6.5–7.0 km/s, corresponding to the upper part of the lower crustal refractor. Thus gabbro or other rock types may well be abundant constituents below the metamorphics of the lower oceanic crust.

Ophiolites

The most sophisticated and detailed models of the oceanic crust are based on examination of a small number of mafic-ultramafic complexes, the ophiolites, thought by many to be segments of oceanic crust tectonically emplaced on land. Many of the ophiolites (e.g., those of the California coast ranges [*Bailey et al.*, 1970; *Page*, 1972], Costa Rica [*Dengo*, 1962], New Caledonia [*Avias*, 1967], the eastern Celebes [*Kundig*, 1956], northern India [*Gansser*, 1964], southeast Turkey [*Rigo de Righi and Cortesina*, 1964], and the Mediterranean region [*Steinmann*, 1926; *Vuagnat*, 1963; *Pamić*, 1971]) are so faulted, dispersed, and, in some instances, metamorphosed that their examination is unprofitable for purposes of crustal reconstruction. Others (e.g., the Betts cove, Mings bight, and Baie Verte complexes of central Newfoundland) are seemingly intact but inexplicably thin [*Dewey and Bird*, 1971; *Upadhyay et al.*, 1971; *Church and Stevens*, 1971].

A small number of ophiolite complexes (in particular, the Vourinos complex of northern Greece [*Brunn*, 1956; *Moores*, 1969], the Troodos complex of Cyprus [*Bear*, 1960; *Gass and Masson-Smith*, 1963; *Gass*, 1968; *Moores and Vine*, 1971; *Greenbaum*, 1972; *Vine et al.*, 1973; *Gass and Smewing*, 1973], the Semail complex of Oman [*Reinhardt*, 1969; *Allemann and Peters*, 1972], Papua [*Davies*, 1971], and the Bay of Islands complex of western Newfoundland [*Church and Stevens*, 1971; *Williams*, 1971; *Williams and Malpas*, 1972]) are intact, unmetamorphosed, and, in the last three instances, stratigraphically robust. Although they are subject to other interpretations, it has been suggested that the Troodos and Papuan complexes can be geophysically traced to the sea [*Gass and Masson-Smith*, 1963; *Davies*, 1971], a distinction shared only with the Macquarie Island ophiolite complex [*Varne et al.*, 1969; *Varne and Rubenach*, 1972], which is apparently being raised above sea level even at the present time.

The stratigraphic columns representing this select group of ophiolites are presented in Figure 19, along with Raitt's mean oceanic crust and the mean of each velocity model obtained from the sonobuoy data presented earlier in Figure 6. Lithologic, structural, textural, and metamorphic facies relationships observed in these complexes have been incorporated in Figure 19 to facilitate comparison with samples dredged and cored from the oceanic crust and to facilitate interpretation in terms of seismic structure. It should be noted that since these complexes are the subject of current study, their columns are subject to revision. For each ophiolite in Figure 19 the lower crustal refractor has been equated with diabase dikes when they are present in sufficient number. As was shown in the preceding section, the top of the refractor is most likely a boundary dependent on metamorphic grade. Thus the actual position of this boundary may be within the dike swarms.

Ultramafics of the ophiolite column. The ophiolites in Figure 19 are, in many respects, remarkably similar. The deepest level of each consists of a thick unit of ultramafic tectonite composed of harzburgite, dunite, and lherzolite lying in fault contact against country rock. Where the basal contact is exposed, the country rock generally is observed to have a metamorphic 'aureole' of garnet amphibolite in the vicinity of the fault. The uppermost levels of the ultramafics appear to be generally, although not invariably, cumulate in origin. This level exhibits a wide variety of ultramafic lithologies, dunite, harzburgite, and pyroxenite predominating. Cumulate or podiform chromitites are commonly associated with the dunites. Pyroxenites, abundant in the ophiolites only at this level and in the lower levels of the overlying gabbros, tend to be clinopyroxene rich (augite, chrome diopside), as are associated peridotites. The uppermost ultramafics are usually feldspathic peridotites or feldspathic dunites, signaling the first appearance of feldspar as a cumulus phase and the transition to the overlying gabbroic level.

The transition zone or 'Moho' between the ultramafics and the gabbros is often strongly layered with dunite, pyroxenite, anorthosite, feldspathic dunite, wehrlite, norite, and troctolite as the predominant lithologies.

Significantly, the transition zone is often quite abrupt (for example, in the Bay of Islands complex the change from olivine to calcic plagioclase as the predominant cumulus phase occurs in less than 100 m). Finally, the transition zone and the levels adjacent to it are commonly intruded by dikes and pegmatites of pyroxenite, anorthosite, and gabbro.

Gabbros. The thick gabbroic level above the ultramafics, commonly equated in whole or in part with layer 3 [*Gass*, 1968; *Dewey and Bird*, 1971; *Moores and Vine*, 1971], can best be described in terms of three major elements present in varying degree in the ophiolites of Figure 19: cumulate gabbros, massive gabbros, and gabbroic sheeted dikes.

Cumulate gabbros are found, and in many instances are predominant, in the lower levels of each complex shown in Figure 19. Near the Moho transition zone, pyroxenites, troctolites, and anorthosites are common, but upward the cumulate gabbros are for the most part noritic; near the top of the cumulates, gabbros with primary and, in some instances, cumulate hornblende are often encountered. Although layering, particularly in the lower levels, is often extremely well developed, individual layers cannot usually be traced laterally for more than a few hundred meters. The cumulate gabbros grade upward and/or laterally into massive gabbros. With the exception of Papua, where the gabbros are hornblende free, the massive gabbros are often extensively uralitized and saussuritized. In both the cumulate and noncumulate cases the differentiation in the gabbros is extensive: not only do the gabbros become increasingly silica rich upward but also the

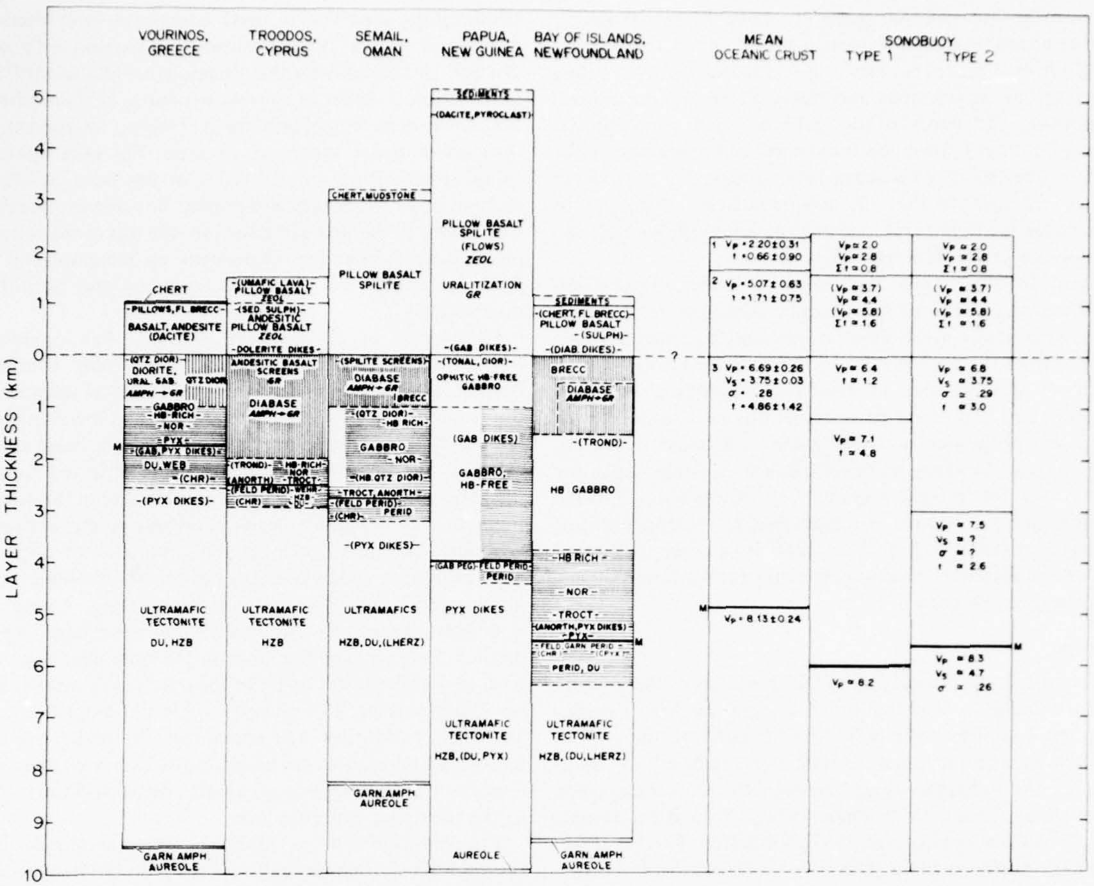

Fig. 19. Comparison of stratigraphic and petrologic field relations in major ophiolite complexes with the seismic structure of the oceanic crust as summarized by *Raitt* [1963] and interpreted from sonobuoy studies. Minor lithologies are in parentheses; lithologies of limited vertical range are between dashed lines; metamorphic facies terms are in italics. Vertical and horizontal striping represents sheeted dikes and cumulate layering, respectively.

petrologic extremes of mafic differentiation, namely, diorites, trondhjemites, and granophyres, are usually found as pods and intrusions at structurally high levels just below the sheeted dikes.

The last and most intriguing element of the gabbroic level is the sheeted dike complex found in the upper levels of four of the five ophiolites examined here. Many authors [*Bear*, 1960; *Gass and Masson-Smith*, 1963; *Moores and Vine*, 1971] consider that these complexes, consisting in the most well-developed instances entirely of narrow one-sided vertical dikes intruded one against the next with no country rock, could have been formed only in a tensional environment such as that thought to exist at ridge crests. This configuration is persuasive and nearly unique to the ophiolites but not ubiquitous among them, being absent, for example, in Papua and only poorly developed in Vourinos.

Viewed more closely, the sheeted dikes are quite complex. Their lower contact is characterized by mutually contradictory (i.e., synchronous) intrusive relations in which the sheeted dikes intrude and are intruded by the underlying massive and cumulate gabbros. In some instances (e.g., Troodos) highly metamorphosed vestiges of extrusive country rock are present as screens. The contact with the overlying extrusive unit is equally complex, being best described in a statistical sense as that point at which the dikes, diminishing in number upward, first constitute less than 50% of the unit. Also, at approximately this point in many complexes the remaining dikes continue upward as feeders for extrusives at higher levels and become more randomly oriented.

The dikes themselves are also internally complex. Many are brecciated [*Reinhardt*, 1969; *Williams and Malpas*, 1972] by a mechanism tentatively identified as gas fluidization. In addition, there appear to be several stages of dike intrusion. Finally, it should be noted that of the minerals originally present in the sheeted dikes, only altered plagioclase and minor relict pyroxene remain, the pyroxene having been partially or completely replaced by hornblende characteristic of the amphibolite facies or by fibrous actinolite of the greenschist facies [*Williams and Malpas*, 1972; *Varne and Rubenach*, 1972]. The metabasites of the sheeted dikes, and in some instances the massive gabbros below, often show evidence of having been pervasively uralitized and sausseritized, apparently through extensive hydrothermal metamorphism.

Extrusives. Overlying the gabbros in all the ophiolites examined is a unit of igneous extrusives composed of pillows, flows, and minor flow breccias of basaltic or andesitic composition. Greenschist facies spilites are common in the lower levels of particularly thick extrusive piles; high-level extrusives are generally in the zeolite facies. Sulphide mineralization is common and apparently associated with late-stage intrusive

activity. Ultramafic extrusives are reported but rare [*Gass and Masson-Smith*, 1963].

Sediments. Intercalated in and lying depositionally upon the extrusives are often found cherts of deep-sea origin, shales, and, in some instances, clastics from the continental margin. These represent the uppermost and final unit of the ophiolites.

Evaluation of the ophiolite hypothesis. Although the ophiolite model of oceanic crustal structure has been presented in some detail above, a question remains: what evidence is there both for and against the hypothesis that the ophiolites are segments of oceanic crust? In response to this question the following arguments can be presented in support of the hypothesis.

1. Cherts and shales forming an integral part of many of the ophiolites are clearly of deep-sea origin.

2. The presence of pillow structures in the extrusives demonstrates formation in a subaqueous environment. That these extrusives are frequently spilites suggests (but does not prove) that this environment was oceanic.

3. There is an excellent correspondence between lithologies obtained in dredge hauls at sea, described in the section on rocks from the lower oceanic crust, and those observed and described above for the ophiolites. This correspondence incorporates not only all major lithologies and metamorphic facies but also extends even to obscure lithologies such as plagioclase peridotite [*Ploshko and Bogdanov*, 1968; *Smith*, 1968], hydrogrossular peridotite [*Switzer et al.*, 1970; *Smith*, 1958], anorthosite, troctolite, and granophyre. As well as can be determined, there is also a rough correlation between the stratigraphic position of a given lithology in the ophiolites and its recovery interval in dredging [*Bonatti et al.*, 1970].

4. If seismic velocities are assigned to the ophiolites on the basis of the observed lithologies discussed above and the laboratory findings presented earlier, the velocity column of the ophiolites is found to be consistent with that of the oceanic crust as determined from seismic refraction studies. Specifically, the extrusives will range in compressional wave velocity V_p between 3.5 and 6.5 km/s (identical to the range of layer 2 velocities) and in shear wave velocity V_s between 1.8 and 3.6 km/s. The lowest velocities will be noted in extremely weathered or pillowed extrusives, the highest velocities in fresh basalts, and intermediate velocities in chlorite-rich greenschist facies metabasalts and moderately weathered or pillowed extrusives.

Velocities in the gabbroic unit will range, on the basis of laboratory studies, from 6.3 to 7.2 km/s for V_p and from 3.3 to 4.0 km/s for V_s, in good agreement with the observed range of velocities for layer 3. In the uppermost, or sheeted dike, level the compressional and shear wave velocities will be those of hornblende metagabbro, 6.8 and 3.8 km/s, respectively. Unmetamorphosed and cumulate gabbros found at intermediate levels will have compressional wave velocities of 7.0–7.2 km/s in the horizontal propagation direction and, in the case of cumulate gabbros, may have velocities as high as 7.4 km/s in the vertical direction owing to the statistical alignment of plagioclase [010] axes in the vertical direction during crystal settling. Since the [010] direction in plagioclase is fast [*Alexandrov and Ryzhova*, 1962; *Ryzhova*, 1964], cumulate gabbros are transversely isotropic, velocities being slow in the horizontal plane of refraction propagation. Although measured velocities in selected directions in cumulate gabbros may approach those of the basal layer of *Sutton et al.* [1969], it is apparent that the velocity of the basal layer cannot be explained in terms of this lithology. Only in the very mafic lower levels of the cumulates, in the vicinity of the gabbro-ultramafic transition zone, are lithologies encountered with compressional wave velocities comparable to those of the basal layer.

Since layer velocities are determined from energy propagating along the uppermost part of a layer, layer 3 velocities in ophiolites should correlate with sheeted dike metamorphic assemblages rather than with the underlying gabbro. It is thus significant that the compressional and shear wave velocities of these assemblages are in specific agreement with those of layer 3. It is also interesting to note that petrologic models equating layer 3 with gabbro on the basis of velocity are thus inconsistent with ophiolite models.

Finally, on the basis of velocity measurements through unserpentinized ultramafics reported elsewhere in the literature [*Birch*, 1960; *Christensen*, 1966*b*], the mantle level of the ophiolites will range in compressional wave velocity from 7.8 to 8.5 km/s, in good agreement with measured oceanic mantle velocities.

5. Internal structural relations in the ophiolites are consistent with formation at the ridge crests. Specifically, the presence of sheeted dikes and cumulates implies continuous creation of void space at a site of tensional spreading; the filling of this space with tholeiitic magma suggests that this site was in the ocean basins.

6. Finally, the high heat flow commonly observed at the ridge crest cannot be explained by thermal conductivity alone; as was demonstrated by *Bottinga* [1974] and *Lister* [1972], a large additional component of heat transfer must occur through water circulation to considerable depths in layer 3. An almost inevitable consequence of such circulation would be pervasive hydrothermal metamorphism comparable to the uralitization, sausseritization, and spilitization observed in the extrusives and upper gabbros of the ophiolites. Where water has been denied access to the lower oceanic crust, as perhaps it has in Papua, such metamorphism would be lacking or incomplete.

Although many features of the ophiolites can best be explained in terms of an oceanic crustal origin, a disconcerting number of features remain inconsistent with the ophiolite hypothesis.

1. Although seismic velocities measured for the ophiolite columns are consistent with those of the oceanic crust, thicknesses, for the most part, are not. Of the five ophiolites examined in Figure 19, only one, the Bay of Islands complex, has both an extrusive layer and a gabbroic layer with thicknesses falling simultaneously within one standard deviation of Raitt's mean thickness estimates for layers 2 and 3. Layer 3 thicknesses for most of the ophiolites, including such petrologically complete complexes as Troodos [*Gass and Masson-Smith*, 1963], Canyon Mountain [*Thayer*, 1963], Vourinos [*Moores*, 1969], Semail [*Reinhardt*, 1969], Mings bight, Baie Verte, and Betts cove [*Dewey and Bird*, 1971], are thin by factors ranging from 2 to 5.

In addition, in no ophiolite has a basal layer of reasonable thickness been found. Recently, *Moores and Jackson* [1974] have equated the basal layer of *Sutton et al.* [1971] to layered cumulates found in the lower sections of ophiolites. The lower-velocity basal layers ($V_p \simeq$ 7.1–7.2 km) are postulated to originate from the presence of olivine cumulate containing as much as 25% plagioclase and 25% pyroxene in the interstices,

and higher-velocity basal layers (~7.6 km/s) are presumably composed of olivine cumulate with less postcumulus material. Simple calculations based on mineral and rock velocities summarized by *Birch* [1960, 1961] and *Christensen* [1965] show that at 2 kbar a rock containing 50% olivine, 25% pyroxene, and 25% plagioclase (An_{80}) would have a compressional wave velocity between 7.8 and 8.0 km/s. Since velocities increase with decreasing pyroxene and plagioclase content, the rocks described by *Moores and Jackson* [1974] cannot be crustal constituents but, on the basis of velocity, belong within the upper mantle ($V_p \simeq 7.8$–8.5 km/s). Lithologies, however, that would produce acceptable basal layer velocities are olivine gabbro [*Christensen*, 1965], partially serpentinized peridotite [*Birch*, 1960, 1961; *Christensen*, 1966*b*], pyroxenites [*Birch*, 1960], and foliated amphibolites [*Christensen*, 1965].

2. Major parts of the extrusive levels of several of the ophiolites (for example, Vourinos and Troodos) are composed not of oceanic tholeiites but of andesitic basalts and andesites [*Moores*, 1969; *Moores and Vine*, 1971]. This composition has prompted *Miyashiro* [1973] to suggest that many of the ophiolites were formed not on the ridge crest but in an island arc environment.

3. Values of heat flow measured at the ridge crests are too low to be consistent with the existence of magma chambers in layer 3 of the size considered necessary to generate major cumulate complexes [*Bottinga and Allegre*, 1973].

4. Sediments interbedded with and immediately overlying the uppermost extrusives of a number of the ophiolites are not of deep-sea origin but are characteristic instead of the continental margin or island arc environment [*Dewey and Bird*, 1971].

5. In the case of at least two of the ophiolites (Troodos and the Bay of Islands) the orientation of the sheeted dikes is currently perpendicular, rather than parallel, to the trend of the ridge crests at which they are thought to have been formed [*Moores and Vine*, 1971; *Williams and Malpas*, 1972].

6. If the M discontinuity lies at a transition between cumulate gabbro and cumulate ultramafics, as it does in the ophiolites [*Moores and Vine*, 1971], mantle refraction velocities will be from cumulate ultramafic levels. This supposition is inconsistent with observed mantle anisotropy, since cumulate ultramafics are, for the most part, transversely isotropic [*Christensen and Crosson*, 1968].

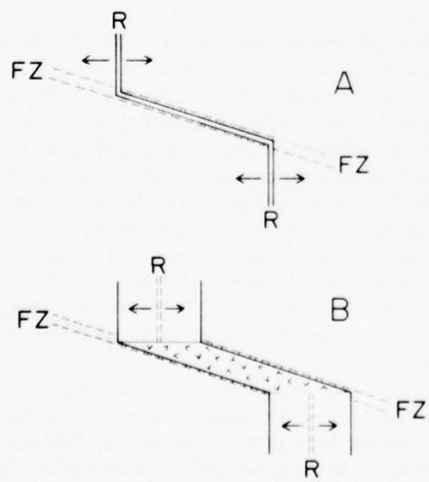

Fig. 20. Formation of new oceanic crust in leaky transform fault zones as a result of a change in the spreading direction [*van Andel et al.*, 1969].

The objections raised above do not argue against an oceanic origin for the ophiolites but emphasize that the ophiolites are not normal oceanic crust. Where, then, might they originate? Three sites answer, in part, this question and the objections raised above.

Marginal basins, leaky transform faults, and immature ridge crests. A number of authors [*Dewey and Bird*, 1971; *Upadhyay et al.*, 1971] have suggested that some ophiolites originated in marginal basins. Such an origin might well explain the andesitic nature of some ophiolite extrusives; rocks of this suite have been recovered, for example, from layer 2 in the Philippine Sea [*Karig*, 1972]. Such an origin is also consistent with the presence of volcano clastic sediments and tuffs typical of marginal basin deposits [*Ingle et al.*, 1973] immediately above some ophiolite extrusives. Still left unexplained, however, is the anomalously thin crust of the ophiolites.

Recent discussions of the composition of the oceanic crust have usually been based on the assumption that crust in the main ocean basins is generated almost entirely along a fairly narrow zone parallel to the ridge crests. Recently, *van Andel et al.* [1969] have proposed a model by which significant amounts of oceanic crust might be formed within fracture zones. This model, as developed for the Vema fracture zone, is illustrated in Figure 20. The initial stage of the opening of a fracture zone requires reorientation of plate movements; for the Vema fracture zone this change is from E10°S to E-W. Following this reorientation, progressive spreading produces an opening rift along the old fracture zone that acts as a site for the emplacement of new crust.

Thompson and Melson [1971] noted several additional fracture zones in the Atlantic in which crust might be forming by this same mechanism. They further attach significance to the alkaline character of many rocks emplaced within these faults, suggesting that oceanic crust formed along leaky transform faults may be different from that formed at ridge crests. In regard to the ophiolites, it may also be significant that the crust in fracture zones is commonly thin and that sheeted dikes formed in such an environment would be perpendicular to the regional trend of the ridge.

Since young crust at ridge crests is commonly thin but thickens with age to 40 m.y. (Figure 4), it follows that the ophiolites may be segments of immature oceanic crust, emplaced on land before reaching normal oceanic crustal thickness. This hypothesis can easily be tested by determining (Table 10) the difference between the time of formation and the time of emplacement for each ophiolite (i.e., the age at the time of emplacement). As can be seen, the ophiolites were invariably young when they were emplaced.

The youth of the ophiolites imposes a considerable restraint on possible mechanisms of emplacement. It is proposed that the most likely mechanism consistent with this phenomenon is the one shown in Figure 21. During the closure of any ocean basin through subduction of one or both of its limbs the ridge crest itself must at some point be subducted. This point is unique in that for the first and only time a thin hot mechanically weak segment of oceanic crust and upper mantle, laced with magma chambers, is presented to the subduction mechanism. That subduction of the ridge crest occurs without incident is unlikely. It is anticipated, rather, that the ridge crest will be dismembered by faulting, major segments, particularly from

TABLE 10. Time Relationships in Some Major Ophiolite Complexes

Location	Time of Formation	Time of Emplacement	Age at Time of Emplacement, m.y.	Reference
Troodos, Cyprus	Lower Campanian	Lower Campanian	<5	*Gass* [1968], *Moores and Vine* [1971], *Vine et al.* [1973]
Vourinos, Greece	Neocomian-Tithonian	Pre-Cenomanian	<35	*Moores* [1974]
Semail, Oman	Cenomanian-Turonian	Lower to middle Maaestrictian	20-30	*Allemann and Peters* [1972]
Papua, New Guinea	Upper Cretaceous	Upper Eocene or Oligocene	35-55	*Davies* [1971]
Bay of Islands, Newfoundland	Arenigian	Middle Ordovician	25	*Williams* [1971]
Macquarie Island, Macquarie ridge	Early to middle Miocene	Present	<20	*Varne and Rubenach* [1972]
Trinity, Calif.	Lower Ordovician	Upper Ordovician	20	*Hopson and Mattinson* [1973]

the upper levels of the outboard plate, being obducted onto the continental margin while the inboard plate is depressed under the approaching continental plate and subducted. Besides being young and thin, ophiolites formed in such a manner would also be expected to (1) have a minimal cover of sediments of pelagic origin, the overlying sediments being composed instead of trench or continental margin deposits, (2) display, at least in some instances, evidence that their upper levels were still partially molten during emplacement, (3) have metamorphic aureoles at their bases, and (4) thin toward the continental block. All these features have, in fact, been observed. Still unexplained, however, is the andesitic composition of the extrusives. In some ophiolites this would no longer pose a problem if the spreading ridge were in a marginal basin.

Finally, it should be noted that if ophiolites are from the ridge crest province, comparison of ophiolite lithologies with those dredged from the fracture zones may be valid, but neither suite is from normal oceanic crust in that both sites are young. It follows that ultramafic tectonites may be from the anomalous mantle; whether they were tectonized during emplacement or not, their fabrics may not be representative of the fabric of the normal oceanic mantle.

SUMMARY AND CONCLUSIONS

Within the framework of Raitt's synthesis of the mean seismic structure of the oceanic crust, patterns of refraction data suggesting regional and local structural differences, seismic anisotropy at intermediate crustal levels, and evolution of seismic structure with age are beginning to emerge.

In a 15-m.y.-wide band to either side of the ridge crest, more than 50% of the sites examined by refraction techniques are floored by anomalous mantle ranging in velocity V_p between 7.2 and 7.8 km/s; layer 3 at these sites is either absent or, if present, thin but of normal velocity (6.8 km/s), whereas layer 2 is somewhat thickened at sites in which layer 3 is missing. The observation of high heat flow and the attenuation of shear waves observed at the ridge crests imply the existence of high-temperature intrusions, and it is thus suggested that the thickening of layer 2 at those sites in which layer 3 is absent may be due to thermal depression of velocities in layer 3 material. At ridge crest sites displaying normal mantle velocities, layer 2 is usually normal, and layer 3 is again thin. Mantle anisotropy appears to be absent to weakly developed [*Whitmarsh*, 1971].

Beyond 15 m.y., sites with anomalous mantle velocities are rare, but mantle anisotropy becomes pronounced, V_p becoming fast ($\simeq$8.3 km/s) perpendicular to the ridge crest and slow ($\simeq$8.0 km/s) parallel to the ridge crest. Layer 3 thickens rapidly away from the ridge crest, reaching a full thickness of approximately 5 km at 40 m.y. Unexpectedly, layer 3 velocities change slowly with age. Velocities of 6.8 km/s, characteristic of layer 3 at the ridge crest, are virtually absent in crust over 80

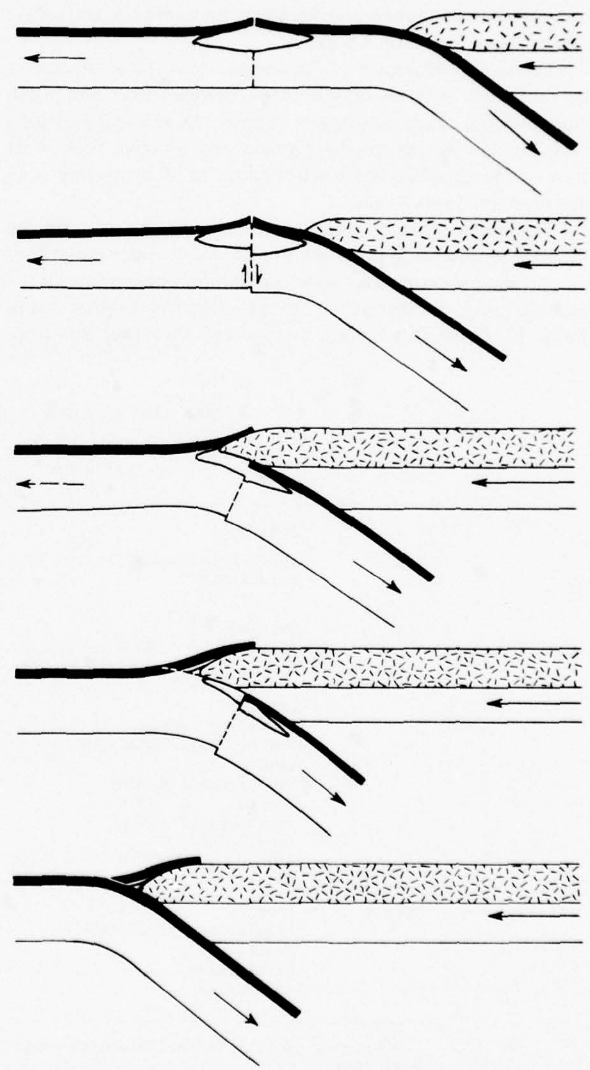

Fig. 21. Ophiolite emplacement during subduction of a ridge crest.

m.y. old, being replaced by a bimodal distribution of velocities with peaks at 6.5 and 7.0 km/s. Also unexpectedly, layer 3 is statistically anisotropic, being slightly faster parallel to the ridge crest than it is perpendicular to the ridge crest.

Differences in seismic structure associated with tectonic province are difficult to delineate at this time owing to poor statistics. Nonetheless, a number of gross features can be outlined. (1) The crust of fracture zones appears to be conventionally three layered but thin; layer 2 velocities are invariably low, presumably owing to brecciation. (2) The crust of offridge rises, back arc rises, and linear island chains is anomalously thick; in the first two instances this excess is distributed within a conventional three-layer structure; in the third, layer 2 is multilayered and two to three times normal thickness, whereas layer 3 is normal in thickness but depressed in velocity. The crust of trenches, troughs, and back arc basins is distinguished only by exceptionally thick sediments.

Finally, the oceanic crust may be divided locally, though not invariably, into at least two structural types based on layer 3 subdivisions detected through sonobuoy studies: type 1, in which layer 3 consists of a thin 6.4-km/s upper level underlain by a thick 7.1-km/s level, and type 2, in which layer 3 consists of two subdivisions of equal thickness, an upper 6.8-km/s level and a 'basal layer' of 7.5 km/s.

The velocity structure of the oceanic crust must ultimately be explained in terms of lithologies dredged from the ocean floor. Within these lithologies (Table 11) are metamorphic rocks of low to intermediate grade and igneous rocks that show evidence of crystal fractionation. In all cases the rocks are predominantly mafic.

Laboratory velocity measurements conducted on dredge samples representing these lithologies show, under conditions of confining pressure and water saturation appropriate to the oceanic crust, the distinctive velocity patterns summarized in Table 12. From this table it is apparent that layer 2 is composed of basalt and probably chlorite-rich metabasite of either basaltic or gabbroic origin. Of the three petrologic models currently proposed in the literature for layer 3 (namely, that layer 3 is composed of either partially serpentinized ultramafics, gabbro, or metabasite), two may be dismissed upon consideration of laboratory and refraction velocity measurements. Compressional and shear wave velocities in partially serpentinized ultramafics are, for the most part, much lower than velocities observed for layer 3; those samples with comparable compressional wave velocities are still incompatible in V_s and σ. Shear wave velocities in normal gabbro (3.8 km/s) are similar to those of layer 3 ($\simeq$3.75 km/s), but measured compressional wave velocities from unmetamorphosed samples (7.0 km/s) are too high. Of the common oceanic lithologies, only hornblende-rich metabasites seem to have values of V_p and V_s that are both consistent with those of layer 3. A model of layer 3 composition based on this lithology alone, however, is incomplete in view of the presence of unmetamorphosed gabbros among the recovered lithologies listed in Table 11. It is thus proposed that hornblende metagabbros predominate in the upper levels of layer 3 sampled by refraction but that unmetamorphosed gabbros predominate at deeper levels.

This relationship is implied in Table 11, which is itself a petrologic model of the oceanic crust constructed simply by listing observed dredged lithologies according to the following premises. (1) Extrusives (and sediments) overlie intrusives. (2) Metamorphic grade increases with depth. (3) In high-temperature facies exhibiting differentiation and cumulate textures the lithologic order is determined by the crystallization order. This model incorporates dredged lithologies into an internally consistent petrologic framework that is, at the same time, consistent with observed refraction and laboratory measurements of seismic velocity. By leaving this model unscaled, the wide range in seismic structure observed in the

TABLE 11. Lithologies Reported From the Sea Floor

Layer	Lithology	
1	Sediments	
2	Tholeiitic basalt (weathered to fresh)	
	Metabasalt*	metabasites
3	Metagabbro+	metabasites
	Amphibolite (schistose and nonschistose)	metabasites
	Aplite	
	Quartz diorite	
	Diorite	
	Nepheline gabbro	
	Primary hornblende gabbro	
	Gabbro	
	Two-pyroxene gabbro	some with cumulate textures
	Norite	some with cumulate textures
	Anorthositic gabbro	some with cumulate textures
	Anorthosite	some with cumulate textures
	Olivine gabbro	some with cumulate textures
	Troctolite	some with cumulate textures
Mantle	Picrite	some with cumulate textures
	Plagioclase peridotite	
	Dunite	as serpentinites, partially serpentinized peridotites
	Harzburgite	as serpentinites, partially serpentinized peridotites
	Lherzolite	as serpentinites, partially serpentinized peridotites

*Includes zeolite facies, prehnite-pumpellyite facies (rare), and greenschist facies (spilite).
+Includes greenschist facies and amphibolite facies.

TABLE 12. Summary of Laboratory Velocity Measurements on Oceanic Rocks (1 kbar)

Lithology	V_p, km/s Range	V_p, km/s Average	V_s, km/s Range	V_s, km/s Average
Basalts (weathered to fresh)	3.7-6.5	5.5	1.8-3.6	2.9
Metabasites				
Chlorite rich	5.2-6.3	5.9	2.8-3.5	3.2
Amphibole rich	6.4-7.2	6.8	3.6-4.1	3.8
Gabbro (fresh, unmetamorphosed)	6.9-7.2	7.0	3.6-3.9	3.8
Ultramafics (serpentinized)	4.1-6.6	5.5	1.8-3.3	2.6

oceanic crust can be attributed to variation in thickness at any level, together with vertical displacements of metamorphic facies boundaries. It is interesting to note that a strong but discontinuous velocity inversion can be predicted in layer 3 wherever low-velocity late differentiates underlie amphibole-rich metabasites and in layer 2 wherever chlorite-rich metabasalts are overlain by fresh unpillowed basalts.

Although this model is consistent with structural and

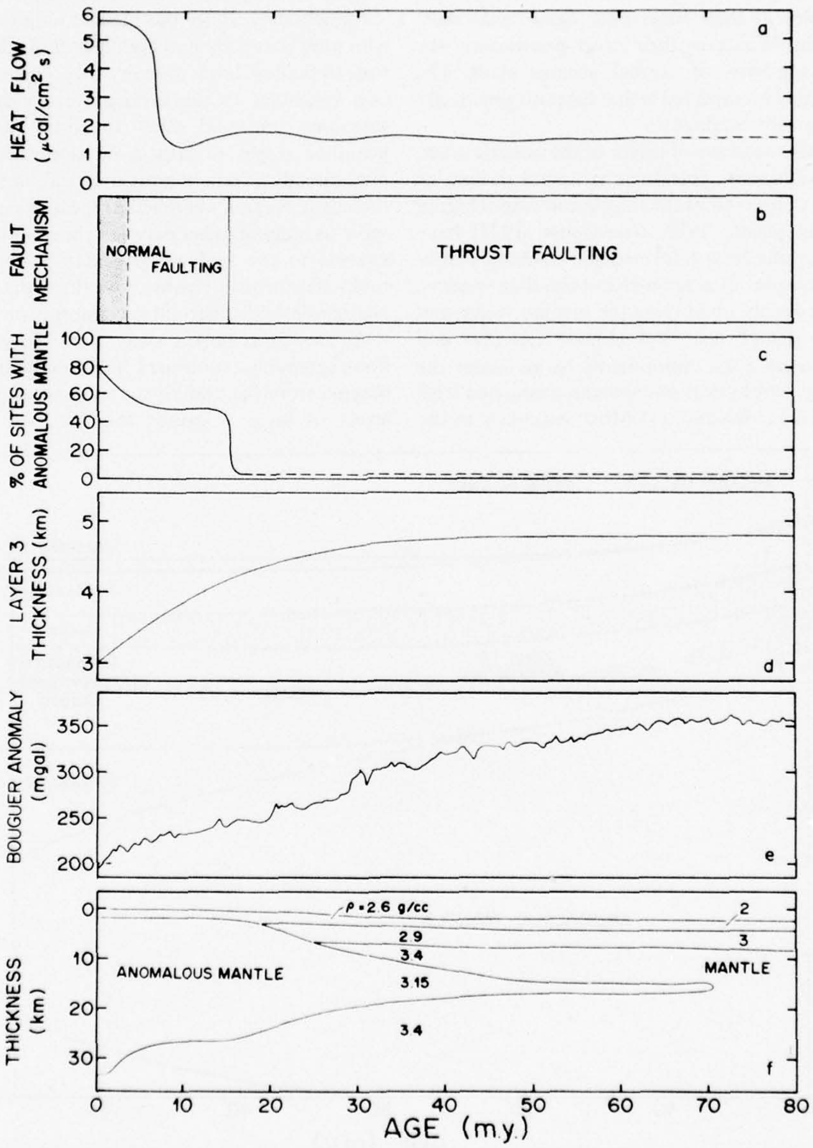

Fig. 22. Geophysical relations at the ridge as a function of sea floor age. The heat flow curve in (*a*) represents the 75% line of *Lee and Uyeda* [1965] for the Atlantic. Fault mechanisms in (*b*) are from *Sykes and Sbar* [1973]; the zone of high seismicity associated with the median valley is indicated by shading. The Bouguer anomaly (*e*) and its interpretation (*f*) are from *Talwani et al.* [1965] for the mid-Atlantic ridge.

petrologic relations in the ophiolites, such support must be embraced with caution. There remains little doubt that the ophiolites derive from the oceanic crust; nonetheless, considerable uncertainty remains concerning the provenance of the ophiolites within the ocean basins themselves. The presence of andesitic basalts and continental clastics in the upper levels of a number of the ophiolites suggests a back-arc basin origin. Alternatively, formation in leaky transform fault zones might explain the presence in many of the ophiolites of an anomalously thin layer 3 and of sheeted dikes perpendicular to the trend of the ridge crests at which they are thought to have been formed. The least restricted, and to us the most attractive, provenance suggested is that the ophiolites are segments of immature ridge crest obducted onto the continental margin during closure of an ocean basin. Such an origin is consistent with the observed youth of the ophiolites at the time of emplacement, the observation that many have metamorphic aureoles at their base, and, again, that most are anomalously thin. Whatever their exact provenance, the ophiolites are not segments of normal oceanic crust. The best that can reasonably be expected is that they are genetically related and petrologically analogous.

In order to consider the mode of origin of the oceanic crust, it is necessary to examine its petrologic structure in light of geophysical relations observed at the mid-ocean ridge (Figure 22). Several authors [*Cann*, 1970; *Greenbaum*, 1972] have suggested that the oceanic crust is formed and essentially completed in a narrow complex of magma chambers, dike swarms, and extrusives immediately underlying the median valley and its associated zone of high heat flow (Figure 22*a* [*Lee and Uyeda*, 1965]). Although crust undoubtedly forms under the median valley, many geophysical phenomena associated with the ridge crest persist far beyond. (1) Most seismicity in the vicinity of the median valley occurs as normal faulting [*Isacks et al.*, 1968], but the seismicity of this mechanism actually continues to approximately 15 m.y., beyond which thrust mechanisms predominate (Figure 22*b* [*Sykes and Sbar*, 1973]). (2) Anomalous mantle velocities are common to 15 m.y. (Figure 22*c*). (3) Layer 3 continues to increase in thickness and volume for 40 m.y. (Figure 22*d*). (4) A strong Bouguer gravity anomaly associated with the presence of the anomalous mantle (masked below the normal mantle beyond 15 m.y.) persists to 70 m.y. (Figures 22*e* and 22*f* [*Talwani et al.*, 1965]).

From these observations it is clear that the formation of oceanic crust is not confined to a narrow vertical zone underlying the ridge median valley. We propose instead that layer 2 and the upper levels of layer 3 form largely under the median valley and that the lower levels of layer 3 thicken under the ridge flanks by offridge intrusion fed from the thinning anomalous mantle in the manner illustrated in Figure 23.

Immediately under the median valley, in a belt coincident with high seismicity and high heat flow, the anomalous mantle rises to shallow levels at many sites, and a liquid tholeiitic fraction continues to the surface via a swarm of continuously spreading tensional dikes to form basaltic extrusives. In primitive stages of crustal development, basaltic extrusives may directly overlie mantle material; in most instances, small turbulent magma chambers, repeatedly invaded from below, serve as staging areas between the mantle and overlying dike swarms to the surface. Seawater, superheated against dike rocks after invasion from above through tension cracks, causes retrograde hydrothermal metamorphism at higher levels.

As this crust moves away from the median valley by sea floor spreading, continued but now intermittent intrusion of magma from the underlying anomalous mantle into the lower levels of layer 3 causes this layer to increase rapidly in

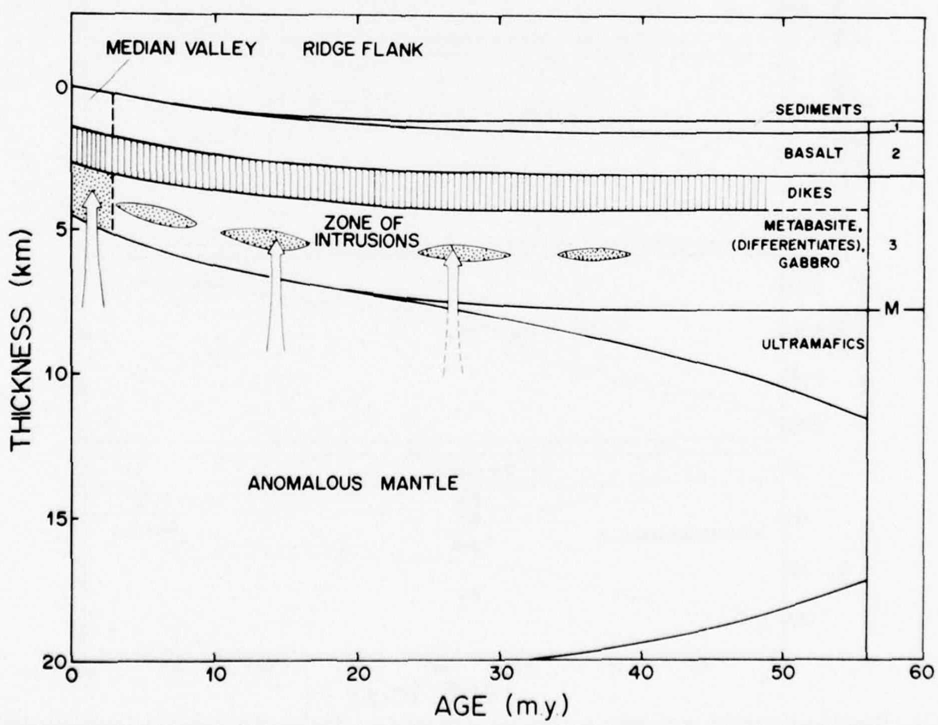

Fig. 23. Generation and evolution of the oceanic crust. The upper levels of the crust are formed largely under the median valley, but layer 3 continues to thicken for nearly 40 m.y. by intermittent offridge intrusion from the anomalous mantle.

thickness. At first, cooling is retarded, and a dense patchwork of cumulate magma chambers, many floored by the anomalous mantle, is maintained. Injection occurs primarily at magmatic levels, and cyclic layering in crystallizing cumulate phases results. Many chambers connect to surface volcanic edifices through late-stage dikes or pipes.

By 15 m.y. the crust is floored, at shallow levels, by a normal mantle composed of cumulate ultramafics and cooled anomalous mantle. Although a change in fault plane solutions at this time suggests that the base of the crust is now locally coupled to mantle convection, gravity anomalies indicate that numerous patches of anomalous mantle still persist at shallow levels in the mantle.

Offridge intrusion, cutting now through the M discontinuity into the lower levels of layer 3, continues to thicken layer 3 at a decelerating pace to 40 m.y., accompanied by minor offridge volcanism and continuous crystallization in the remaining magma chambers, to form massive and cumulate gabbros and, finally, late differentiates. As the crust continues to cool, the final stages of intrusion will be small cross-cutting dikes and apophyses, many with chilled margins, introduced at any level.

Beyond 40 m.y. the lowering of isotherms by continued cooling will introduce retrograde metamorphism to deeper levels. The upper levels of layer 3, becoming chlorite rich, will lower in velocity from 6.8 to approximately 6.5 km/s, as is shown in Figure 3; deeper levels in the gabbro will convert to amphibolite along avenues of water penetration. Should water eventually penetrate to the upper mantle, partial serpentinization would seem inevitable. It should be noted in this regard that the high-velocity basal layer of *Sutton et al.* [1971] has been detected to date only in old crust or in the vicinity of fracture zones.

In the model presented above, we have attempted to explain geophysical observations of the oceanic crust in terms of a petrologic model consistent with information on rocks obtained from dredging. The crustal model adopted was founded in its general form by simple consideration of the rocks reported from oceanic regions, but to obtain information on the relative abundances of these rocks at various levels within the crust, it was necessary to review experimental work bearing on the velocities of compressional and shear waves in oceanic rocks and to compare these velocities with oceanic seismic structure. Within the framework of the model thus obtained, ophiolites represent immature ridge crest that has been obducted at an early stage of crustal evolution onto continental margins, their variability reflecting the complex, almost chaotic, tectonic and intrusive relations at centers of spreading. Thus old crustal segments will rarely be observed on land; their detailed study must await the results of deep-ocean drilling.

Acknowledgments. We are indebted to Tj. H. van Andel, E. Bonatti, R. L. Fisher, J. Hawkins, C. R. B. Lister, and G. Thompson for providing many of the dredge samples used for the experimental studies. Rocks from the Deep-Sea Drilling Project were provided through the assistance of the National Science Foundation. H. Williams gave many helpful suggestions for collecting samples from the Newfoundland ophiolites. In addition, we wish to thank R. McConaghy, M. Mulcahey, P. Lage, G. H. Shaw, R. Ramananantoandro, K. V. Campbell, D. Fountain, R. Carlson, M. Brown, P. Hoddinott, M. Stroh, and J. L. Vance for providing valuable technical support over the past five years for experimental and, in several instances, field phases of this study. Financial support was provided by the Office of Naval Research (contract N-00014-67-A-0103-0014), the National Science Foundation (grant GA-36138), and the Geological Society of America (grant 1680-73).

REFERENCES

Alexandrov, K. S., and T. V. Ryzhova, Elastic properties of rock-forming minerals, 3, Feldspars, *Bull. Acad. Sci. USSR, Geophys. Ser.*, Engl. Transl., no. 2, 129–131, 1962.

Allemann, F., and T. Peters, The ophiolite-radiolarite belt of the North-Oman Mountains, *Eclogae. Geol. Helv.*, *65*, 657–697, 1972.

Aumento, F., Magmatic evolution on the mid-Atlantic ridge, *Earth Planet. Sci. Lett.*, *2*, 225–230, 1967.

Aumento, F., The mid-Atlantic ridge near 45°N, 2, Basalts from the area of Confederation Peak, *Can. J. Earth Sci.*, *5*, 1–21, 1968.

Aumento, F., Diorites from the mid-Atlantic ridge at 45°N, *Science*, *165*, 1112–1113, 1969.

Aumento, F., and B. D. Loncarevic, The mid-Atlantic ridge near 45°N, 3, Bald Mountain, *Can. J. Earth Sci.*, *6*, 11–23, 1969.

Aumento, F., and H. Loubat, The mid-Atlantic ridge near 45°N, 16, Serpentinized ultramafic intrusions, *Can. J. Earth Sci.*, *8*, 631–663, 1971.

Avias, J., Overthrust structure of the main ultrabasic New Caledonian massives, *Tectonophysics*, *4*, 531–541, 1967.

Bailey, E. H., M. C. Blake, Jr., and D. L. Jones, On-land Mesozoic oceanic crust in California coast ranges, *U.S. Geol. Surv. Prof. Pap.*, *700-C*, C70–C81, 1970.

Barrett, D. L., and F. Aumento, The mid-Atlantic ridge near 45°N, 11, Seismic velocity, density and layering of the crust, *Can. J. Earth Sci.*, *70*, 1117–1124, 1970.

Bear, L. M., The geology and mineral resources of the Akaki-Lythrodondhe area, *Mem. Geol. Surv. Dep. Cyprus*, *3*, 1–122, 1960.

Birch, F., The velocity of compressional waves in rocks to 10 kbar, 1, *J. Geophys. Res.*, *65*, 1083–1102, 1960.

Birch, F., The velocity of compressional waves in rocks to 10 kbar, 2, *J. Geophys. Res.*, *66*, 2199–2224, 1961.

Bogdanov, Y. A., and V. V. Ploshko, Magmatic and metamorphic rocks of the Romanche trench, *Dokl. Akad. Nauk. SSSR*, *177*, 909–912, 1967.

Bonatti, E., Ultramafic rocks from the mid-Atlantic ridge, *Nature*, *219*, 363–364, 1968.

Bonatti, E., J. Honnorez, and G. Ferrara, Equatorial mid-Atlantic ridge: Petrologic and Sr isotopic evidence for an alpine type rock assemblage, *Earth Planet. Sci. Lett.*, *9*, 247–256, 1970.

Bosshard, E., and D. J. MacFarlane, Crustal structure of the western Canary Islands from seismic refraction and gravity data, *J. Geophys. Res.*, *75*, 4901–4918, 1970.

Bottinga, Y., Thermal aspects of sea-floor spreading, and the nature of the suboceanic lithosphere, *Tectonophysics*, *21*, 15–38, 1974.

Bottinga, Y., and C. J. Allegre, Thermal aspects of sea-floor spreading and the nature of the oceanic crust, *Tectonophysics*, *18*, 1–17, 1973.

Bowin, C. O., A. J. Nalwalk, and J. B. Hersey, Serpentinized peridotite from the north wall of the Puerto Rico trench, *Geol. Soc. Amer. Bull.*, *77*, 257–270, 1966.

Brace, W. F., Resistivity of saturated crustal rocks to 40 km based on laboratory studies, in *The Structure and Physical Properties of the Earth's Crust, Geophys. Monogr. Ser.*, vol. 14, edited by J. G. Hancock, pp. 243–256, AGU, Washington, D. C., 1971.

Brunn, J. H., Contribution à l'étude géologique du Pinde septentrional et d'une partie de la Macedonie occidentale, *Ann. Geol. Pays Hellen.*, *7*, 1–358, 1956.

Bunce, E. T., and D. A. Fahlquist, Geophysical investigation of the Puerto Rico trench and outer ridge, *J. Geophys. Res.*, *67*, 3955–3972, 1962.

Bunce, E. T., D. A. Fahlquist, and J. W. Clough, Seismic refraction and reflection measurements—Puerto Rico outer ridge, *J. Geophys. Res.*, *74*, 3082–3094, 1969.

Cann, J. R., Geological processes at mid-ocean ridge crests, *Geophys. J. Roy. Astron. Soc.*, *15*, 331–341, 1968.

Cann, J. R., Spilites from the Carlsberg ridge, Indian Ocean, *J. Petrology*, *10*, 1–19, 1969.

Cann, J. R., New model for the structure of the ocean crust, *Nature*, *226*, 928–930, 1970.

Cann, J. R., and B. M. Funnell, Palmer ridge: A section through the upper part of the ocean crust, *Nature*, *213*, 661–664, 1967.

Cann, J. R., and F. J. Vine, An area on the crest of the Carlsberg ridge: Petrology and magnetic survey, *Phil. Trans. Roy. Soc. London*, *259*, 198–217, 1966.

Carmichael, D., G. Carpenter, A. Hubbard, K. McCamy, and W. McDonald, A recording ocean bottom seismograph, *J. Geophys. Res.*, *78*, 8748–8750, 1973.

Chernysheva, V. I., and P. L. Bezrukov, Serpentinite from the crest of the Indo-Arabian ridge, *Dokl. Akad. Nauk SSSR, 166*, 207–210, 1966.

Christensen, N. I., Compressional wave velocities in metamorphic rocks at pressures to 10 kbar, *J. Geophys. Res., 70*, 6147–6164, 1965.

Christensen, N. I., Shear wave velocities in metamorphic rocks at pressures to 10 kbar, *J. Geophys. Res., 71*, 3549–3556, 1966*a*.

Christensen, N. I., Elasticity of ultrabasic rocks, *J. Geophys. Res., 71*, 5921–5931, 1966*b*.

Christensen, N. I., Compressional wave velocities in basic rocks, *Pac. Sci., 22*, 41–44, 1968.

Christensen, N. I., Composition and evolution of the oceanic crust, *Mar. Geol., 8*, 139–154, 1970*a*.

Christensen, N. I., Possible greenschist facies metamorphism of the oceanic crust, *Geol. Soc. Amer. Bull., 81*, 905–908, 1970*b*.

Christensen, N. I., Compressional wave velocities in basalts from the Juan de Fuca ridge, *J. Geophys. Res., 75*, 2773–2775, 1970*c*.

Christensen, N. I., The abundance of serpentinites in the oceanic crust, *J. Geol., 80*, 709–719, 1972*a*.

Christensen, N. I., Seismic anisotropy in the lower oceanic crust, *Nature, 237*, 450–451, 1972*b*.

Christensen, N. I., Compressional and shear wave velocities at pressures to 10 kilobars for basalts from the East Pacific rise, *Geophys. J. Roy. Astron. Soc., 28*, 425–429, 1972*c*.

Christensen, N. I., and R. S. Crosson, Seismic anisotropy in the upper mantle, *Tectonophysics, 6*, 93–107, 1968.

Christensen, N. I., and M. H. Salisbury, Sea floor spreading, progressive alteration of layer 2 basalts, and associated changes in seismic velocities, *Earth Planet. Sci. Lett., 15*, 367–375, 1972.

Christensen, N. I., and M. H. Salisbury, Velocities, elastic moduli and weathering-age relations for Pacific layer 2 basalts, *Earth Planet. Sci. Lett., 19*, 461–470, 1973.

Christensen, N. I., and G. H. Shaw, Elasticity of mafic rocks from the mid-Atlantic ridge, *Geophys. J. Roy. Astron. Soc., 20*, 271–284, 1970.

Church, W. R., and R. K. Stevens, Early Paleozoic ophiolite complexes of the Newfoundland Appalachians as mantle-oceanic crust sequences, *J. Geophys. Res., 76*, 1460–1466, 1971.

Cox, C. S., The electrical conductivity of the oceanic lithosphere, in *The Structure and Physical Properties of the Earth's Crust, Geophys. Monogr. Ser.*, vol. 14, edited by J. G. Hancock, pp. 227–233, AGU, Washington, D. C., 1971.

Davies, H. L., Peridotite-gabbro-basalt complex in eastern Papua: An overthrust plate of oceanic mantle and crust, *Bull. Bur. Mineral Resour. Geol. Geophys. Aust., 128*, 1–47, 1971.

Deffeyes, K. S., The axial valley; a steady-state feature of terrain, in *The Megatectonics of Continents and Oceans*, edited by C. H. Johnson and R. C. Smith, pp. 194–222, Rutgers University Press, Brunswick, N. J., 1970.

Den, N., W. J. Ludwig, S. Murauchi, J. I. Ewing, H. Hotta, N. T. Edgar, T. Yoshii, T. Asanuma, K. Hagiwara, T. Sato, and S. Ando, Seismic refraction measurements in the northwest Pacific basin, *J. Geophys. Res., 74*, 1421–1434, 1969.

Den, N., W. J. Ludwig, S. Murauchi, M. Ewing, H. Hotta, T. Asanuma, T. Yoshii, A. Kubotera, and K. Hagiwara, Sediments and structure of the Eauripik-New Guinea rise, *J. Geophys. Res., 76*, 4711–4723, 1971.

Dengo, G., Tectonic-igneous sequence in Costa Rica, in *Petrologic Studies (Buddington Volume)*, edited by A. E. J. Engel, H. L. James, and B. F. Leonard, pp. 133–161, Geological Society of America, Boulder, Colo., 1962.

Dewey, J. F., and J. M. Bird, Origin and emplacement of the ophiolite suite: Appalachian ophiolites in Newfoundland, *J. Geophys. Res., 76*, 3179–3206, 1971.

Dietz, R. S., Alpine serpentines as oceanic rind fragments, *Geol. Soc. Amer. Bull., 74*, 947–752, 1963.

Dortman, N. B., and M. Sh. Magid, New data on velocity of elastic waves in crystalline rocks as a function of moisture, *Int. Geol. Rev., 11*, 517–523, 1969.

Elder, J. W., Physical processes in geothermal areas, in *Terrestrial Heat Flow, Geophys. Monogr. Ser.*, vol. 8, edited by W. H. K. Lee, pp. 211–239, AGU, Washington, D. C., 1965.

Engel, A. E. J., and C. G. Engel, Composition of basalt from the mid-Atlantic ridge, *Science, 144*, 1330–1333, 1964.

Engel, A. E. J., C. G. Engel, and R. G. Havens, Chemical characteristics of oceanic basalts and the upper mantle, *Geol. Soc. Amer. Bull., 76*, 719–734, 1965.

Engel, C. G., and R. L. Fisher, Lherzolite, anorthosite, gabbro and basalt dredged from the mid-Indian Ocean ridge, *Science, 166*, 1136–1141, 1969.

Ewing, J. I., and M. Ewing, Seismic refraction measurements in the Atlantic Ocean basins, in the Mediterranean Sea, on the mid-Atlantic ridge, and in the Norwegian Sea, *Geol. Soc. Amer. Bull., 70*, 291–318, 1959.

Ewing, J. I., and M. Ewing, Sediment distribution on the mid-ocean ridges with respect to spreading of the sea-floor, *Science, 156*, 1590–1593, 1967.

Ewing, J. I., and R. Houtz, Mantle reflections in air gun-sonobuoy profiles, *J. Geophys. Res., 74*, 6706–6709, 1969.

Ewing, J. I., W. J. Ludwig, M. Ewing, and S. L. Eittreim, Structure of the Scotia Sea and Falkland plateau, *J. Geophys. Res., 76*, 7118–7137, 1971.

Ewing, M., A. P. Crary, and H. M. Rutherford, Geophysical investigations in the emerged and submerged Atlantic coastal plain, 1, Methods and results, *Geol. Soc. Amer. Bull., 48*, 753–802, 1937.

Ewing, M., G. P. Woollard, and A. C. Vine, Geophysical investigations in the emerged and submerged Atlantic coastal plain, 3, Barnegat Bay, New Jersey, section, *Geol. Soc. Amer. Bull., 50*, 257–296, 1939.

Ewing, M., L. V. Hawkins, and W. J. Ludwig, Crustal structure of the Coral Sea, *J. Geophys. Res., 75*, 1953–1962, 1970.

Fenwick, D. K. B., M. J. Keen, C. Keen, and A. Lambert, Geophysical studies of the continental margin northeast of Newfoundland, *Can. J. Earth Sci., 5*, 483–500, 1968.

Fisher, R. L., and C. G. Engel, Ultramafic and basaltic rocks dredged from the nearshore flank of the Tonga trench, *Geol. Soc. Amer. Bull., 80*, 1373–1378, 1969.

Fox, P. J., E. Schreiber, and B. C. Heezen, The geology of the Caribbean crust: Tertiary rocks from the Aves ridge, *Tectonophysics, 12*, 89–109, 1971.

Fox, P. J., E. Schreiber, and J. J. Peterson, The geology of the oceanic crust: Compressional wave velocities of oceanic rocks, *J. Geophys. Res., 78*, 5155–5172, 1973.

Francis, T. G., and I. T. Porter, Median valley seismology: The mid-Atlantic ridge near 45°N, *Geophys. J. Roy. Astron. Soc., 34*, 279–311, 1973.

Francis, T. G., and R. W. Raitt, Seismic refraction measurements in the southern Indian Ocean, *J. Geophys. Res., 72*, 3015–3041, 1967.

Francis, T. G., and G. G. Shor, Jr., Seismic refraction measurements in the northwest Indian Ocean, *J. Geophys. Res., 71*, 427–449, 1966.

Furumoto, A. S., G. P. Woollard, J. F. Campbell, and D. M. Hussong, Variation in the thickness of the crust in the Hawaiian archipelago, in *The Crust and Upper Mantle of the Pacific Area, Geophys. Monogr. Ser.*, vol. 12, edited by L. Knopoff, C. L. Drake, and P. J. Hart, pp. 94–111, AGU, Washington, D. C., 1968.

Furumoto, A. S., J. F. Campbell, and D. M. Hussong, Seismic refraction surveys along the Hawaiian ridge, Kauai to Midway, *Bull. Seismol. Soc. Amer., 61*, 147–166, 1971.

Gansser, A., *The Geology of the Himalayas*, pp. 123–128, Interscience, New York, 1964.

Gass, I. G., Is the Troodos massif of Cyprus a fragment of Mesozoic ocean floor?, *Nature, 220*, 39–42, 1968.

Gass, I. G., and D. Masson-Smith, The geology and gravity anomalies of the Troodos massif, Cyprus, *Phil. Trans. Roy. Soc. London, Ser. A, 255*, 417–467, 1963.

Gass, I. G., and J. D. Smewing, Intrusion, extrusion and metamorphism at constructive margins: Evidence from the Troodos massif, Cyprus, *Nature, 242*, 26–29, 1973.

Goslin, J., P. Beauzart, J. Francheteau, and X. Le Pichon, Thickening of the oceanic layer in the Pacific Ocean, *Mar. Geophys. Res., 1*, 418–427, 1972.

Greenbaum, D., Magmatic processes at ocean ridges: Evidence from the Troodos massif, Cyprus, *Nature Phys. Sci., 238*, 18–21, 1972.

Gutenberg, B., *Physics of the Earth's Interior*, pp. 28–36, Academic, New York, 1959.

Hart, R. A., Chemical exchange between sea water and deep ocean basalts, *Earth Planet. Sci. Lett., 9*, 269–279, 1970.

Hart, R. A., A model for chemical exchange in the basalt-seawater system of oceanic layer II, *Can. J. Earth Sci., 10*, 799–816, 1973.

Hawkins, J. W., J. G. Sclater, and G. Hornhaus, Petrologic and geophysical characteristics of the Lau basin ridge—A spreading center behind the Tonga arc (abstract), *Geol. Soc. Amer. Abstr. Programs, 2*, 571, 1970.

Hekinian, R., Rocks from the mid-oceanic ridge in the Indian Ocean, *Deep Sea Res.*, *15*, 195-213, 1968.
Hekinian, R., Chemical and mineralogical differences between abyssal hill basalts and ridge tholeiites in the eastern Pacific Ocean, *Mar. Geol.*, *11*, 77-91, 1971.
Hekinian, R., and F. Aumento, Rocks from the Gibbs fracture zone and the Minia seamount near 53°N in the Atlantic Ocean, *Mar. Geol.*, *14*, 47-72, 1973.
Helmberger, D. V., The crust-mantle transition in the Bering Sea, *Bull. Seismol. Soc. Amer.*, *58*, 179-214, 1968.
Helmberger, D. V., and G. B. Morris, A travel time and amplitude interpretation of a marine refraction profile: Primary waves, *J. Geophys. Res.*, *74*, 483-494, 1969.
Helmberger, D. V., and G. B. Morris, A travel time and amplitude interpretation of a marine refraction profile: Transformed shear waves, *Bull. Seismol. Soc. Amer.*, *60*, 593-600, 1970.
Hess, H. H., History of ocean basins, in *Petrologic Studies (Buddington Volume)*, edited by A. E. J. Engel, H. L. James, and B. F. Leonard, pp. 599-620, Geological Society of America, Boulder, Colo., 1962.
Hess, H. H., Seismic anisotropy of the uppermost mantle under oceans, *Nature*, *203*, 629-631, 1964*a*.
Hess, H. H., The oceanic crust, the upper mantle and the Magaguez serpentinized peridotite, in *A Study of Serpentinite*, *Publ. 1188*, edited by C. A. Burke, pp. 169-175, National Academy of Sciences-National Research Council, Washington, D. C., 1964*b*.
Hill, M. N., Seismic refraction shooting in an area of the eastern Atlantic, *Phil. Trans. Roy. Soc. London, Ser. A*, *244*, 561-596, 1952.
Hill, M. N., Recent geophysical exploration of the ocean floor, *Phys. Chem. Earth*, *2*, 129-163, 1957.
Hopson, C. A., and J. M. Mattinson, Ordovician and Late Jurassic ophiolite assemblages in the Pacific Northwest (abstract), *Geol. Soc. Amer. Abstr. Programs*, *5*, 57, 1973.
Houtz, R., J. I. Ewing, and P. Buhl, Seismic data from sonobuoy stations in the northern and equatorial Pacific, *J. Geophys. Res.*, *75*, 5093-5111, 1970.
Hughes, D. S., and J. L. Kelly, Variation of elastic wave velocity with saturation in sandstone, *Geophysics*, *17*, 739-752, 1952.
Hussong, D. M., Detailed structural interpretations of the Pacific oceanic crust using ASPER and ocean bottom seismometer methods, Ph.D. thesis, 165 pp., Univ. of Hawaii, Honolulu, 1972.
Hussong, D. M., A. A. Nowroozi, M. E. Odegard, and G. H. Sutton, Crustal structure under an ocean bottom seismometer using explosive sources (abstract), *Eos Trans. AGU*, *50*, 644, 1969.
Hyndman, R. D., Seismic velocities of basalts from DSDP leg 26 (abstract), *Eos Trans. AGU*, *54*, 1026, 1973.
Ingle, J. C., Jr., D. E. Karig, A. H. Bouma, C. H. Ellis, N. Haile, I. Koizumi, H. Y. Ling, I. MacGregor, C. Moore, H. Ujiie, T. Watanabe, S. M. White, and M. Yasui, Western Pacific floor, *Geotimes*, *18*, 22-25, 1973.
Isacks, B., J. Oliver, and L. R. Sykes, Seismology and the new global tectonics, *J. Geophys. Res.*, *73*, 5855-5899, 1968.
Karig, D. E., Structural framework of the west Philippine basin (abstract), *Geol. Soc. Amer. Abstr. Programs*, *4*, 180-181, 1972.
Kay, R., N. J. Hubbard, and P. Gast, Chemical characteristics and origin of oceanic ridge volcanic rocks, *J. Geophys. Res.*, *75*, 1581-1613, 1970.
Keen, C. E., and D. L. Barrett, A measurement of seismic anisotropy in the Northeast Pacific, *Can. J. Earth Sci.*, *8*, 1056-1064, 1971.
Keen, C. E., and B. D. Loncarevic, Crustal structure on the eastern seaboard of Canada: Studies on the continental margin, *Can. J. Earth Sci.*, *3*, 65-76, 1966.
Kundig, E., Geology and ophiolite problems of East-Celebes, *Verh. Kon. Ned. Geol. Mijnbourvk. Genoot.*, *16*, 210-235, 1956.
Lee, W. H. K., and S. Uyeda, Review of heat flow data, in *Terrestrial Heat Flow*, *Geophys. Monogr. Ser.*, vol. 8, edited by W. H. K. Lee, pp. 87-190, AGU, Washington, D. C., 1965.
Le Pichon, X., Models and structure of the oceanic crust, *Tectonophysics*, *7*, 385-401, 1969.
Le Pichon, X., R. E. Houtz, C. L. Drake, and J. E. Nafe, Crustal structure of the mid-ocean ridges, 1, Seismic refraction measurements, *J. Geophys. Res.*, *70*, 319-339, 1965.
Lister, C. R. B., On the thermal balance of a mid-ocean ridge, *Geophys. J. Roy. Astron. Soc.*, *26*, 515-535, 1972.
Lister, C. R. B., and B. T. R. Lewis, An ocean bottom seismometer suitable for arrays (abstract), *Eos Trans. AGU*, *55*, 357, 1974.
Ludwig, W. J., J. I. Ewing, M. Ewing, S. Murauchi, N. Den, S. Asano, H. Hotta, M. Hayakawa, T. Asanuma, K. Ichikawa, and I. Ichikawa, Sediments and structure of the Japan trench, *J. Geophys. Res.*, *71*, 2121-2137, 1966.
Ludwig, W. J., J. E. Nafe, E. S. W. Simpson, and S. Sacks, Seismic refraction measurements on the southeast African continental margin, *J. Geophys. Res.*, *73*, 3707-3719, 1968.
Ludwig, W. J., S. Murauchi, N. Den, M. Ewing, H. Hotta, R. Houtz, T. Yoshii, T. Asanuma, K. Hagiwara, T. Sato, and S. Ando, Structure of Bowers ridge, Bering Sea, *J. Geophys. Res.*, *76*, 6350-6375, 1971.
Ludwig, W. J., S. Murauchi, N. Den, P. Buhl, H. Hotta, M. Ewing, T. Asanuma, T. Yoshii, and N. Sakajiri, Structure of east China Sea-west Philippine Sea margin off southern Kyushu, Japan, *J. Geophys. Res.*, *78*, 2526-2536, 1973.
Matthews, D. H., A. S. Laughton, D. T. Pugh, E. T. W. Jones, J. Sunderland, M. Takin, and M. Bacon, Crustal structure and origin of Peake and Freen deeps, N.E. Atlantic, *Geophys. J. Roy. Astron. Soc.*, *18*, 517-542, 1969.
Maynard, G. L., G. H. Sutton, and D. M. Hussong, Seismic observations in the Solomon Islands and Darwin rise regions using repetitive sources (abstract), *Eos Trans. AGU*, *50*, 206, 1969.
McConnell, R. K., Jr., R. N. Gupta, and J. T. Wilson, Compilation of deep crustal seismic refraction profiles, *Rev. Geophys. Space Phys.*, *4*, 41-100, 1966.
Melson, W. G., and G. Thompson, Layered basic complex in oceanic crust, Romanche fracture, equatorial Atlantic Ocean, *Science*, *168*, 817-820, 1970.
Melson, W. G., and G. Thompson, Petrology of a transform fault zone and adjacent ridge segments, *Phil. Trans. Roy. Soc. London, Ser. A*, *268*, 423-441, 1971.
Melson, W. G., and Tj. H. van Andel, Metamorphism in the mid-Atlantic ridge, 22°N. latitude, *Mar. Geol.*, *4*, 165-186, 1966.
Menard, H. W., Sea-floor spreading, topography and the second layer, *Science*, *157*, 923-924, 1967.
Miyashiro, A., The Troodos ophiolite complex was probably formed in an island arc, *Earth Planet. Sci. Lett.*, *19*, 218-224, 1973.
Miyashiro, A., F. Shido, and M. Ewing, Composition and origin of serpentinites from the mid-Atlantic ridge near 24° and 30° north latitude, *Contrib. Mineral. Petrol.*, *23*, 117-127, 1969*a*.
Miyashiro, A., F. Shido, and M. Ewing, Diversity and origin of abyssal tholeiite from the mid-Atlantic ridge near 24° and 30° north latitude, *Contrib. Mineral. Petrol.*, *23*, 38-52, 1969*b*.
Miyashiro, A., F. Shido, and M. Ewing, Crystallization and differentiation in abyssal tholeiites and gabbros from mid-oceanic ridges, *Earth Planet. Sci. Lett.*, *7*, 361-365, 1970*a*.
Miyashiro, A., F. Shido, and M. Ewing, Petrologic models for the mid-Atlantic ridge, *Deep Sea Res.*, *17*, 109-123, 1970*b*.
Miyashiro, A., F. Shido, and M. Ewing, Metamorphism in the mid-Atlantic ridge near 24° and 30°N, *Phil. Trans. Roy. Soc. London, Ser. A*, *268*, 589-603, 1971.
Moores, E. M., Petrology and structure of the Vourinos ophiolitic complex of northern Greece, *Geol. Soc. Amer. Spec. Pap.*, *118*, 1-74, 1969.
Moores, E. M., Reexamination of the Vourinos ophiolite, Greece (abstract), *Eos Trans. AGU*, *55*, 444, 1974.
Moores, E. M., and E. M. Jackson, Ophiolites and ocean crust, *Nature*, *250*, 136-139, 1974.
Moores, E. M., and F. J. Vine, The Troodos massif, Cyprus, and other ophiolites as oceanic crust: Evaluation and implications, *Phil. Trans. Roy. Soc. London, Ser. A*, *268*, 443-466, 1971.
Muir, I. D., and C. E. Tilley, Basalts from the northern part of the mid-Atlantic ridge, *J. Petrology*, *7*, 193-211, 1966.
Murauchi, S., N. Den, S. Asano, H. Hotta, T. Yoshii, T. Asanuma, K. Hagiwara, K. Ichikawa, T. Sato, W. J. Ludwig, J. I. Ewing, N. T. Edgar, and R. E. Houtz, Crustal structure of the Philippine Sea, *J. Geophys. Res.*, *73*, 3143-3171, 1968.
Murauchi, S., W. J. Ludwig, N. Den, H. Hotta, T. Asanuma, T. Yoshii, A. Kubotera, and K. Hagiwara, Structure of the Sulu Sea and the Celebes Sea, *J. Geophys. Res.*, *78*, 3437-3447, 1973.
Nicholls, G. D., A. J. Nalwalk, and E. E. Hays, The nature and composition of rock samples dredged from the mid-Atlantic ridge between 22°N and 52°N, *Mar. Geol.*, *1*, 333-343, 1964.
Nur, A., and G. Simmons, The effect of saturation on velocity in low porosity rocks, *Earth Planet. Sci. Lett.*, *7*, 183-193, 1969.
Officer, C. B., J. I. Ewing, J. F. Hennion, D. G. Harkrider, and D. E. Miller, Geophysical investigations in the eastern Caribbean: Summary of 1955 and 1956 cruises, *Phys. Chem. Earth*, *3*, 17-109, 1959.
Oxburgh, E. R., and D. L. Turcotte, Mid-ocean ridges and geotherm

distribution during mantle convection, *J. Geophys. Res.*, *73*, 2643–2661, 1968.

Page, B. M., Oceanic crust and mantle fragment in subduction complex near San Luis Obispo, California, *Geol. Soc. Amer. Bull.*, *83*, 957–972, 1972.

Pamić, J., Some petrological features of Bosnian peridotite-gabbro complexes in the Dinaride zone of Yugoslavia, *Tschermaks Mineral. Petrogr. Mitt.*, *15*, 14–42, 1971.

Peterson, J. J., P. J. Fox, and E. Schreiber, Newfoundland ophiolites and the geology of the oceanic layer, *Nature*, *247*, 194–196, 1974.

Phillips, J. D., G. Thompson, R. P. Von Herzen, and V. T. Bowen, Mid-Atlantic ridge near 43°N latitude, *J. Geophys. Res.*, *74*, 3069–3081, 1969.

Ploshko, V. V., and Y. A. Bogdanov, Ultrabasites of the deep-water Romanche trench, *Izv. Akad. Nauk SSSR*, *12*, 82–93, 1968.

Poster, C. K., Ultrasonic velocities in rocks from the Troodos massif, Cyprus, *Nature*, *243*, 2–3, 1973.

Quon, S. H., and E. G. Ehlers, Rocks of the northern part of the mid-Atlantic ridge, *Geol. Soc. Amer. Bull.*, *74*, 1–7, 1963.

Raitt, R. W., The crustal rocks, in *The Sea*, vol. 3, edited by M. N. Hill, pp. 85–102, John Wiley, New York, 1963.

Raitt, R. W., G. G. Shor, Jr., G. B. Morris, and H. K. Kirk, Mantle anisotropy in the Pacific Ocean, *Tectonophysics*, *12*, 173–186, 1971.

Reinhardt, B. M., On the genesis and emplacement of ophiolites in the Oman Mountains geosyncline, *Schweiz. Mineral. Petrogr. Mitt.*, *49*, 1–30, 1969.

Rigo de Righi, M., and A. Cortesina, Gravity tectonics in foothills structure belt of southeast Turkey, *Amer. Ass. Petrol. Geol. Bull.*, *48*, 1911–1937, 1964.

Ryzhova, T. V., Elastic properties of plagioclase, *Bull. Acad. Sci. USSR, Geophys. Ser.*, Engl. Transl., no. 7, 633–635, 1964.

Shido, F., A. Miyashiro, and M. Ewing, Crystallization of abyssal tholeiites, *Contrib. Mineral. Petrol.*, *31*, 251–266, 1971.

Shor, G. G., Jr., Refraction and reflection techniques and procedure, in *The Sea*, vol. 3, edited by M. N. Hill, pp. 20–38, John Wiley, New York, 1963.

Shor, G. G., Jr., P. Dehlinger, H. K. Kirk, and W. S. French, Seismic refraction studies off Oregon and northern California, *J. Geophys. Res.*, *73*, 2175–2194, 1968.

Shor, G. G., Jr., H. W. Menard, and R. W. Raitt, Structure of the Pacific basin, in *The Sea*, vol. 4, edited by A. E. Maxwell, pp. 3–27, John Wiley, New York, 1971*a*.

Shor, G. G., Jr., H. K. Kirk, and H. W. Menard, Crustal structure of the Melanesian area, *J. Geophys. Res.*, *76*, 2562–2586, 1971*b*.

Simmons, G., The velocity of shear waves in rocks to 10 kbar, 1, *J. Geophys. Res.*, *69*, 1123–1130, 1964.

Smith, C. H., Bay of Islands igneous complex, western Newfoundland, *Geol. Surv. Can. Mem.*, *290*, 1–132, 1958.

Steinmann, A., Die ophiolitischen Zonen in den mediterranen Kettengebirgen, *Int. Geol. Congr. 14th*, *2*, 637–667, 1926.

Sutton, G. H., G. L. Maynard, and D. M. Hussong, Marine crustal seismic refraction studies using repetitive sources and sonobuoys (abstract), in *Program of Annual Meeting*, Seismological Society of America, Oakland, Calif., 1969.

Sutton, G. H., G. L. Maynard, and D. M. Hussong, Widespread occurrence of a high-velocity basal layer in the Pacific crust found with repetitive sources and sonobuoys, in *The Structure and Physical Properties of the Earth's Crust, Geophys. Monogr. Ser.*, vol. 14, edited by J. G. Heacock, pp. 193–209, AGU, Washington, D. C., 1971.

Switzer, A., A. Melson, and G. Thompson, Garnet from the mid-Atlantic ridge near 43°N latitude, *Geol. Soc. Amer. Bull.*, *81*, 895–898, 1970.

Sykes, L. R., and M. L. Sbar, Intraplate earthquakes, lithospheric stresses and the driving mechanism of plate tectonics, *Nature*, *245*, 298–302, 1973.

Talwani, M., X. Le Pichon, and M. Ewing, Crustal structure of the mid-oceanic ridges, 2, Computed model from gravity and seismic refraction data, *J. Geophys. Res.*, *70*, 341–352, 1965.

Talwani, M., C. C. Windisch, and M. G. Langseth, Jr., Reykjanes ridge crest: A detailed geophysical study, *J. Geophys. Res.*, *76*, 473–517, 1971.

Thayer, T. P., The Canyon Mountain complex, Oregon, and the Alpine mafic magma stem, *U.S. Geol. Surv. Prof. Pap.*, *475C*, C82–C85, 1963.

Thompson, G., Trace-element distributions in fractionated oceanic rocks, 2, Gabbros and related rocks, *Chem. Geol.*, *12*, 99–111, 1973.

Thompson, G., and W. G. Melson, The petrology of oceanic crust across fracture zones in the Atlantic Ocean: Evidence of a new kind of sea-floor spreading, *J. Geol.*, *80*, 526–538, 1972.

Upadhyay, H. D., J. F. Dewey, and E. R. W. Neale, The Betts cove ophiolite complex, Newfoundland: Appalachian oceanic crust and mantle, *Proc. Geol. Ass. Can.*, *24*, 27–34, 1971.

van Andel, Tj. H., J. D. Phillips, and R. P. Von Herzen, Rifting origin for the Vema fracture in the North Atlantic, *Earth Planet. Sci. Lett.*, *5*, 296–300, 1969.

Varne, R., and M. J. Rubenach, Geology of Macquarie Island and its relationship to oceanic crust, in *Antarctic Oceanology II: The Australian–New Zealand Sector, Antarctic Res. Ser.*, vol. 19, edited by D. E. Hayes, pp. 251–266, AGU, Washington, D. C., 1972.

Varne, R., R. D. Gee, and P. G. J. Quilty, Macquarie Island and the cause of oceanic linear magnetic anomalies, *Science*, *166*, 230–232, 1969.

Vuagnat, M., Remarques sur la trilogie serpentinites-gabbros-diabases dans le basin de la Méditerranée occidentale, *Geol. Rundsch.*, *53*, 336–358, 1963.

Vine, F. T., and H. H. Hess, Sea floor spreading, in *The Sea*, vol. 4, edited by A. E. Maxwell, pp. 587–622, John Wiley, New York, 1971.

Vine, F. J., C. K. Poster, and I. G. Gass, Aeromagnetic survey of the Troodos igneous massif, Cyprus, *Nature Phys. Sci.*, *244*, 34–38, 1973.

Wager, L. R., and W. A. Deer, Geological investigations in east Greenland, 3, The petrology of the Skaergaard intrusion, Kangerdluzssaug, east Greenland, *Medd. Groenland*, *105*, 1–353, 1939.

Wenner, D. B., and H. P. Taylor, Jr., Oxygen and hydrogen isotope studies of the serpentinization of ultramafic rocks in oceanic environments and continental ophiolite complexes, *Amer. J. Sci.*, *273*, 207–239, 1973.

Whitmarsh, R. B., Seismic anisotropy of the uppermost mantle absent beneath the east flank of the Reykjanes ridge, *Bull. Seismol. Soc. Amer.*, *61*, 1351–1368, 1971.

Williams, H., Mafic-ultramafic complexes in western Newfoundland Appalachians and the evidence for transportation: A review and interim report, *Proc. Geol. Ass. Can.*, *24*, 9–25, 1971.

Williams, H., and J. Malpas, Sheeted dikes and brecciated dike rocks within transported igneous complexes, Bay of Islands, western Newfoundland, *Can. J. Earth Sci.*, *9*, 1216–1229, 1972.

Wyllie, M. R. J., A. R. Gregory, and G. H. F. Gardner, An experimental investigation of factors affecting elastic wave velocities in porous media, *Geophysics*, *23*, 459–493, 1958.

Yoshii, T., W. J. Ludwig, N. Den, S. Murauchi, M. Ewing, H. Hotta, P. Buhl, T. Asanuma, and N. Sakajiri, Structure of southwest Japan margin of Shikoku, *J. Geophys. Res.*, *78*, 2517–2525, 1973.

(Received June 18, 1974;
accepted September 10, 1974.)

Reprinted from Karig, D.E., Ingle, J.C., Jr., et al., 1975
Initial Reports of the Deep Sea Drilling Project, Volume XXXI, Washington (U.S. Government Printing Office)

27. ELASTIC WAVE VELOCITIES IN VOLCANIC AND PLUTONIC ROCKS RECOVERED ON DSDP LEG 31

N.I. Christensen, R.L. Carlson, M.H. Salisbury, and D.M. Fountain,
Department of Geological Sciences, University of Washington, Seattle, Washington

INTRODUCTION

In this paper information is presented on compressional and shear wave velocities, bulk densities, and elastic constants for several samples of basement rock obtained from Sites 292, 293, 294, and 296. The velocities have been measured to 4.0 or 6.0 kb using a pulse transmission technique similar to that described by Birch (1960).

The rocks studied from Site 292 are fine-grained basalts with intersertal to subophitic textures; all samples are vesicular and slightly altered. The rocks from Site 293 are of particular significance in that they may represent samples from the lower oceanic crust. Compressional wave velocities were measured in metadiabase containing abundant actinolite after clinopyroxene (31-293-18-1, 90-93 cm); granulated-chloritized gabbro (31-293-19-1, 108-111 cm); hornblende metagabbro of amphibolite facies grade (293-20-1, 100-103 cm); and gabbro tending towards anorthositic gabbro, often with cumulate textures and strong preferred orientation of plagioclase (31-293-20-1, 136-139 cm; 31-293-21-1, 5-8 cm; 31-293-21-1, 32-35 cm; and 31-293-21-2, 11-14 cm). The sample from Site 294 is a fine-grained, altered basalt with an intersertal texture, whereas the sample from Site 296 is a lapilli tuff.

DATA

The velocities and bulk densities of the samples are given in Table 1. The samples were stored in water immediately after their recovery. Since it has been shown that at pressures below a few kilobars, water saturation significantly increases compressional wave velocities (e.g., Wyllie et al., 1958; Nur and Simmons, 1969; Christensen, 1970), the velocities were measured under saturated conditions. Pore pressures were maintained at values lower than external pressures by placing 100-mesh screen between the samples and copper jackets.

Ratios of compressional to shear velocities (V_p/V_s), Poisson's ratios (σ), seismic parameters (ϕ), bulk moduli

TABLE 1
Compressional (P) and Shear (S) Wave Velocities

Sample (Interval in cm)	Bulk Density	Mode	Velocity (km/sec) at Varying Pressures							
			0.2 kb	0.4 kb	0.6 kb	0.8 kb	1.0 kb	2.0 kb	4.0 kb	6.0 kb
292-41-2, 37-40	2.567	P	4.63	4.71	4.78	4.84	4.89	5.06	5.28	–
	2.567	S	2.41	2.45	2.48	2.50	2.53	2.62	2.69	–
292-41-5, 40-43	2.611	P	4.88	4.93	4.97	5.01	5.04	5.21	5.39	–
	2.611	S	2.48	2.52	2.56	2.59	2.62	2.71	2.80	–
292-42-5, 29-32	2.607	P	5.04	5.09	5.13	5.16	5.19	5.29	5.41	–
	2.607	S	2.64	2.66	2.68	2.70	2.72	2.77	2.83	–
292-43-4, 40-43	2.675	P	4.98	5.04	5.09	5.13	5.16	5.26	5.36	–
	2.675	S	2.66	2.69	2.71	2.73	2.74	2.79	2.84	–
292-44-4, 48-51	2.688	P	5.09	5.16	5.21	5.24	5.27	5.34	5.45	–
	2.688	S	2.73	2.75	2.77	2.78	2.79	2.84	2.89	–
292-46, CC	2.792	P	5.33	5.39	5.43	5.47	5.50	5.61	5.73	–
293-18-1, 90-93	2.828	P	6.21	6.23	6.25	6.26	6.27	6.33	6.44	6.53
293-19-1, 108-111	2.848	P	6.51	6.53	6.55	6.57	6.58	6.63	6.70	6.74
293-20-1, 100-103	2.853	P	6.49	6.56	6.62	6.67	6.71	6.80	6.86	–
293-20-1, 136-139	2.832	P	6.80	6.85	6.89	6.93	6.95	7.02	7.10	7.16
293-21-1, 5-8	2.939	P	6.80	6.83	6.85	6.87	6.88	6.95	7.05	7.10
293-21-1, 32-35	2.938	P	6.77	6.82	6.85	6.88	6.91	7.00	7.07	–
293-21-2, 11-14	2.933	P	6.99	7.01	7.03	7.05	7.06	7.11	7.17	7.23
294-7-1, 116-119	2.462	P	4.63	4.69	4.73	4.75	4.78	4.88	5.04	5.14
	2.462	S	2.30	2.35	2.38	2.42	2.45	2.55	2.66	–
296-56-6, 10-13	1.985	P	3.93	3.95	3.96	3.97	3.98	4.00	4.02	–

(K) compressibilities (β), shear moduli (μ), Young's moduli (E), and Lamé's constant (λ) calculated from densities and velocities are given for selected pressures in Table 2. Shear velocities and elastic constants are not reported for the samples from Site 293 because of probable anisotropy of these rocks resulting from strong preferred mineral orientation.

VELOCITY-DENSITY RELATIONS

In a previous report, Christensen et al. (1974) suggested that velocity-density relations for DSDP basalts might be more appropriately described by a nonlinear curve than by the linear solutions commonly used. Figure 1 shows a plot of velocity versus density for water-saturated DSDP basalts at 0.5 kb from this study, and from previous work (Christensen and Salisbury, 1972, 1973; Christensen et al., 1974). The data have been fit with both linear and nonlinear solutions with equations:

$$V_p = 3.56\rho - 4.26 \text{ km/sec}$$

and

$$V_p = 0.08\rho^{3.63} + 2.33 \text{ km/sec}$$

The coarse-grained, high-velocity samples recovered from Site 293 fall predictably above the basalt data distribution and have not been included in these solutions. The basalt from Site 294 is unusually rich in calcite which accounts for its anomalously high velocity with respect to either solution.

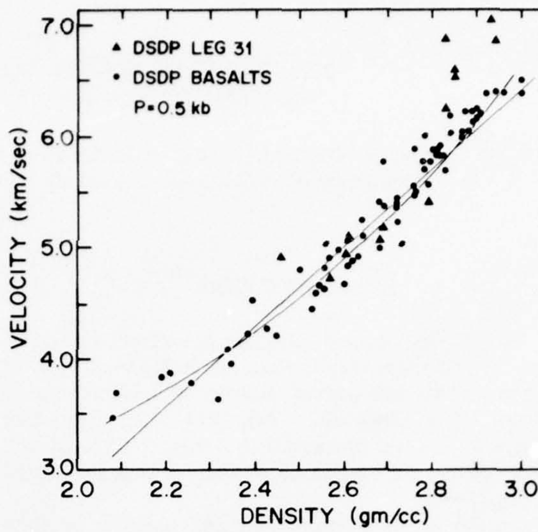

Figure 1. *Compressional wave velocity versus bulk density for DSDP basalts and samples from Leg 31 at 0.5 kb. Included are least squares, linear, and nonlinear solutions to the data.*

DISCUSSION

Examination of Table 1 suggests that at pressures appropriate to the sea floor (0.4-0.6 kb), velocities increase with basement recovery depth at both Sites 292 (Figure 2) and 293. At Site 292, observed velocity gradients (Table 3) are clearly related to increasing density accompanying a decrease in both vesicularity and weathering with depth. At Site 293, velocity differences are associated with a change in lithology from metadiabase through hornblende metagabbro to anorthositic gabbro.

TABLE 2
Elastic Constants

Sample (Interval in cm)	Pressure (kb)	V_p/V_s	σ	Φ (km/sec)^2	K (mb)	β (mb^{-1})	μ (mb)	E (mb)	λ (mb)
31-292-41-2, 37-40	0.4	1.92	0.32	14.16	0.36	2.75	0.15	0.40	0.26
	1.0	1.94	0.32	15.38	0.40	2.53	0.16	0.43	0.29
	2.0	1.94	0.32	16.46	0.42	2.36	0.18	0.46	0.31
	4.0	1.96	0.32	18.14	0.47	2.13	0.19	0.49	0.35
31-292-41-5, 40-43	0.4	1.96	0.32	15.80	0.41	2.42	0.17	0.44	0.30
	1.0	1.93	0.32	16.24	0.43	2.35	0.18	0.47	0.31
	2.0	1.92	0.31	17.24	0.45	2.21	0.19	0.50	0.32
	4.0	1.93	0.32	18.53	0.49	2.05	0.21	0.54	0.35
31-292-42-5, 29-32	0.4	1.91	0.31	16.46	0.43	2.33	0.18	0.48	0.31
	1.0	1.91	0.31	17.00	0.44	2.25	0.19	0.51	0.32
	2.0	1.91	0.31	17.67	0.46	2.16	0.20	0.53	0.33
	6.0	1.91	0.31	18.54	0.49	2.05	0.21	0.55	0.35
31-292-43-4, 40-43	0.4	1.87	0.30	15.74	0.42	2.37	0.19	0.50	0.29
	1.0	1.88	0.30	16.62	0.45	2.24	0.20	0.52	0.31
	2.0	1.89	0.30	17.25	0.46	2.16	0.21	0.54	0.32
	4.0	1.89	0.30	17.83	0.48	2.08	0.22	0.56	0.34
31-292-44-4, 48-51	0.4	1.88	0.30	16.54	0.44	2.25	0.20	0.53	0.31
	1.0	1.88	0.30	17.30	0.47	2.15	0.21	0.55	0.33
	2.0	1.88	0.30	17.74	0.48	2.09	0.22	0.57	0.33
	4.0	1.88	0.30	18.44	0.50	2.00	0.23	0.59	0.35
31-294-7-1, 116-119	0.4	1.99	0.33	14.62	0.36	2.77	0.14	0.36	0.27
	1.0	1.95	0.32	14.82	0.37	2.73	0.15	0.39	0.27
	2.0	1.91	0.31	15.09	0.37	2.68	0.16	0.42	0.27
	4.0	1.89	0.31	15.86	0.39	2.53	0.17	0.46	0.28

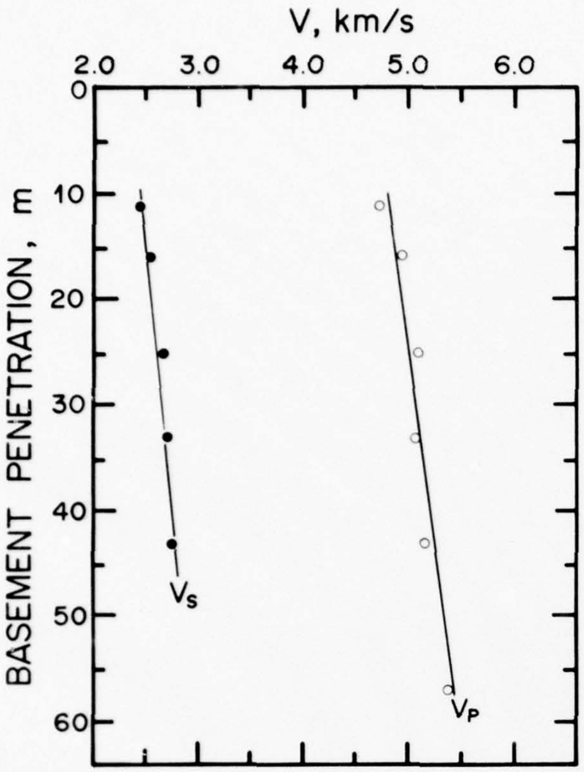

Figure 2. *Measured velocity versus basement penetration at Site 292.*

TABLE 3
Compressional and Shear Wave Velocity Gradients

	$\partial V_p/\partial z$ $\frac{(km/sec)}{m}$	$\partial V_s/\partial z$ $\frac{(km/sec)}{m}$
Site 292	0.012	0.009

Straightforward comparisons of seismic refraction data for the Philippine Sea (Murauchi et al., 1968) with velocity data presented here are difficult because of both poor overlap of refraction lines with DSDP sites and the structural complexities seemingly inherent to marginal basins (Karig, 1971). Site 292, for instance, lies on the flank of the Benham Rise, whereas Sites 293 and 296 mark the extensions of the Central Basin Fault and the Palau-Kyushu Ridge, respectively. General seismic properties of the main basin of the Philippine Sea, however, are correlative with the seismic properties of crystalline rocks recovered on Leg 31. The mean Layer 2 velocity reported for the abyssal plains of the Philippine Sea (Murauchi et al., 1968) is 4.86 km/sec with a standard deviation of 0.18 km/sec, a range which clearly embraces most of the velocities at 0.4-0.6 kb of volcanic rocks recovered from Sites 292 and 294 (Table 1). This general agreement suggests that basalts similar to those measured in this study constitute a large portion of the crustal basement of the basins of the Philippine Sea. Layer 3 of the abyssal plains in this region has a mean V_p of 6.76 km/sec with a standard deviation of 0.14 km/sec. Velocities (at 1 kb) determined for the plutonic rocks recovered from Site 293 (Table 1), the highest yet reported for DSDP samples, fall within the range of layer 3 velocities implying that these rocks may be important petrologic elements of Layer 3 in the Philippine Sea. It is suggested that tectonic activity of the Central Basin Fault may have introduced these rocks to the ocean floor from the deeper levels of the crust in this region. Alternatively, these rocks may have formed in situ as new ocean crust within a leaky transform fault by mechanisms outlined by van Andel et al. (1969). It is interesting to note that the samples examined are similar to those commonly observed in both dredge hauls in main basin fracture zones and in ophiolite complexes. Verification of these implications, however, depends on future determinations of the shear wave velocities of these rocks and the shear wave velocity structure in the neighborhood of the Central Basin Fault.

ACKNOWLEDGMENTS

We wish to thank R. McConaghy and M. Brown for technical assistance. This investigation was supported by the Office of Naval Research Contract N-00014-67-A-0014 and National Science Foundation Grant GA-36138.

REFERENCES

Birch, F., 1960. The velocity of compressional waves in rocks to 10 kilobars, I: J. Geophys. Res., v. 65, p. 1083.

Christensen, N.I., 1970. Compressional wave velocities in basalts from the Juan de Fuca Ridge: J. Geophys. Res., v. 75, p. 2773.

Christensen, N.I. and Salisbury, M.H., 1972. Sea floor spreading, progressive alteration of Layer 2 basalts, and associated changes in seismic velocities: Earth Planet. Sci. Lett., v. 15, p. 367.

———, 1973. Velocities, elastic moduli and weathering-age relations for Pacific Layer 2 basalts: Earth Planet. Sci. Lett., v. 19, p. 461.

Christensen, N.I., Fountain, D.M., Carlson, R.L., and Salisbury, M.H., 1974. Velocities and elastic moduli of volcanic and sedimentary rocks recovered on DSDP Leg 25: *In* Simpson, E.S.W., Schlich, R., et al., Initial Reports of the Deep Sea Drilling Project, Volume 25: Washington (U.S. Government Printing Office), p. 357.

Karig, D.E., 1971. Origin and development of marginal basins in the Western Pacific: J. Geophys. Res., v. 76, p. 2542.

Murauchi, S., Den, N., Asano, S., Hotta, H., Yoshii, T., Asanuma, T., Hagiwara, K., Ichikawa, K., Sato, T., Ludwig, W.J., Ewing, J.I., Edgar, N.T., and Houtz, R.E., 1968. Crustal structure of the Philippine Sea: J. Geophys. Res., v. 73, p. 3143.

Nur, A. and Simmons, G., 1969. The effect of saturation on velocity in low porosity rocks: Earth Planet. Sci. Lett., v. 7, p. 183.

van Andel, Tj.H., Phillips, J.D., and von Herzen, R.P., 1969. Rifting origin for the Vema Fracture in the North Atlantic: Earth Planet. Sci. Lett., v. 5, p. 296.

Wyllie, M.R.J., Gregory, A.R., and Gardner, G.G.F., 1958. An experimental investigation of factors affecting elastic wave velocities in porous media: Geophysics, v. 23, p. 459.

Constitution of the Lower Continental Crust Based on Experimental Studies of Seismic Velocities in Granulite

NIKOLAS I. CHRISTENSEN *Department of Geological Sciences and Graduate Program in Geophysics, University of Washington, Seattle, Washington 98195*
DAVID M. FOUNTAIN *Department of Geological Sciences, University of Washington, Seattle, Washington 98195*

ABSTRACT

Rocks of the granulite facies have been proposed as major constituents of the lower continental crust. To evaluate this possibility, compressional and shear wave velocities have been determined to pressures of 10 kb for 10 granulite samples, thus enabling comparisons of seismic data for the lower crust with the velocities and elastic properties of granulite rocks. The samples selected for this study range in composition from granitic to basaltic, with bulk densities of 2.68 to 3.09 g/cm³. At 6 kb, compressional (V_p) and shear (V_s) wave velocities range from 6.39 to 7.49 km/sec and from 3.36 to 4.25 km/sec, respectively. Velocities in granulite rocks are shown to vary systematically with variations in mineralogical constitution. Both V_p and V_s increase with increasing pyroxene, amphibole, and garnet. Velocities increase with an increasing ratio of pyroxene to amphibole in hornblende-granulite subfacies rocks of approximately equivalent chemical compositions. Decreasing quartz content in granulite rocks produces an increase in V_p and an accompanying decrease in V_s, thereby significantly changing Poisson's ratio. The range of velocities measured for the granulite samples is similar to the range of seismic velocities reported for the lower continental crust; thus, the hypothesis that granulite rocks are major lower crustal constituents is further strengthened. Furthermore, it is shown that lower crustal composition is extremely variable, and therefore valid discussions of composition must be limited to specific regions where seismic velocities are well known. The use of seismic velocities in estimating lower crustal composition is illustrated for the Canadian Shield in Ontario and Manitoba. *Key words: crustal structure, Canadian Shield.*

INTRODUCTION

During the past two decades, extensive efforts have been made by seismologists to decipher the structure and seismic velocity distribution within the continental crust. In spite of these efforts, little progress has been made in forging petrologic interpretations of crustal composition from seismic data. The delineation of the crust of the continents into a "granitic" layer overlying a "basaltic" layer by Jeffreys (1926), in fact, still pervades modern literature of explosion seismology (for example, Roller and Healy, 1963; Hill and Pakiser, 1966; Ocola and Meyer, 1972). Russian seismologists (Kosminskaya and Riznichenko, 1964), however, argue that the apparent seismic layering of the continental crust is due to horizontal "metamorphic fronts." This suggestion is very appealing, because lower crustal hydrostatic pressures of 6 to 10 kb and temperatures of as much as 700°C at the Mohorovičić discontinuity (Lachenbruch, 1970) can combine to provide an appropriate environment for high-grade metamorphism. A straightforward application of these pressure-temperature conditions to conventional metamorphic-facies diagrams (Hietanen, 1967; Turner, 1968) indicates that the rocks of the lower crust may be in the granulite facies.

Granulite-facies rocks are abundant within stable Precambrian shield areas and, to a much lesser extent, are components of younger orogens (see Oliver, 1969, for review). The widespread occurrence of granulite in the shield areas is attributed to extensive denudation coupled with tectonic activity to expose lower levels of continental crust. On the basis of this argument, den Tex and Vogel (1962) suggested that the granulite terranes of Cabo Ortegal in Spain represent unroofed lower continental crust. Lambert (1971) argued for a similar lower crustal origin for the granulite terranes of the Yilgarn Block and the Musgrave Range of Australia. In a comprehensive discussion of the setting, metamorphic associations, and general mineralogy and composition of granulite-facies rocks, den Tex (1965) concluded that within the crust there is a gradual transition from rocks of a granitic series (including hydrous migmatite and high-temperature metamorphic rocks) to rocks of the granulite facies, the latter being the major constituent below the Conrad discontinuity. He estimated a lower crustal composition of 50 percent acidic granulite and intermediate charnockite and 50 percent mafic granulite and eclogite.

Another occurrence of granulite-facies rocks is as xenoliths in diatremes, which have long been subject to scrutiny because the eclogite and peridotite xenoliths in them are commonly thought to be samples of the upper mantle. Granulite-facies rocks have also been reported in diatremes in San Juan County, Utah (McGetchin and Silver, 1972), northeastern Arizona (Watson and Morton, 1969), Riley County, Kansas (Brookins and Wood, 1970), Delegate, Australia (Lovering and White, 1969), and South Africa (Wagner, 1928). The close association of granulite xenoliths with eclogite and peridotite leads one to suspect that the granulite xenoliths have been brought up from the lower crust. On the basis of the sizes of xenoliths from the Moses Rock Pipe, McGetchin and Silver (1972) constructed a crustal model in which a major part of the lower crust is composed of mafic granulite rocks.

One method of obtaining estimates of crustal composition is to compare seismological data with laboratory measurements of rock velocities. Because granulite-facies rocks may well be abundant in the lower crust, it is necessary to determine their velocities and elastic properties. Christensen (1969) reported compressional and shear wave velocities for granulite-facies rocks at hydrostatic pressures to 10 kb (the approximate pressure at the continental crust–mantle boundary; see also Goodacre, 1972, and Ramananantoandro and Manghnani, 1972). We report here the measurement of compressional and shear wave velocities and the elastic constants of granulite-facies rocks of considerably varying chemical composition and mineralogy to hydrostatic pressures of 10 kb. We have

Geological Society of America Bulletin, v. 86, p. 227–236, 7 figs., February 1975, Doc. no. 50212.

found that seismic velocities and the related elastic constants of granulite rocks vary systematically with mineralogy. The data are used to estimate lower crustal mineral compositions in selected regions where detailed crustal seismic information is available.

NOTATION

V_p, compressional wave velocity, km/sec^{-1}
V_s, shear wave velocity, km/sec^{-1}
ρ, bulk density, g/cc
σ, Poisson's ratio
B, compressibility, Mb^{-1}
λ, Lamés' constant, Mb
μ, shear modulus, Mb
E, Young's modulus, Mb
K, bulk modulus, Mb
ϕ, seismic parameter (km/sec^{-1})^2

SAMPLE DESCRIPTIONS

Beginning with the early work of Eskola (1920), metamorphic rocks have been classified into various facies based on assemblages of mineral phases that form in various temperature-pressure regimes. The granulite facies was originally defined to include regionally metamorphosed rocks in which only anhydrous minerals are stable (Eskola, 1939). Later classifications have both subdivided the granulite-facies rocks into subfacies and expanded upon the original definition to include rocks transitional between the amphibolite and granulite facies. Although more comprehensive subdivisions have been proposed for the granulite facies (for example, de Waard, 1965a, 1965b), the twofold subdivision of Turner and Verhoogen (1960) is particularly appropriate for a discussion of the elasticity of granulite rocks and will be used throughout this paper. According to this classification, granulite facies are subdivided into the hornblende-granulite subfacies and the pyroxene-granulite subfacies. Rocks from the latter subfacies are formed at higher temperatures for given water pressures and lack the hydrous minerals hornblende and biotite.

Ten granulite samples that show a wide range in composition and density were selected for this study. Modal analyses obtained by point counting two or three thin sections from each sample are given in Table 1, in which the samples are arranged in order of increasing density, the more granitic and syenitic granulite rocks being near the top and the more mafic at the bottom. Five of the samples contain hornblende and (or) biotite and thus are classified within the hornblende-granulite subfacies.

Sample 1 is representative of granulite described in detail by Smith (1969) as hypersthene-quartz-andesine gneiss from the southern block of the New Jersey highlands. Although the sample selected for our study is compositionally layered, no preferred mineral orientation is apparent either in hand sample or in thin section.

Sample 2, from Tichborne, Ontario, is gray gneiss of the Grenville province and has been described in detail by Giovanella (1965). The rock contains primarily feldspar and quartz and exhibits a strong lineation in hand sample. The lineation is due to linear concentrations of pyroxene that lack preferred orientation (Giovanella, 1965).

The samples of California granulite (samples 3, 6, 8) that form part of the core of the Santa Lucia Range were collected along the Pacific coast approximately 25 km southeast of Point Sur. Although there is considerable variation in composition among the three rocks, it is apparent from their mineralogy (Table 1) that they were formed under conditions of hornblende-granulite–subfacies metamorphism. The mafic minerals within the samples show distinct preferred orientation, even though mineral segregation is lacking. The petrography and chemistry of these rocks have been described in detail by Compton (1960).

The samples of New York granulite collected near Saranac Lake (samples 4, 5, 7) have been described as charnockitic gneiss by Buddington (1952) and as quartz syenite gneiss by Davis (1971). Compositional banding and preferred mineral orientation are weakly developed in the specimens we studied from this area. Sample 7 is texturally similar to samples 4 and 5 but lacks quartz and contains more pyroxene (Table 1).

Samples 9 and 10 are mafic representatives of the granulite facies. Sample 9, described by Barrus (1970), contains abundant hornblende and pyroxene, placing it within the hornblende-granulite subfacies. A strong lineation of hornblende is evident in hand sample and thin section. Sample 10, described by Schmid (1967), is from the Ivrea-Verbano zone in the Italian Alps. The rock shows no obvious preferred mineral orientation or compositional layering. Pyroxene and garnet are abundant, producing the highest density of the rocks included in this study.

TABLE 1. MODAL ANALYSES (PERCENTAGES BY VOLUME)

Sample no. and locality	Qtz	Mi	Pl	Ho	Py	Others
1, New Jersey highlands	24	1	67	..	6	2 ma
2, Tichborne, Ontario	21	7	63	..	4	3 ma, 1 bi, 1 ga
3, Santa Lucia Mtns., California	7	..	74	8	8	2 bi, 1 ma
4, Saranac Lake, New York	2	43*	36	..	11	1 ga, 3 my, 4 ma
5, Saranac Lake, New York	3	48*	30	4	9	5 my, 1 ma
6, Santa Lucia Mtns., California	2	..	53	22	18	3 bi, 2 ma
7, Adirondack Mtns., New York	..	30*	32	..	38	..
8, Santa Lucia Mtns., California	6	..	32	54	4	3 ga, 1 ma
9, Wind River Mtns., Wyoming	..	..	36	42	22	..
10, Valle d'Ossola, Italy	..	1	60	..	26	9 ga, 4 ma

Note: bi = biotite, ga = garnet, ho = hornblende, ma = magnetite, mi = microcline, my = myrmekite, pl = plagioclase, py = pyroxene, qtz = quartz.

* Perthitic microcline.

EXPERIMENTAL TECHNIQUE AND DATA

Three mutually perpendicular cores, 2.54 cm in diameter and 5 to 7 cm in length, were cut from each specimen. Bulk densities (Table 2) were calculated using the weights and dimensions of the cores. The cores were jacketed with copper foil, and transducers, electrodes, and rubber tubing were assembled on each end in a manner similar to the procedure described by Birch (1960).

Velocities were obtained from the travel times of elastic waves through samples of known length using the pulse transmission technique (Birch, 1960). Barium titanate and AC-cut quartz transducers of 2 MHz frequencies were used to generate and receive compressional and shear waves, respectively. The pressure-generating system consists of a two-stage intensifier using a low-viscosity oil for the pressure medium. Pressure was measured by observing the change in electrical resistance of a calibrated manganin coil located on the high-pressure side of the intensifier.

The velocities given in Table 2 are uncorrected for length changes resulting from compression at elevated pressures. For most rocks, this correction lowers velocity at 10 kb approximately 0.02 km/sec and is significant only in calculating elastic constants and pressure derivatives of velocity. The compressional and shear wave velocities are estimated to be accurate to 0.5 percent and 1 percent, respectively (Christensen and Shaw, 1970).

Ratios of V_p to V_s and the elastic constants of the granulite samples calculated from the relations between elastic constants, velocities, and density (Birch, 1961) are given in Table 3. The velocities and densities used for the calculations were corrected for compression using an iterative technique and the dynamically determined compressibilities.

SEISMIC VELOCITIES AND GRANULITE MINERALOGY

Birch (1961) has shown that, to a first approximation, compressional wave velocities are linearly related to density for rocks of constant mean atomic weight. On the basis of shear wave velocity measurements by Simmons (1964), Kanamori and Mizutani (1965), and Christensen (1966a, 1966b), Christensen (1968) demonstrated that a similar relationship exists between shear velocity and density. The mean atomic weight (m) of a rock is calculated from its chemical analysis with the relation $m = (\sum x_i/m_i)^{-1}$, where m_i and x_i are the mean atomic weight and proportion by weight of oxide i, respectively. Calculations by Birch (1961) have shown that most common rocks have mean atomic weights between 20 and 22 and that differences in mean atomic weights of rock are primarily related to iron content — higher iron content gives a higher mean atomic weight.

In granulite, iron is often located in the crystal lattices of pyroxene, amphibole, garnet, biotite, and magnetite. An increase in the percentages of these minerals at the expense of feldspar and quartz will thus increase mean atomic weight. For the granulite samples included in this study, the percentages of iron-bearing minerals show a tendency to increase with increasing density (Tables 1, 2); therefore, mean atomic weight increases with increasing density, and velocities should not follow lines of constant mean atomic weight. In Figure 1, granulite velocities at 6 kb and Poisson's ratios calculated from the velocities are plotted against bulk density. Also shown are mean atomic weight lines $m = 21$ determined for compressional wave velocities by Birch (1961) and shear wave velocities by Christensen (1968). Although the velocity-density data do not follow lines of constant mean atomic weight, a linear relation between V_p and ρ is apparent. The least-squares linear solution is given by

$$V_p = 0.31 + 2.27\rho,$$

with a correlation coefficient of 0.95. Compressional wave velocities for the higher density granulite rocks fall below the constant mean atomic weight line 21 (that is, toward lines of higher mean atomic weight), as predicted from their mineralogy. Shear velocities, however, do not show a linear relation between density and velocity; for granulite rocks with densities below approximately 2.85 g/cc, the shear velocities decrease with increasing density, and above 2.85 g/cc, the velocities increase with increasing density. Poisson's ratio first increases with increasing density and then decreases (Fig. 1), with the exception of sample 10.

The unusual relation between shear velocity and density is readily explained by the mineralogy of the granulite rocks. The increase in shear velocity with increasing density for granulite rocks with densities above 2.85 g/cc is due to increasing pyroxene, hornblende, and garnet content. These minerals have higher aggregate velocities than feldspars and quartz (Table 4). The relatively low shear velocity and high Poisson's ratio for sample 10 are related to the high feldspar content of this rock (Tables 1, 4). For the lower density samples, there is a decrease in quartz content with increasing density. Compared to many other common silicates, quartz has a relatively low compressional wave velocity and a high shear wave velocity (a low Poisson's ratio). Thus, decreasing quartz content will increase compressional wave velocity and *decrease* shear wave velocity, as observed

TABLE 2. COMPRESSIONAL AND SHEAR WAVE VELOCITIES (KM/SEC)

Sample no. and locality	Bulk density (g/cm³)	p = 0.4 kb		p = 1.0 kb		p = 2.0 kb		p = 4.0 kb		p = 6.0 kb		p = 8.0 kb		p = 10.0 kb	
		V_p	V_s	V_p	V_s	V_p	V_s	V_p	V_s	V_p	V_s	V_p	V_s	V_p	V_s
1, New Jersey Highlands	2.671	6.13	3.68	6.25	3.72	6.350	3.762	6.428	3.790	6.482	3.805	6.518	3.814	6.542	3.820
	2.693	6.32	3.55	6.43	3.59	6.510	3.620	6.595	3.642	6.640	3.650	6.669	3.653	6.690	3.655
	2.678	6.32	3.67	6.40	3.69	6.469	3.721	6.548	3.744	6.595	3.758	6.628	3.767	6.650	3.773
Mean	2.681	6.26	3.63	6.36	3.67	6.443	3.701	6.523	3.725	6.572	3.738	6.605	3.745	6.627	3.749
2, Tichborne, Ontario	2.715	5.99	3.29	6.05	3.34	6.162	3.414	6.308	3.526	6.406	3.587	6.464	3.613	6.483	3.620
	2.709	5.99	3.20	6.09	3.26	6.195	3.341	6.339	3.466	6.432	3.539	6.482	3.575	6.507	3.586
	2.713	5.94	3.25	6.03	3.33	6.140	3.417	6.292	3.538	6.390	3.603	6.439	3.635	6.460	3.644
Mean	2.712	5.97	3.25	6.06	3.31	6.166	3.391	6.313	3.510	6.409	3.576	6.462	3.608	6.483	3.617
3, Santa Lucia Mtns., California	2.729	6.28	3.24	6.45	3.29	6.541	3.324	6.648	3.348	6.715	3.362	6.772	3.373	6.795	3.380
	2.726	6.41	3.46	6.47	3.50	6.515	3.555	6.572	3.599	6.615	3.630	6.655	3.655	6.690	3.679
	2.729	6.48	3.59	6.55	3.64	6.632	3.683	6.700	3.717	6.738	3.749	6.772	3.765	6.800	3.770
Mean	2.728	6.39	3.43	6.49	3.48	6.563	3.521	6.640	3.555	6.689	3.580	6.733	3.598	6.762	3.610
4, Saranac Lake, New York	2.846	6.17	3.22	6.43	3.31	6.553	3.350	6.635	3.382	6.672	3.396	6.705	3.405	6.731	3.410
	2.771	5.99	3.24	6.32	3.32	6.500	3.375	6.637	3.415	6.698	3.438	6.738	3.458	6.771	3.472
	2.873	6.13	3.25	6.43	3.37	6.573	3.415	6.695	3.450	6.752	3.468	6.784	3.481	6.800	3.490
Mean	2.830	6.09	3.24	6.40	3.33	6.542	3.380	6.656	3.416	6.707	3.434	6.742	3.448	6.767	3.457
5, Saranac Lake, New York	2.806	6.26	3.38	6.46	3.43	6.575	3.485	6.687	3.539	6.754	3.556	6.800	3.560	6.830	3.568
	2.866	5.97	3.29	6.26	3.37	6.410	3.417	6.531	3.452	6.580	3.462	6.603	3.468	6.615	3.470
	2.862	6.24	3.26	6.47	3.31	6.616	3.378	6.732	3.453	6.775	3.486	6.807	3.497	6.833	3.508
Mean	2.845	6.16	3.31	6.40	3.37	6.534	3.427	6.650	3.481	6.703	3.501	6.737	3.508	6.759	3.515
6, Santa Lucia Mtns., California	2.892	6.79	3.66	6.88	3.70	6.951	3.736	7.030	3.769	7.085	3.792	7.120	3.811	7.149	3.823
	2.916	6.32	3.58	6.60	3.63	6.725	3.659	6.813	3.675	6.855	3.682	6.890	3.686	6.920	3.688
	2.890	6.67	3.58	6.75	3.61	6.820	3.642	6.883	3.672	6.920	3.690	6.949	3.700	6.975	3.709
Mean	2.899	6.60	3.61	6.75	3.65	6.832	3.679	6.909	3.705	6.953	3.721	6.986	3.732	7.015	3.740
7, Adirondack Mtns., New York	2.963	6.71	3.71	6.78	3.74	6.858	3.778	6.943	3.808	6.983	3.828	7.015	3.845	7.042	3.855
	2.905	6.75	3.70	6.82	3.73	6.888	3.762	6.970	3.790	7.012	3.805	7.047	3.818	7.077	3.823
	2.916	6.80	3.63	6.86	3.71	6.935	3.750	7.003	3.785	7.040	3.804	7.071	3.816	7.096	3.821
Mean	2.928	6.75	3.68	6.82	3.73	6.894	3.763	6.972	3.794	7.012	3.812	7.044	3.826	7.072	3.833
8, Santa Lucia Mtns., California	2.995	6.11	3.50	6.38	3.60	6.600	3.679	6.779	3.751	6.865	3.785	6.931	3.804	6.980	3.812
	2.993	6.41	3.59	6.71	3.71	6.940	3.810	7.125	3.896	7.221	3.934	7.300	3.953	7.379	3.960
	2.960	6.25	3.49	6.44	3.60	6.650	3.667	6.818	3.724	6.897	3.744	6.950	3.753	6.987	3.759
Mean	2.983	6.26	3.53	6.51	3.63	6.730	3.719	6.907	3.790	6.994	3.821	7.060	3.837	7.115	3.844
9, Wind River Mtns., Wyoming	3.048	6.83	4.07	7.07	4.11	7.181	4.160	7.256	4.212	7.310	4.248	7.354	4.272	7.396	4.288
	3.048	7.33	4.03	7.42	4.09	7.499	4.141	7.573	4.197	7.616	4.230	7.642	4.252	7.660	4.263
	3.010	6.65	3.62	6.84	3.72	7.021	3.836	7.119	3.945	7.175	3.985	7.220	4.005	7.254	4.018
Mean	3.035	6.94	3.91	7.11	3.97	7.234	4.046	7.316	4.118	7.367	4.154	7.405	4.176	7.434	4.190
10, Valle d'Ossola, Italy	3.055	6.10	3.47	6.79	3.74	7.098	3.851	7.306	3.954	7.430	4.000	7.502	4.027	7.520	4.054
	3.132	6.35	3.54	6.78	3.75	7.143	3.904	7.400	4.008	7.486	4.041	7.530	4.070	7.555	4.097
	3.067	6.08	3.43	6.50	3.63	6.924	3.775	7.174	3.877	7.284	3.906	7.338	3.903	7.377	3.956
Mean	3.085	6.18	3.48	6.68	3.71	7.055	3.843	7.293	3.946	7.400	3.982	7.457	4.000	7.484	4.036

for the granulite samples plotted in Figure 1. This observation may prove to have important implications in future interpretations of crustal low-velocity zones. Several seismic investigations (for example, Landisman and others, 1971; Mueller and Landisman, 1966) have cited evidence for the presence of compressional wave low-velocity zones in the continental crust. It is possible that decreasing quartz content with depth in crustal rocks could cause a velocity inversion of quite a different sort: one for shear waves but not for compressional waves. At present, however, because very little information is available on shear wave velocities in the continental crust, there is no evidence either supporting or disproving the existence of crustal shear wave low-velocity zones.

The mineralogies of the granulite rocks are related in a complex manner to the velocities. To a first approximation, compressional wave velocities in granulite rocks increase systematically with increasing pyroxene, amphibole, and garnet content.

TABLE 3. ELASTIC CONSTANTS CALCULATED FROM V_p, V_s, AND ρ

Pressure (kb)	V_p/V_s	σ	ϕ (km/sec)^2	K (Mb)	β (Mb^{-1})	μ (Mb)	E (Mb)	λ (Mb)
				Sample 1				
0.4	1.72	0.25	21.6	0.58	1.73	0.35	0.88	0.34
2.0	1.74	0.25	23.2	0.62	1.60	0.37	0.92	0.38
6.0	1.76	0.26	24.4	0.66	1.51	0.38	0.95	0.41
10.0	1.77	0.26	24.9	0.68	1.47	0.38	0.96	0.42
				Sample 2				
0.4	1.84	0.29	21.6	0.59	1.70	0.29	0.74	0.40
2.0	1.82	0.28	22.6	0.62	1.62	0.31	0.80	0.41
6.0	1.79	0.27	23.9	0.65	1.53	0.35	0.89	0.42
10.0	1.79	0.27	24.3	0.67	1.49	0.36	0.91	0.43
				Sample 3				
0.4	1.86	0.30	25.1	0.69	1.46	0.32	0.83	0.47
2.0	1.86	0.30	26.5	0.72	1.38	0.34	0.87	0.50
6.0	1.87	0.30	27.5	0.76	1.32	0.35	0.91	0.52
10.0	1.87	0.30	28.1	0.78	1.29	0.36	0.93	0.54
				Sample 4				
0.4	1.88	0.30	23.1	0.65	1.53	0.30	0.77	0.46
2.0	1.94	0.32	27.5	0.78	1.28	0.32	0.85	0.57
6.0	1.95	0.32	29.1	0.82	1.20	0.33	0.88	0.61
10.0	1.96	0.32	29.6	0.85	1.18	0.34	0.90	0.62
				Sample 5				
0.4	1.66	0.30	23.3	0.66	1.51	0.31	0.81	0.46
2.0	1.90	0.31	27.0	0.80	1.30	0.33	0.88	0.55
6.0	1.91	0.31	28.4	0.82	1.23	0.35	0.92	0.58
10.0	1.92	0.31	29.0	0.83	1.20	0.35	0.92	0.60
				Sample 6				
0.4	1.83	0.29	26.2	0.76	1.32	0.38	0.97	0.51
2.0	1.86	0.30	28.6	0.83	1.21	0.39	1.01	0.57
6.0	1.87	0.30	29.8	0.87	1.15	0.40	1.04	0.60
10.0	1.88	0.30	30.3	0.89	1.13	0.41	1.06	0.62
				Sample 7				
0.4	1.84	0.29	27.5	0.81	1.24	0.40	1.02	0.54
2.0	1.83	0.29	28.6	0.84	1.19	0.41	1.07	0.56
6.0	1.84	0.29	29.7	0.87	1.14	0.43	1.10	0.59
10.0	1.85	0.29	30.2	0.89	1.12	0.43	1.12	0.61
				Sample 8				
0.4	1.77	0.27	22.5	0.67	1.49	0.37	0.94	0.42
2.0	1.81	0.28	26.8	0.80	1.25	0.41	1.06	0.52
6.0	1.83	0.29	29.3	0.88	1.14	0.43	1.12	0.59
10.0	1.85	0.29	30.7	0.93	1.08	0.44	1.14	0.63
				Sample 9				
0.4	1.77	0.27	27.8	0.84	1.19	0.46	1.18	0.53
2.0	1.78	0.27	30.5	0.93	1.08	0.50	1.27	0.60
6.0	1.77	0.27	31.1	0.95	1.05	0.53	1.33	0.60
10.0	1.77	0.27	31.6	0.97	1.03	0.53	1.36	0.61
				Sample 10				
0.4	1.78	0.27	22.0	0.68	1.47	0.37	0.95	0.43
2.0	1.84	0.29	30.0	0.93	1.08	0.46	1.18	0.62
6.0	1.86	0.30	33.5	1.04	0.96	0.49	1.27	0.71
10.0	1.85	0.29	34.1	1.06	0.94	0.50	1.31	0.73

Figure 2 shows modal percentages of these minerals (Table 1) with compressional wave velocities between 4 and 10 kb. The data in Figure 2 also emphasize the importance of pyroxene versus amphibole content (that is, subfacies mineralogy) on compressional wave velocities. Because pyroxenes have significantly higher velocities than amphiboles (Table 4), granulite rocks of the pyroxene-granulite subfacies have higher velocities than hornblende-granulite–subfacies rocks of roughly equivalent percentages of mafic minerals. It follows that in hornblende-granulite–subfacies rocks, the amount of hornblende relative to pyroxene will significantly influence velocities. For example, samples 8 and 9 have approximately equivalent percentages of total amphibole plus pyroxene (Table 1; Fig. 2); however, due primarily to a greater percentage of pyroxene, sample 9 has higher velocities. Additional comparisons of samples 3 and 4 and samples 6 and 7 (Fig. 2) also illustrate this influence of metamorphic grade on velocities.

A more detailed examination of the influence of mineralogy on elastic properties may be made with the use of triangular velocity-mineralogy diagrams similar to those used by Christensen (1966b) for ultramafic mineral assemblages. Velocities of the individual mineral components for these diagrams can be obtained from theoretical Voigt-Reuss-Hill averages of single-crystal elastic constants (Table 4). It should be emphasized that the velocities given in Table 4 are for atmospheric pressure determinations, and there is uncertainty about the correct technique to be used to calculate aggregate velocities from single-crystal data (Birch, 1972; Thomsen, 1972). Nevertheless, calculations of rock velocities from Voigt-Reuss-Hill averages tend to agree quite well with measured velocities at pressures above 1 to 2 kb when the effects of grain boundary cracks on velocity are negligible (Christensen, 1965, 1966a).

In the following discussion, the emphasis will be on changes in velocity that accompany changes in mineralogy, rather than on the values of the aggregate velocities themselves. In this way, the averaging technique used to obtain single-crystal aggregate velocities has less importance, and the effects of pressure on mineral velocities, which are unknown for many of the minerals listed in Table 4, can, to a first approximation, be neglected. Aggregate velocities and Poisson's ratios have been calculated for four major three-component mineral assemblages typical of granulite-facies rocks: bronzite + quartz + plagioclase (An_{29}), bronzite + perthite + plagioclase (An_{29}), bronzite + hornblende + plagioclase (An_{56}), and bronzite + garnet + plagioclase

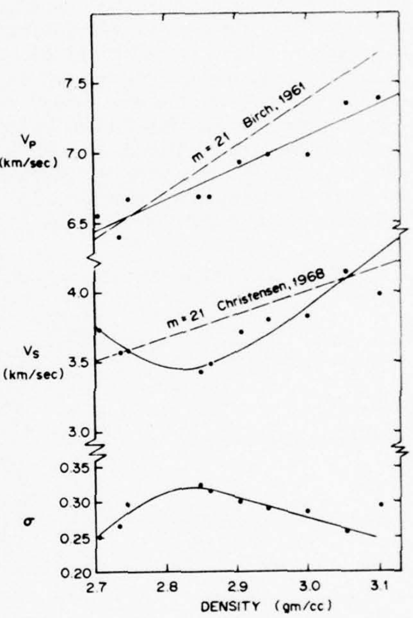

Figure 1. Compressional wave velocity, shear wave velocity, and Poisson's ratio at 6 kb versus density for granulite-facies rocks.

TABLE 4. AGGREGATE VELOCITIES AT ATMOSPHERIC PRESSURE FOR SELECTED MINERALS COMMON IN GRANULITE

Mineral	Composition	Density (g/cc)	V_p (km/s)	V_s (km/s)	Reference
Microcline		2.56	6.01	3.34	Alexandrov and Ryzhova, 1962
Perthite	79% Or, 19% Ab, 2% An	2.56	5.91	3.25	Ryzhova and Alexandrov, 1965
Plagioclase	9% An	2.61	6.07	3.34	Ryzhova, 1964
Plagioclase	24% An	2.64	6.22	3.40	Ryzhova, 1964
Plagioclase	29% An	2.64	6.35	3.44	Ryzhova, 1964
Quartz		2.65	6.05	4.09	McSkimin and others, 1965
Plagioclase	53% An	2.68	6.57	3.53	Ryzhova, 1964
Plagioclase	56% An	2.69	6.62	3.57	Ryzhova, 1964
Biotite		3.05	5.26	2.87	Alexandrov and Ryzhova, 1961a
Hornblende		3.15	7.04	3.81	Alexandrov and Ryzhova, 1961b
Diopside		3.31	7.70	4.38	Alexandrov and others, 1964
Bronzite	85% En	3.34	7.84	4.75	Kumazawa, 1969
Garnet	Almandite-pyrope	4.16	8.53	4.76	Soga, 1967
Garnet	Almandite	4.18	8.52	4.77	Verma, 1960
Magnetite		5.18	7.40	4.20	Doraiswami, 1947

(An_{53}). The results of these calculations are shown in Figures 3 and 4.

Samples 1, 2, and 3 are plotted in Figure 3(a). The diagrams of Figure 3(a) predict that these rocks should have nearly equal shear velocities, whereas compressional wave velocities of sample 3 should be significantly higher than those of samples 1 and 2. This agrees well with the measured velocities (Table 2). More importantly, Figure 3(a) illustrates the effect of quartz on the aggregate properties of granulite-facies rocks. Along the line from point A to point B on the diagrams, V_p increases, but V_s decreases. This direction corresponds to the direction of the maximum decrease in Poisson's ratio. Note that this direction does not coincide with the direction of maximum decrease of the percentage of quartz, because Poisson's ratio is controlled by three mineral components, not quartz alone.

The assemblage bronzite + perthite + An_{29} (Fig. 3) differs from the previous assemblage by the substitution of perthite for quartz. Granulite samples of this mineralogy (4, 5, 7) are plotted in Figure 3(b). It is clear that the differences between V_p and V_s between sample 7 and samples 4 and 5 are primarily due to differences in pyroxene content, because the velocity contours are subparallel to lines of constant pyroxene percentage. Thus, a small change in the percentage of pyroxene will greatly influence the aggregate velocity. Figure 3(b) also shows that the velocity contours for V_p and V_s are nearly parallel to each other, in marked contrast to the velocity contours for Figure 3(a). This difference again points to the unusual elastic behavior of quartz in influencing overall elastic properties of granulite-facies rocks.

Samples 6, 8, and 9 are plotted in Figure 4(a), the bronzite + hornblende + An_{56} assemblage. This assemblage illustrates the interplay of pyroxene and hornblende in determining the elastic properties of granulite-facies rocks. Consider any line of constant pyroxene + hornblende. As this line is followed in the direction of increasing pyroxene [for example, A to B, in Fig. 4(a)] compressional wave velocities increase. Thus the diagram illustrates the effect of increasing pyroxene at the expense of hornblende on compressional wave velocities, as discussed earlier in conjunction with Figure 2. One should keep in mind, however, that recent measurements in our laboratory of velocities in hornblendite indicate that the hornblende shear velocity in Table 4 and Figure 4(a) may be low by as much as 0.3 km/sec.

Figure 4(b) illustrates the bronzite + garnet + An_{53} assemblage appropriate to sample 10. The important fact here is that V_p is relatively insensitive to the percentage of bronzite (note that the velocity contours are perpendicular to the lines of equal percentage of bronzite). The compressional wave velocity is changed most readily by changing the ratio of garnet to plagioclase.

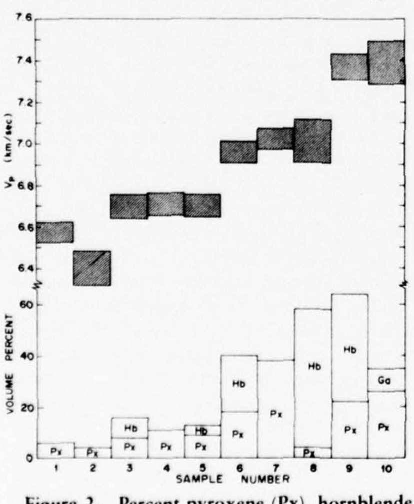

Figure 2. Percent pyroxene (Px), hornblende (Hb), and garnet (Ga) for granulite-facies rocks and ranges of compressional wave velocities between 4 and 10 kb.

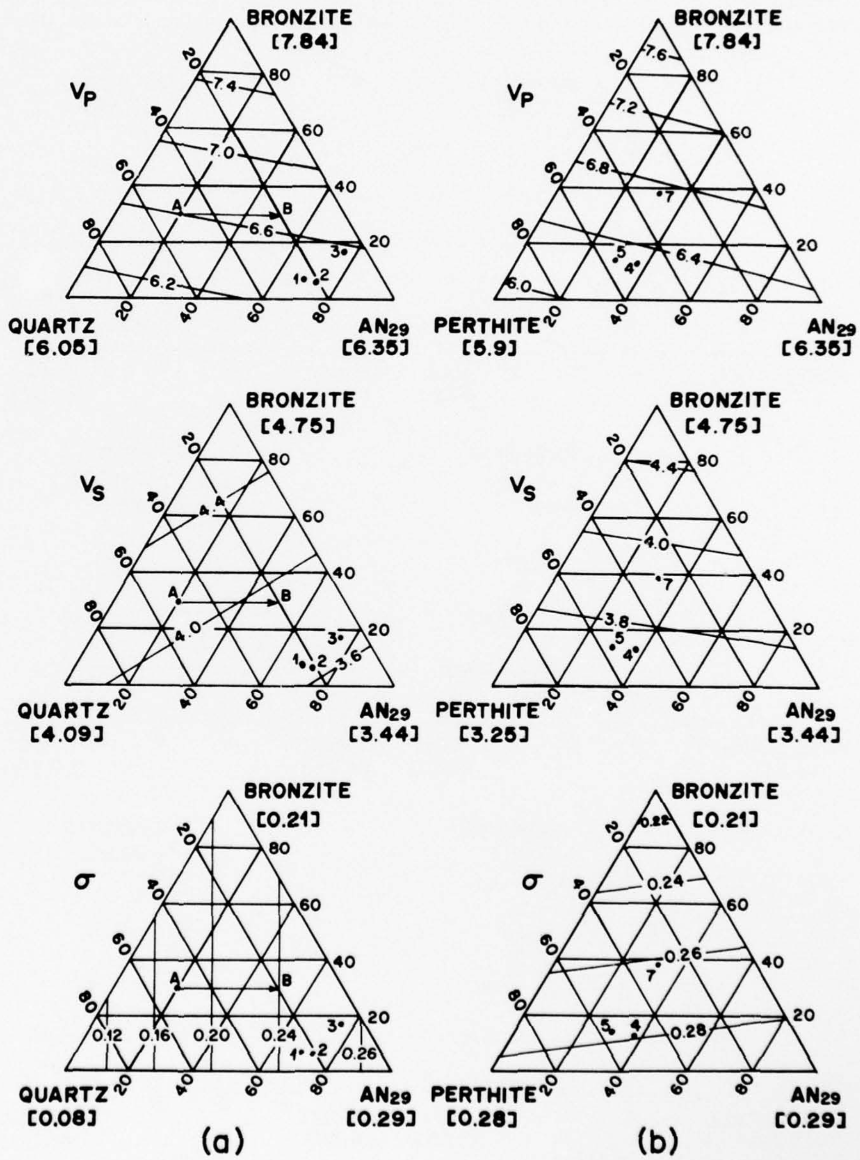

Figure 3. Aggregate values of compressional and shear wave velocity and Poisson's ratio for assemblages (a) bronzite + quartz + An_{29} and (b) bronzite + perthite + An_{29}.

COMPOSITION OF THE LOWER CONTINENTAL CRUST

Estimates of lower crustal composition based on field relations have been, to some extent, substantiated by experimental studies of high-temperature and high-pressure mineralogic assemblages. Kennedy's (1959) preliminary experiments on the gabbro-eclogite phase transformation for basaltic compositions showed that mineral assemblages characteristic of granulite-facies metamorphism (pyroxene + plagioclase ± garnet ± quartz) are stable up to the eclogite stability field and, on the basis of extrapolations, suggested that these assemblages should be stable at the pressure-temperature conditions of the lower continental crust. Subsequent experiments conducted by Yoder and Tilley (1962), Cohen and others (1967), Ito and Kennedy (1970, 1971), and Kennedy and Ito (1972) provided data in support of Kennedy (1959). Ringwood and Green's (1964) preliminary results, however, indicated that eclogite mineral assemblages may be the stable phases for basaltic compositions at lower crustal pressure-temperature conditions. In more detailed work that followed (Ringwood and Green, 1966a, 1966b; Green and Ringwood, 1967, 1972), extrapolations of extremely high pressure gabbro-granulite-eclogite stability data to the lower pressures and temperatures expected for the continental crust further suggested that under anhydrous conditions, eclogite and possibly garnet granulite are the stable phases of basaltic composition in the crust.

Fewer data are available on the stability of high-pressure and high-temperature mineral assemblages for intermediate and acidic compositions. Green and Lambert (1965), however, studying crystallization of various mineral phases in a starting material of granitic composition, found that granulite-facies mineral assemblages (quartz + plagioclase + alkali feldspar + pyroxene ± garnet) are stable at the pressure-temperature conditions of the lower crust. These authors thus suggested that these laboratory-generated assemblages have natural analogs in many acid granulite and charnockite terranes. In a more recent study of gabbroic anorthosite and diorite compositions, T. H. Green (1970) also found granulite mineralogies of these compositions to be stable assemblages under lower crustal conditions. There are, therefore, data from experimental studies indicating that granulite-facies assemblages of acidic and intermediate compositions may be important stable phases of the lower crust.

Variability in Lower Crustal Composition

Although experimental investigations on mineral stability fields at relatively high temperatures and pressures and estimates of pressure and temperature conditions within the crust suggest that rocks of the granulite facies may be ubiquitous constituents of the deep crust of the continents, any valid petrologic model for the lower crust based on granulite-facies mineralogy must satisfy comparisons of seismic data with observed velocities in granulite-facies rocks. The most widely accepted models of continental structure have been those determined through explosion seismology. Most crustal models are considered to be either two layered, the deeper layer separated from the upper layer by the Conrad discontinuity, or essentially one layered, with a shallow refractor at depths of a few kilometers extending to the Mohorovičić discontinuity. In some seismic refraction investigations, however, more than two layers have been reported (Hall and Hajnal, 1973; Mitchell and Landisman, 1971). These traditional pictures of the Earth's crust are undoubtedly oversimplified (James and Steinhart, 1966); we hope that future thorough examinations of velocity-depth relations will define continuous velocity profiles, which, in conjunction with laboratory measurement of rock velocities, will provide important information on changes in composition with depth.

A summary of more than 200 compressional wave velocities for crustal refractors at depths greater than 10 km in the lower

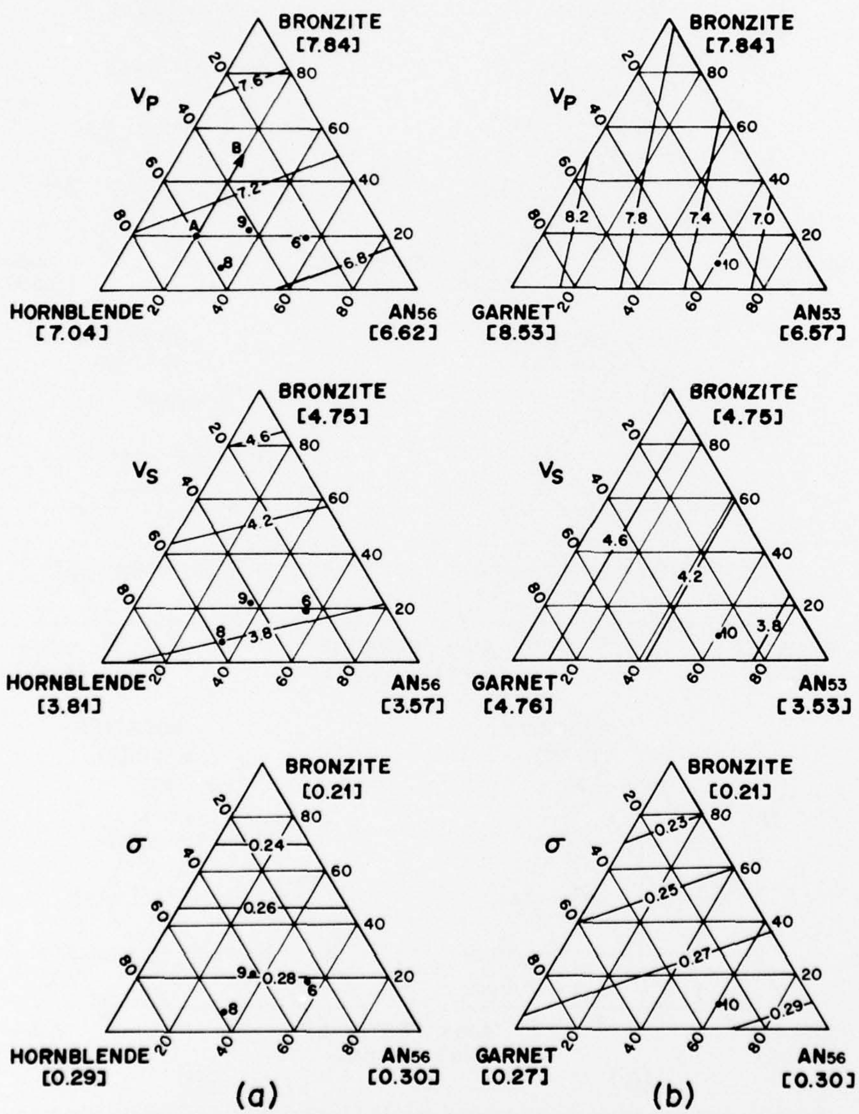

Figure 4. Aggregate values of compressional and shear wave velocity and Poisson's ratio for assemblages (a) bronzite + hornblende + An_{56} and (b) bronzite + garnet + An_{53}.

continental crust is shown in Figure 5. A limitation of 10-km depth allows observations of continental crust below what would conventionally be called the Conrad discontinuity and precludes data from one-layer solutions. Figure 5 shows that lower crustal refractors exhibit an extremely wide range of compressional wave velocities, which suggests that the lower crust is quite variable in composition. Because of this variability, it should be emphasized that overall estimates of crustal composition are at present extremely tenuous (Poldervaart, 1955; Taylor, 1964; Taylor and White, 1965; Pakiser and Robinson, 1966; Wedepohl, 1969; Ronov and Yaroshevsky, 1969).

Also illustrated in Figure 5 is the range of compressional wave velocities between 4 and 10 kb for the 10 granulite-facies rocks we are concerned with here. The range of velocities for the granulite samples is clearly similar to the range of seismic velocities determined for the lower crust. As discussed in the preceding section, the variability of velocities for the samples is clearly related to their range of mineralogy and chemistry. Thus, if the lower crust is composed of granulite-facies mineral assemblages, a significant chemical and mineralogic inhomogeneity of the lower crust is implied.

Composition of the Crust Below the Canadian Shield

In the past few years, several seismic investigations have provided significant observations that allow more detailed analyses of crustal composition than were previously possible for classical two-layered crustal models. These observations included crustal shear velocities and hence Poisson's ratios, information on positive crustal velocity gradients, velocity reversals within the crust (Landisman and others, 1971), changes in Poisson's ratio with depth (Suzuki, 1965), and crustal anisotropy (Dorman, 1972). To show how some of these can be used to obtain a general picture of lower crustal composition, seismic observations for one particular region, the Canadian Shield, will be discussed.

Seismic refraction studies in Ontario and Manitoba (south and southwest of Hudson Bay) summarized by Hall and Hajnal (1973) provide excellent data for a comparison of refraction results with laboratory data. This region has been chosen because both compressional and shear wave velocities are reported, the stated accuracy of the measurements is high (most velocities are reported accurate to ± 0.05 km/sec), and the region has been covered both extensively and in detail (84 deep seismic recordings). The crustal models determined for this region are summarized in Figure 6 (see Hall and Hajnal, 1973, for further details of these models). Figure 6(a) is determined from profiles straddling the boundary between the Churchill geologic province and the Superior geologic province and represents the crustal structure of the Churchill province. The west Ontario and east Manitoba models [Fig. 6(b), (c)] are for a region farther to the south and thus represent the crustal structure of the Superior province.

Refracted velocities for crust beneath the Conrad discontinuity [termed the Riel discontinuity by Hall and Hajnal (1973)] in these models are 6.95, 6.85, and 6.81 km/sec, and the eastern Manitoba section shows an additonal sub-Conrad refractor of 7.1 km/sec. Clearly these velocities are within the range of compressional wave velocities measured for granulite-facies rocks in this study. Knowledge of compressional wave velocity of the lower crust, however, does not provide adequate information to determine lower crustal composition; inspection of Figures 3 and 4 shows that a given V_p can be indicative of any number of mineral assemblages. If V_s is known, Poisson's ratio, a parameter

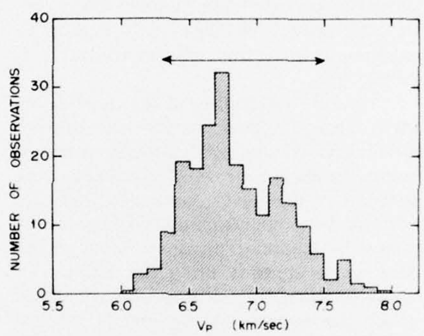

Figure 5. Histogram of compressional wave velocities for lower crust at depths greater than 10 km. Arrow indicates range of compressional wave velocities between 4 and 10 kb reported for granulite-facies rocks.

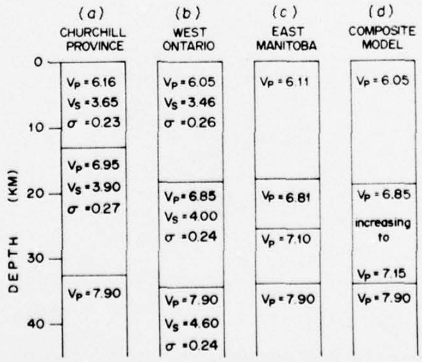

Figure 6. Velocity models for Churchill province, west Ontario, and east Manitoba, and composite model for Canadian Shield (after Hall and Hajnal, 1973).

thought to be insensitive to pressure and temperature (Crosson and Christensen, 1967; Fagerne and Kanestrøm, 1973) can be calculated and used in conjunction with V_p as a constraint on crustal composition. Superposition of the triangular diagrams for V_p and σ (Figs. 3, 4) produce intersections between V_p contours and σ contours that represent an estimate of composition for specific values of V_p and σ. Thus, if these two parameters are known for the lower crust of a region and granulite-facies stability is assumed, it may be possible to estimate lower crustal composition. Because the triangular diagrams (Figs. 3, 4) were calculated from atmospheric pressure values of elastic constants of the component minerals, a correction must be made for pressure. The average disagreement between the predicted velocities and those measured at 6 kb for the granulite samples is 0.2 km/sec; therefore, each velocity contour in Figures 3 and 4 has been augmented by that amount. Employing the corrected diagram for the assemblage bronzite + quartz + An_{29} [Fig. 7 (a)], an approximate estimate of 50 percent An_{29}, 27 percent bronzite, and 23 percent quartz can be made for the mineralogy of the lower crust of west Ontario ($V_p = 6.85$ km/sec, $\sigma = 0.24$). Figure 7(a) also predicts a mineralogy of 63 percent An_{29}, 31 percent bronzite, and 6 percent quartz for the lower crust of the Churchill province section ($V_p = 6.95$ km/sec, $\sigma = 0.26$). An alternate possibility of 65 percent An_{29}, 30 percent bronzite, and 5 percent perthite is given for the Churchill province mineralogy [Fig. 7(b)]. Note that the two estimates for the Churchill province section differ only by the substitution of a small percentage of perthite for quartz.

The two estimates for one region indicate the nonuniqueness of this approach. If more than the four mineral assemblages presented here had been examined, more estimates for one region may have been possible. It should be stressed that the variation of temperature with depth was not considered, because the change of V_p with temperature for many of the minerals used is not adequately known. The correction for pressure may also be in error. It is clear, however, that possible estimates of lower crustal composition cannot be made by use of compressional wave velocities alone. Although V_p measurements for the lower crust of the two regions discussed above are nearly equivalent, knowledge of Poisson's ratio in each case allows calculation of different compositions.

Hall and Hajnal (1973), in developing a composite model for the Canadian Shield, found evidence for a positive velocity gradient in the lower crust:

$$V_p = 6.70 \text{ km/sec} + 0.02\, z,$$

where z is the depth in kilometers. Thus, the refracted velocity at the Conrad discon-

tinuity of 6.85 km/sec leads to a velocity of 7.15 km/sec at the base of the crust, a change of 0.3 km/sec. A similar gradient was observed in the Grenville province by Berry and Fuchs (1973). It is interesting that, for the rocks examined in this study, the average change of V_p over an equivalent pressure range of 6 to 10 kb is only 0.1 km/sec. This is significantly less than the change observed in the Canadian Shield and would be diminished further if the effect of temperature increases expected in the lower crust (Lachenbruch, 1970) were considered. Thus, the only way to explain this velocity gradient is by change of mineralogy with increasing depth with or without a change in chemistry. This suggested change of mineralogy with depth is expressed in the east Manitoba section by the sub-Conrad refractor of 7.10 km/sec. Goodacre's (1972) analysis of refraction data for Canada also implied a change of composition with depth. Other regions in which evidence for velocity gradients exist are Missouri (Stewart, 1968), Oklahoma (Mitchell and Landisman, 1971), and the western United States (Prodehl, 1970), showing that positive velocity gradients are not unique to the Canadian Shield. Steinhart and Meyer (1961) emphasized that many time-distance curves from seismic experiments can also be interpreted as resulting from velocity gradients instead of layers of constant velocity. Thus, in addition to lateral variations of composition, there is considerable evidence to suggest that the lower continental crust is further complicated by changes in mineralogy with depth.

SUMMARY AND CONCLUSIONS

Velocities and elastic constants of granulite-facies rocks are related to the elastic properties of their constituent minerals. To a first approximation, velocities and Poisson's ratios of granulite rocks can be predicted from their mineralogy with simple three-component diagrams. The diagrams are particularly useful in understanding how variations in mineralogy affect seismic velocities. Because these diagrams show that a variety of mineral combinations can have equivalent compressional wave velocities, the interpretation of lower crustal seismic wave velocities in terms of granulite-facies mineralogy requires shear-velocities in addition to compressional wave velocities.

Our knowledge of the structure and composition of the lower continental crust is still incomplete. However, the wide range of seismic compressional wave velocities implies extreme variability in composition. Because experimental studies of mineral stabilities suggest that common igneous rocks are unstable throughout the lower continental crust, we must turn to metamorphic assemblages in estimating lower crustal mineralogy. As has been shown from the velocity measurements presented in this paper, the range of lower continental crustal velocities can readily be explained in terms of granulite-facies mineralogy.

It should be emphasized that seismic velocity measurements do not rule out the possibility of amphibolite-facies rocks as being significant or even dominant constituents of the lower continental crust. In addition to temperature considerations, the nature of regional metamorphism in the deep crust depends upon the relation of water pressure to load pressure (see Binns, 1969, for review); unfortunately, present estimates of the distribution of water in the lower crust are highly subjective. Compressional wave velocities at 6 kb for amphibolite-facies rocks reported by Christensen (1965) vary from 6.15 to 7.75 km/sec, which is similar to the variation observed for granulite-facies rocks. Shear wave velocities of amphibolite-facies rocks (Christensen, 1966a) are also comparable with granulite shear wave velocities.

Because of the variability of mineral composition and therefore chemical composition implied by lower crustal seismic velocities, any estimate of average lower crustal composition based on seismic velocities must await a much more thorough study of velocity distributions within the crust. It is highly probable that in some regions the lower crust consists of granulite-facies mineralogy of intermediate composition, whereas overall compositions in other regions might be much different. In addition to regions of relatively uniform lower crustal composition, there undoubtedly are areas in which there are significant vertical changes in composition with depth, as has been discussed for the Canadian Shield.

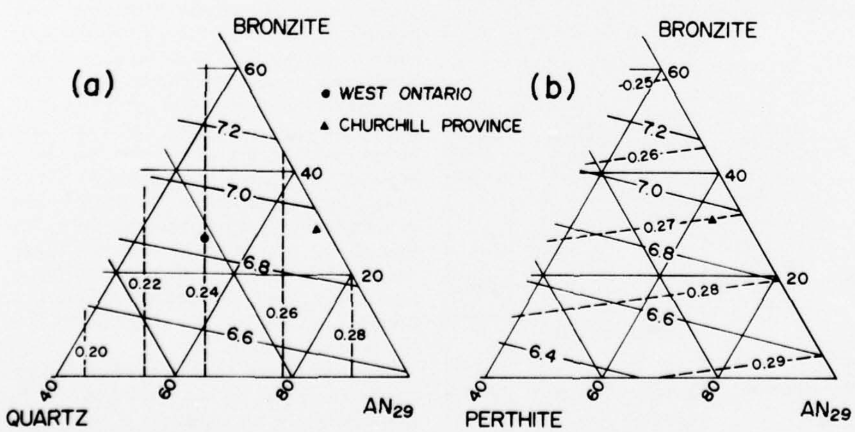

Figure 7. Compressional wave velocities and Poisson's ratios for assemblages (a) bronzite + quartz + An_{29} and (b) bronzite + perthite + An_{29}. Intersections of lines of constant V_p and σ (circle and small triangle) yield estimates of mineralogy for west Ontario and Churchill province velocity models.

ACKNOWLEDGMENTS

This study was supported by National Science Foundation Grant GA-36138 and the Office of Naval Research Contract N-00014-67-A-0103-0014. We thank Matthew H. Salisbury for critically reading the manuscript and providing helpful suggestions.

REFERENCES CITED

Alexandrov, K. S., and Ryzhova, T. V., 1961a, Elastic properties of rock-forming minerals. 2, Layered silicates: Acad. Sci. USSR Bull., Geophys. Ser. (English trans.), no. 11, p. 871–875.

——1961b, Elastic properties of rock-forming minerals. 1, Pyroxenes and amphiboles: Acad. Sci. USSR Bull., Geophys. Ser. (English trans.), no. 9, p. 1165–1168.

——1962, Elastic properties of rock-forming minerals. 3, Feldspars: Acad. Sci. USSR Bull., Geophys. Ser. (English trans.), no. 2, p. 129–131.

Alexandrov, K. S., Ryzhova, T. V., and Belikov, B. P., 1964, The elastic properties of pyroxenes: Soviet Physics-Crystallography, v. 8, p. 589–591.

Barrus, B., 1970, The petrology of the Precambrian rocks of the High Peaks area, Wind River Mountains, Fremont County, Wyoming [Ph.D. thesis]: Seattle, Univ. Washington, 86 p.

Berry, M. J., and Fuchs, K., 1973, Crustal structure of the Superior and Grenville provinces of the northeastern Canadian Shield: Seismol. Soc. America Bull., v. 63, p. 1393–1432.

Binns, R. A., 1969, Hydrothermal investigations of the amphibolite-granulite facies boundary: Geol. Soc. Australia Spec. Pubs., v. 2, p. 341–344.

Birch, F., 1960, The velocity of compressional waves in rocks to 10 kilobars; Part 1: Jour. Geophys. Research, v. 65, p. 1083–1102.
——1961, The velocity of compressional waves in rocks to 10 kilobars, Part 2: Jour. Geophys. Research, v. 66, p. 2199–2224.
——1972, Numerical experiments on the velocities in aggregates of olivine: Jour. Geophys. Research, v. 77, p. 6385–6391.
Brookins, D. G., and Wood, M. J., 1970, Rb-Sr geochronologic investigation of basic and ultrabasic xenoliths from the Stockdale Kimberlite, Riley County, Kansas: Kansas Geol. Survey Bull., v. 199, pt. 2, 12 p.
Buddington, A. F., 1952, Chemical petrology of some metamorphosed Adirondack gabbroic, syenitic and quartz syenitic rocks (Bowen volume): Am. Jour Sci., p. 37–84.
Christensen, N. I., 1965, Compressional wave velocities in metamorphic rocks at pressures to 10 kilobars: Jour. Geophys. Research, v. 70, p. 6147–6164.
——1966a, Shear wave velocities in metamorphic rocks at pressures to 10 kilobars: Jour. Geophys. Research, v. 71, p. 3549–3556.
——1966b, Elasticity of ultrabasic rocks: Jour. Geophys. Research, v. 71, p. 5921–5931.
——1968, Chemical changes associated with upper mantle structure: Tectonophysics, v. 6, p. 331–342.
——1969, Granulite facies metamorphism of the lower continental crust: EOS (Am. Geophys. Union Trans.), v. 50, p. 673.
Christensen, N. I., and Shaw, G. H., 1970, Elasticity of mafic rocks from the Mid-Atlantic Ridge: Royal Astron. Soc. Geophys. Jour., v. 20, p. 271–284.
Cohen, L. H., Ito, K., and Kennedy, G. C., 1967, Melting and phase relations in an anhydrous basalt to 40 kilobars: Am. Jour. Sci., v. 265, p. 475–518.
Compton, R. R., 1960, Charnockitic rocks of Santa Lucia Range, California: Am. Jour. Sci., v. 258, p. 609–636.
Crosson, R. S., and Christensen, N. I., 1967, Compositions of the Earth's crust and upper mantle from Poisson's ratio: Am. Geophys. Union Trans., v. 48, p. 200.
Davis, B.T.C., 1971, Bedrock geology of the St. Regis quadrangle, New York: New York State Mus. and Sci. Service Map and Chart Ser. no. 16, scale 1:62,500, 34 p.
den Tex, E., 1965, Metamorphic lineages of orogenic plutonism: Geologie en Mijnbouw, v. 44, p. 105–132.
den Tex, E., and Vogel, D. E., 1962, A "granulitgebirge" at Cabo Ortegal (N.W. Spain): Geol. Rundschau, v. 52, p. 95–112.
de Waard, D., 1965a, The occurrence of garnet in the granulite-facies terrane of the Adirondack Highlands: Jour. Petrology, v. 6, p. 165–191.
——1965b, A proposed subdivision of the granulite facies: Am. Jour. Sci., v. 263, p. 455–461.
Doraiswami, M. S., 1947, Elastic constants of magnetite, pyrite, and chromite: Indian Acad. Sci. Proc., ser. A, v. 25, p. 413–416.
Dorman, L. M., 1972, Seismic crustal anisotropy in northern Georgia: Seismol. Soc. America Bull., v. 43, p. 39–45.
Eskola, P., 1920, The mineral facies of rocks: Norsk. Geol. Tidsskr., v. 6, p. 143–194.
——1939, Die metamorphen Gesteine, *in* Barth, T.F.W., Correns, C. W., and Eskola, P., eds., Die Entstehung der Gesteine: Berlin, Springer, p. 351–355.
Fagerne, V., and Kanestrøm, R., 1973, Variations in the upper mantle structure as derived from P_n and S_n waves: Pure and Appl. Geophysics, v. 109, p. 1762–1772.
Giovanella, C. A., 1965, Petrology of the Precambrian rocks at Tichborne, southeastern Ontario [Ph.D. thesis]: Seattle, Univ. Washington, 78 p.
Goodacre, A. K., 1972, Generalized structure and composition of the deep crust and upper mantle in Canada: Jour. Geophys. Research, v. 77, p. 3146–3161.
Green, D. H., and Lambert, I. B., 1965, Experimental crystallization of anhydrous granite at high pressures and temperatures: Jour. Geophys. Research, v. 70, p. 5259–5268.
Green, D. H., and Ringwood, A. E., 1967, An experimental investigation of the gabbro to eclogite transformation and its petrological applications: Geochim. et Cosmochim. Acta, v. 31, p. 767–833.
——1972, A comparison of recent experimental data on the gabbro-garnet granulite-eclogite transition: Jour. Geology, v. 80, p. 277–288.
Green, T. H., 1970, High pressure experimental studies on the mineralogical constitution of the lower crust: Physics Earth and Planetary Interiors, v. 3, p. 441–450.
Hall, D. H., and Hajnal, Z., 1973, Deep seismic crustal studies in Manitoba: Seismol. Soc. America Bull., v. 63, p. 885–910.
Hietanen, A., 1967, On the facies series in various types of metamorphism: Jour. Geology, v. 75, p. 187–214.
Hill, D. P., and Pakiser, L. C., 1966, Crustal structure between the Nevada Test Site and Boise, Idaho, from seismic-refraction measurements, *in* Steinhart, J. S., and Smith, T. J., eds., The earth beneath the continents: Am. Geophys. Union Geophys. Mon. 13, p. 391–419.
Ito, K., and Kennedy, G. C., 1970, The fine structure of the basalt-eclogite transition: Mineralog. Soc. America Spec. Paper 3, p. 77–83.
——1971, An experimental study of the basalt-garnet granulite-eclogite transition, *in* Heacock, J. G., ed., The structure and physical properties of the Earth's crust: Am. Geophys. Union Geophys. Mon. 14, p. 303–314.
James, D. E., and Steinhart, J. S., 1966, Structure beneath continents: A critical review of explosion studies, 1960–1965, *in* Steinhart, D. E., and Smith, T. J., eds., The earth beneath the continent: Am. Geophys. Union Geophys. Mon. 10, p. 293–333.
Jeffreys, H., 1926, On near earthquakes: Royal Astron. Soc. Monthly Notes, Geophys. Supp., v. 1, p. 385–402.
Kanamori, H., and Mizutani, H., 1965, Ultrasonic measurements of elastic constants of rocks under high pressures: Earthquake Research Inst. Bull., v. 43, p. 173–194.
Kennedy, G. C., 1959, The origin of continents, mountain ranges, and ocean basins: Am. Jour. Sci., v. 47, p. 491–504.
Kennedy, G. C., and Ito, K., 1972, Comments on: "A comparison of recent experimental data on the gabbro-garnet granulite-eclogite transition": Jour. Geology, v. 80, p. 289–292.
Kosminskaya, I. P., and Riznichenko, Y. V., 1964, Seismic studies of the Earth's crust, *in* Odishaw, H., ed., Research in geophysics 2: Cambridge, M.I.T. Press, p. 81–122.
Kumazawa, M., 1969, The elastic constants of single-crystal orthopyroxene: Jour. Geophys. Research, v. 74, p. 5973–5980.
Lachenbruch, A. H., 1970, Crustal temperature and heat production: Implications of the linear heat flow relation: Jour. Geophys. Research, v. 75, p. 3291–3300.
Lambert, I. B., 1971, The composition and evolution of the deep continental crust: Geol. Soc. Australia Spec. Pubs., v. 3, p. 419–428.
Landisman, M., Mueller, S., and Mitchell, B. J., 1971, Review of evidence for velocity inversions in the continental crust, *in* Heacock, J. G., ed., The structure and physical properties of the Earth's crust: Am. Geophys. Union Geophys. Mon. 14, p. 11–34.
Lovering, J. F., and White, A.J.R., 1969, Granulitic and eclogitic inclusions from basic pipes of Delegate, Australia: Contr. Mineralogy and Petrology, v. 21, p. 9–52.
McGetchin, T. R., and Silver, L. T., 1972, A crustal–upper mantle model for the Colorado Plateau based on observations of crystalline rock fragments in the Moses Rock Dike: Jour. Geophys. Research, v. 77, p. 7022–7037.
McSkimin, H. J., Andreatch, P., Jr., and Thurston, R. W., 1965, Elastic moduli of quartz versus hydrostatic pressure at 25° and −195.8°C: Jour. Appl. Physics, v. 36, p. 1624–1632.
Mitchell, B., and Landisman, M., 1971, Geophysical measurements in the southern Great Plains, *in* Heacock, J. G., ed., The structure and physical properties of the Earth's crust: Am. Geophys. Union Geophys. Mon. 14, p. 77–93.
Mueller, S., and Landisman, M., 1966, Seismic studies of the Earth's crust in continents. I, Evidence for a low-velocity zone in the upper part of the lithosphere: Royal Astron. Soc. Geophys. Jour., v. 10, p. 525–538.
Ocola, L. C., and Meyer, R. P., 1972, Crustal low-velocity zones under the Peru-Bolivia altiplano: Royal Astron. Soc. Geophys. Jour., v. 30, p. 199–209.
Oliver, R. L., 1969, Some observations on the distribution and nature of granulite-facies terrains: Geol. Soc. Australia Spec. Pubs., v. 2, p. 259–268.
Pakiser, L. C., and Robinson, R., 1966, Composition and evolution of the continental crust as suggested by seismic observations: Tectonophysics, v. 3, p. 547–557.
Poldervaart, A., 1955, The chemistry of the Earth's crust, *in* Poldervaart, A., ed., Crust of the Earth: Geol. Soc. America Spec. Paper 62, p. 119–144.
Prodehl, C., 1970, Seismic refraction study of crustal structure in the western United States: Geol. Soc. America Bull., v. 81, p. 2629–2646.
Ramananantoandro, R., and Manghnani, M., 1972, Compressional wave velocities in

granulites and eclogites to 10 kbar: EOS (Am. Geophys. Union Trans.), v. 53, p. 1119.

Ringwood, A. E., and Green, D. H., 1964, Experimental investigations bearing on the nature of the Mohorovičić discontinuity: Nature, v. 201, p. 566–567.

——1966a, Petrologic nature of the stable continental crust, *in* Steinhart, J. S., and Smith, T. J., eds., The earth beneath the continents: Am. Geophys. Union Geophys. Mon. 10, p. 611–619.

——1966b, An experimental investigation of the gabbro-eclogite transformation and some geophysical implications: Tectonophysics, v. 3, p. 383–427.

Roller, J. C., and Healy, J. H., 1963, Seismic-refraction measurements of crustal structure between Santa Monica Bay and Lake Mead: Jour. Geophys. Research, v. 68, p. 5837–5849.

Ronov, A. B., and Yaroshevsky, A. A., 1969, Chemical composition of the Earth's crust, *in* Hart, P. J., ed., The Earth's crust and upper mantle: Am. Geophys. Union Geophys. Mon. 13, p. 37–57.

Ryzhova, T. V., 1964, Elastic properties of plagioclase: Acad. Sci. USSR Bull., Geophys. Ser. (English Trans.), no. 7, p. 633–635.

Ryzhova, T. V., and Alexandrov, K. S., 1965, The elastic properties of potassium-sodium feldspars: Acad. Sci. USSR Bull., Earth Physics Ser. (English Trans.), no. 1, p. 53–56.

Schmid, R., 1967, Zur Petrographie und Struktur der Zone Ivrea-Verbano Zwischen Valle d'Ossola und Val Grande (Prov. Novara, Italien): Schweizer. Mineralog. u. Petrog. Mitt., v. 47, p. 935–1119.

Simmons, G., 1964, The velocity of shear waves in rocks to 10 kbars: Jour. Geophys. Research, v. 69, p. 1123–1130.

Smith, B. L., 1969, The Precambrian geology of the central and northeastern parts of the New Jersey Highlands, *in* Subitsky, S., ed., Geology of selected areas in New Jersey and eastern Pennsylvania and guidebook of excursions: New Brunswick, N.J., Rutgers Univ., p. 35–47.

Soga, N., 1967, The elastic constants of garnet under pressure and temperature: Jour. Geophys. Research, v. 72, p. 4227–4234.

Steinhart, J. S., and Meyer, R. P., 1961, Explosion studies of continental structure: Carnegie Inst. Washington Pub., v. 622, 409 p.

Stewart, S. W., 1968, Crustal structure in Missouri by seismic refraction methods: Seismol. Soc. America Bull., v. 58, p. 291–323.

Suzuki, Z., 1965, Maine seismic experiment — A study of shear waves: Seismol. Soc. America Bull., v. 55, p. 425–439.

Taylor, S. R., 1964, Abundance of chemical elements in the continental crust: A new table: Geochim. et. Cosmochim. Acta, v. 28, p. 1273–1286.

Taylor, S. R., and White, A.J.R., 1965, Geochemistry of andesites and the growth of continents: Nature, v. 208, p. 271–273.

Thomsen, L., 1972, Elasticity of polycrystals and rocks: Jour. Geophys. Research, v. 77, p. 315–327.

Turner, F. J., 1968, Metamorphic petrology; mineralogical and field aspects: New York, McGraw-Hill Pub. Co., p. 403.

Turner, F. J., and Verhoogen, J., 1960, Igneous and metamorphic petrology: New York, McGraw-Hill Pub. Co., p. 694.

Verma, R. K., 1960, Elasticity of some high density crystals: Jour. Geophys. Research, v. 65, p. 757–766.

Wagner, P. A., 1928, The evidence of the kimberlite pipes on the constitution of the outer part of the earth: South African Jour. Sci., v. 25, p. 127–148.

Watson, K. D., and Morton, D. M., 1969, Eclogite inclusions in kimberlite pipes at Garnet Ridge, northeastern Arizona: Am. Mineralogist, v. 54, p. 267–285.

Wedepohl, K. H., 1969, Composition and abundance of common igneous rocks, *in* Wedepohl, K. H., ed., Handbook of geochemistry 1: Berlin, Springer-Verlag, p. 227–249.

Yoder, H. S., Jr., and Tilley, C. E., 1962, Origin of basalt magmas: An experimental study of natural and synthetic rock systems: Jour. Petrology, v. 3, p. 342–532.

MANUSCRIPT RECEIVED BY THE SOCIETY APRIL 24, 1974

REVISED MANUSCRIPT RECEIVED JULY 22, 1974

REPORT DOCUMENTATION PAGE

READ INSTRUCTIONS BEFORE COMPLETING FORM

1. REPORT NUMBER: TR # 337	2. GOVT ACCESSION NO.	3. RECIPIENT'S CATALOG NUMBER
4. TITLE (and Subtitle): The Petrologic Nature of the Lower Oceanic Crust and Upper Mantle		5. TYPE OF REPORT & PERIOD COVERED
		6. PERFORMING ORG. REPORT NUMBER
7. AUTHOR(s): Nikolas I. Christensen		8. CONTRACT OR GRANT NUMBER(s): N-00014-67-A-0103-0014
9. PERFORMING ORGANIZATION NAME AND ADDRESS: University of Washington, Department of Oceanography, Seattle, Washington 98195		10. PROGRAM ELEMENT, PROJECT, TASK AREA & WORK UNIT NUMBERS: Project NR 083012
11. CONTROLLING OFFICE NAME AND ADDRESS: Office of Naval Research, La Jolla, California		12. REPORT DATE: 1975
		13. NUMBER OF PAGES
14. MONITORING AGENCY NAME & ADDRESS (if different from Controlling Office)		15. SECURITY CLASS. (of this report): Unclassified
		15a. DECLASSIFICATION/DOWNGRADING SCHEDULE

16. DISTRIBUTION STATEMENT (of this Report)

Approved for public release; distribution unlimited

17. DISTRIBUTION STATEMENT (of the abstract entered in Block 20, if different from Report)

18. SUPPLEMENTARY NOTES

Reprint from: Kristjansson (ed.), Geodynamics of Iceland and the North Atlantic Area, D. Reidel Publishing Company, Dordrecht-Holland.

19. KEY WORDS (Continue on reverse side if necessary and identify by block number)

Seismic Velocities, Oceanic Crust, Upp~~er Mantle, Op~~hiolite, Anisotropy, Iceland.

20. ABSTRACT (Continue on reverse side if necessary and identify by block number)

ABSTRACT. The compositions of the lower oceanic crust and upper mantle are investigated using data from high pressure experiments of compressional and shear wave velocities in rocks. Four compositional models for the lower oceanic crust are considered: 1) partially serpentinized peridotite, 2) gabbro, 3) metabasalt and metagabbro and 4) an ophiolite model consisting of metamorphosed sheeted dikes overlying late differentiates and cumulate gabbros. Comparisons of compressional wave velocities (V_p) from dredged oceanic rocks with layer 3 refraction velocities show that perido-

(continued on back)

tites 30 to 40% serpentinized, unaltered gabbro, metagabbro and metabasalt all have velocities similar to observed lower crustal velocities. Thus compressional wave velocity measurements alone will not distinguish between the various crustal models. Although only a limited amount of refraction data on shear wave velocities (V_s) are available, it appears that lower crustal Poisson's ratios, calculated from V_p and V_s, are significantly lower than measured values in partially serpentinized peridotite and unaltered gabbro. In support of models 3 and 4 it is shown that Poisson's ratios of metabasalt and metagabbro, on the other hand, agree well with seismic data from the upper portion layer 3. The low Poisson's ratios reported for the lower crust of Iceland ($\sim$ 0.27) suggest that metabasalt and metagabbro are abundant constituents of layer 3. The 7.4 km/sec layer, often found between layer 3 and oceanic upper mantle in the Pacific Ocean, is interpreted as most likely being composed of peridotite, 10 to 20% serpentinized, or feldspathic

---

SECURITY CLASSIFICATION OF THIS PAGE (When Data Entered)

REPORT DOCUMENTATION PAGE		READ INSTRUCTIONS BEFORE COMPLETING FORM
1. REPORT NUMBER TR#338	2. GOVT ACCESSION NO.	3. RECIPIENT'S CATALOG NUMBER
4. TITLE (and Subtitle) Velocities of Compressional and Shear Waves in DSDP Leg 27 Basalts		5. TYPE OF REPORT & PERIOD COVERED
		6. PERFORMING ORG. REPORT NUMBER
7. AUTHOR(s) N. I. Christensen, M. H. Salisbury, D. M. Fountain, and R. L. Carlson		8. CONTRACT OR GRANT NUMBER(s) N-00014-67-A-0103-0014
9. PERFORMING ORGANIZATION NAME AND ADDRESS University of Washington Department of Oceanography Seattle, Washington 98195		10. PROGRAM ELEMENT, PROJECT, TASK AREA & WORK UNIT NUMBERS Project NR 083012
11. CONTROLLING OFFICE NAME AND ADDRESS Office of Naval Research La Jolla, California		12. REPORT DATE 1975
		13. NUMBER OF PAGES 5
14. MONITORING AGENCY NAME & ADDRESS(if different from Controlling Office)		15. SECURITY CLASS. (of this report) Unclassified
		15a. DECLASSIFICATION/DOWNGRADING SCHEDULE

16. DISTRIBUTION STATEMENT (of this Report)

Approved for public release; distribution unlimited.

17. DISTRIBUTION STATEMENT (of the abstract entered in Block 20, if different from Report)

18. SUPPLEMENTARY NOTES

Reprint from: Initial Reports of the Deep Sea Drilling Project Vol. XXVII, Washington (U.S. Government Printing Office) 1974, 445-449.

19. KEY WORDS (Continue on reverse side if necessary and identify by block number)

Oceanographic data. Basalt, Velocities, Oceanic Crust

20. ABSTRACT (Continue on reverse side if necessary and identify by block number)

Two holes drilled during Leg 27 into basalt achieved significant penetrations of 38.5 meters at Site 259 and 47.5 meters at Site 261. The relatively deep drill penetrations into layer 2 provide a unique opportunity to examine variations in seismic velocity as a function of depth and thus to measure seismic-velocity gradients in the upper levels of Layer 2 directly. With increasing depth at both sites, weathering effects become less pronounced and seismic velocities increase. Projecting the observed velocity gradients downward, it is apparent that weathering extends to at least 70 and 55 meters at Sites 259 and 261, respectively.

DD FORM 1 JAN 73 1473 EDITION OF 1 NOV 65 IS OBSOLETE
S/N 0102-014-6601

Unclassified

SECURITY CLASSIFICATION OF THIS PAGE (When Data Entered)

Unclassified

SECURITY CLASSIFICATION OF THIS PAGE (When Data Entered)

REPORT DOCUMENTATION PAGE		READ INSTRUCTIONS BEFORE COMPLETING FORM
1. REPORT NUMBER TR# 339	2. GOVT ACCESSION NO	3. RECIPIENT'S CATALOG NUMBER
4. TITLE (and Subtitle) Structure and Constitution of the Lower Oceanic Crust.		5. TYPE OF REPORT & PERIOD COVERED
		6. PERFORMING ORG. REPORT NUMBER
7. AUTHOR(s) Nikolas I. Christensen and Matthew H. Salisbury		8. CONTRACT OR GRANT NUMBER(s) N-00014-67-A-0103-0014
9. PERFORMING ORGANIZATION NAME AND ADDRESS University of Washington Department of Oceanography Seattle, Washington 98195		10. PROGRAM ELEMENT, PROJECT, TASK AREA & WORK UNIT NUMBERS Project NR 083012
11. CONTROLLING OFFICE NAME AND ADDRESS Office of Naval Research La Jolla, California		12. REPORT DATE February, 1975
		13. NUMBER OF PAGES 29
14. MONITORING AGENCY NAME & ADDRESS (if different from Controlling Office)		15. SECURITY CLASS. (of this report) Unclassified
		15a. DECLASSIFICATION/DOWNGRADING SCHEDULE

16. DISTRIBUTION STATEMENT (of this Report)

Approved for public release; distribution unlimited.

17. DISTRIBUTION STATEMENT (of the abstract entered in Block 20, if different from Report)

18. SUPPLEMENTARY NOTES

Reprint from: Reviews of Geophysics and Space Physics v. 113, Feb. 1975.

19. KEY WORDS (Continue on reverse side if necessary and identify by block number)

Oceanic Crust, Seismic Structure, ~~Seismic Velocities,~~ Petrology, Ophiolites.

20. ABSTRACT (Continue on reverse side if necessary and identify by block number)

Any petrologic model of the lower oceanic crust must be consistent with three sets of data: (1) the seismic structure of the oceanic crust, (2) the petrology of oceanic dredge samples, and (3) laboratory measurements of seismic velocity through such samples. A review of these data indicates that within the framework of earlier three-layer models of oceanic seismic structure *the crust is internally complex and* varies markedly with age, azimuth, and tectonic province. Mantle compressional wave velocities V_p are anomalously low under the ridge (7.2-7.7 km/s) but increase to 8.0-8.3 km/s beyond 15 m.y.; layer 3 thickens by 2 km within 40 m.y. of formation and decreases in V_p from 6.8 to 6.5 km/s within 80 m.y.; both the mantle and layer 3 are statistically anisotropic. Dredge lithologies consist predominantly of serpentinized ultramafics and mafic igneous rocks ranging from basalt to gabbro, the gabbro often showing evidence of fractionation. Metamorphism of mafic rocks from zeolite to amphibolite facies grade is

(continued on back)

DD FORM 1 JAN 73 1473 EDITION OF 1 NOV 65 IS OBSOLETE
S/N 0102-014-6601

Unclassified

SECURITY CLASSIFICATION OF THIS PAGE (When Data Entered)

common. Velocities in oceanic serpentinites and basalts are generally lower than layer 3 refraction velocities. Unaltered gabbros have compressional wave velocities of approximately 7.0 km/s, which is high for layer 3, together with shear wave velocities V_s of 3.8 km/s and values of Poisson's ratio σ of 0.30. Metabasites containing hornblende and plagioclase have values of V_p = 6.8 km/s, V_s = 3.8 km/s, and σ = 0.28, in good agreement with those of layer 3. On the basis of petrology and velocity it is suggested that layer 3 is composed of hornblende metagabbro underlain by normal gabbro. In a model consistent with geophysical observations of heat flow, seismicity, gravity, and seismic structure at the ridge it is proposed that layer 2 and the upper levels of layer 3 form near the median valley but that deeper levels of layer 3 thicken for 40 m.y. by intermittent offridge intrusion fed from the underlying anomalous mantle. Ophiolites in such a model represent segments of thin immature ridge crest obducted onto continental margins during subduction of a spreading ridge.

Unclassified

SECURITY CLASSIFICATION OF THIS PAGE (When Data Entered)

REPORT DOCUMENTATION PAGE

READ INSTRUCTIONS BEFORE COMPLETING FORM

1. REPORT NUMBER: TR#340
2. GOVT ACCESSION NO.
3. RECIPIENT'S CATALOG NUMBER
4. TITLE (and Subtitle): Elastic Wave Velocities in Volcanic and Plutonic Rocks Recovered on DSDP Leg 31
5. TYPE OF REPORT & PERIOD COVERED
6. PERFORMING ORG. REPORT NUMBER
7. AUTHOR(s): N. I. Christensen, R. L. Carlson, M. H. Salisbury, and D. M. Fountain
8. CONTRACT OR GRANT NUMBER(s): N-00014-67-A-0103-0010
9. PERFORMING ORGANIZATION NAME AND ADDRESS: University of Washington, Department of Oceanography, Seattle, Washington 98195
10. PROGRAM ELEMENT, PROJECT, TASK AREA & WORK UNIT NUMBERS: Project NR 083012
11. CONTROLLING OFFICE NAME AND ADDRESS: Office of Naval Research, La Jolla, California
12. REPORT DATE: 1975
13. NUMBER OF PAGES: 3
14. MONITORING AGENCY NAME & ADDRESS (if different from Controlling Office)
15. SECURITY CLASS. (of this report): Unclassified
15a. DECLASSIFICATION/DOWNGRADING SCHEDULE
16. DISTRIBUTION STATEMENT (of this Report): Approved for public release; distribution unlimited.
17. DISTRIBUTION STATEMENT (of the abstract entered in Block 20, if different from Report)
18. SUPPLEMENTARY NOTES: Reprint from: Initial Reports of the Deep Sea Drilling Project Vol. XXXI, Washington (U.S. Government Printing Office) 1975, 607-609.
19. KEY WORDS (Continue on reverse side if necessary and identify by block number): Oceanographic data. Velocities, Oceanic Crust, Basalt, Gabbro
20. ABSTRACT (Continue on reverse side if necessary and identify by block number):

Velocities and densities are reported for several samples of basement rock obtained from Sites 292, 293, 294, and 296 of the Deep Sea Drilling Project. Velocities in gabbroic rocks and metabasites recovered from Site 293 are correlative with seismic velocities determined for Layer 3. The lower crustal origin for these rocks is further supported by the similarity in lithology between these samples, dredge haul samples from fracture zones and rocks found in ophiolite complexes.

DD FORM 1 JAN 73 1473 EDITION OF 1 NOV 65 IS OBSOLETE
S/N 0102-014-6601

Unclassified

SECURITY CLASSIFICATION OF THIS PAGE (When Data Entered)

SECURITY CLASSIFICATION OF THIS PAGE (When Data Entered)

REPORT DOCUMENTATION PAGE

READ INSTRUCTIONS BEFORE COMPLETING FORM

1. REPORT NUMBER TR# 341	2. GOVT ACCESSION NO.	3. RECIPIENT'S CATALOG NUMBER
4. TITLE (and Subtitle) Constitution of the Lower Continental Crust Based on Experimental Studies of Seismic Velocities in Granulite		5. TYPE OF REPORT & PERIOD COVERED
		6. PERFORMING ORG. REPORT NUMBER
7. AUTHOR(s) Nikolas I. Christensen and David M. Fountain		8. CONTRACT OR GRANT NUMBER(s) N-00014-67-A-0103-0014
9. PERFORMING ORGANIZATION NAME AND ADDRESS University of Washington Department of Oceanography Seattle, Washington 98195		10. PROGRAM ELEMENT, PROJECT, TASK AREA & WORK UNIT NUMBERS Project NR 083012
11. CONTROLLING OFFICE NAME AND ADDRESS Office of Naval Research La Jolla, California		12. REPORT DATE February, 1975
		13. NUMBER OF PAGES 10
14. MONITORING AGENCY NAME & ADDRESS(if different from Controlling Office)		15. SECURITY CLASS. (of this report)
		15a. DECLASSIFICATION/DOWNGRADING SCHEDULE

16. DISTRIBUTION STATEMENT (of this Report)

Approved for public release; distribution unlimited

17. DISTRIBUTION STATEMENT (of the abstract entered in Block 20, if different from Report)

18. SUPPLEMENTARY NOTES

Reprint from: Geological Society of America Bulletin, V. 86, p. 227-236, Feb. 1975.

19. KEY WORDS (Continue on reverse side if necessary and identify by block number)

Crustal Structure, Canadian Shield, Granulite, Seismic Velocities

20. ABSTRACT (Continue on reverse side if necessary and identify by block number)

Rocks of the granulite facies have been proposed as major constituents of the lower continental crust. To evaluate this possibility, compressional and shear wave velocities have been determined to pressures of 10 kb for 10 granulite samples, thus enabling comparisons of seismic data for the lower crust with the velocities and elastic properties of granulite rocks. The samples selected for this study range in composition from granitic to basaltic, with bulk densities of 2.68 to 3.09 g/cm³. At 6 kb, compressional (V_p) and shear (V_s) wave velocities range from 6.39 to 7.49 km/sec and from 3.36 to 4.25 km/sec, respectively. Velocities in granulite rocks are shown to vary systematically with variations in mineralogical constitution. Both V_p and V_s increase with in-

(continued on back)

DD FORM 1 JAN 73 1473 EDITION OF 1 NOV 65 IS OBSOLETE
S/N 0102-014-6601

Unclassified

SECURITY CLASSIFICATION OF THIS PAGE (When Data Entered)

creasing pyroxene, amphibole, and garnet. Velocities increase with an increasing ratio of pyroxene to amphibole in hornblende-granulite subfacies rocks of approximately equivalent chemical compositions. Decreasing quartz content in granulite rocks produces an increase in V_p and an accompanying decrease in V_s, thereby significantly changing Poisson's ratio. The range of velocities measured for the granulite samples is similar to the range of seismic velocities reported for the lower continental crust; thus, the hypothesis that granulite rocks are major lower crustal constituents is further strengthened. Furthermore, it is shown that lower crustal composition is extremely variable, and therefore valid discussions of composition must be limited to specific regions where seismic velocities are well known. The use of seismic velocities in estimating lower crustal composition is illustrated for the Canadian Shield in Ontario and Manitoba. *Key words: crustal structure, Canadian Shield.*

FOR UNCLASSIFIED TECHNICAL REPORTS, REPRINTS, & FINAL REPORTS
PUBLISHED BY OCEANOGRAPHIC CONTRACTORS
OF THE OCEAN SCIENCE & TECHNOLOGY DIVISION
OF THE OFFICE OF NAVAL RESEARCH
(REVISED SEPTEMBER, 1975)

1 Director of Defense Research and Engineering
Office of the Secretary of Defense
Washington, D.C. 20301
ATTN: Office Assistant Director (Research)

12 Defense Documentation Center
Cameron Station
Alexandria, Virginia 22314

Office of Naval Research
Department of the Navy
Arlington, Virginia 22217
3 ATTN: Code 480
1 ATTN: Code 460
1 ATTN: Code 102-OS
6 ATTN: Code 102IP
1 Cognizant ONR Branch Office

1 ONR Resident Representative

Director
Naval Research Laboratory
Washington, D.C. 20390
6 ATTN: Library, Code 2620

Commander
Naval Oceanographic Office
Washington, D.C. 20390
1 ATTN: Code 1640
1 ATTN: Code 70

1 Director
National Oceanographic Data Center
National Oceanic & Atmospheric Administration
Rockville, Maryland 20882